QUADRATURE SIGNAL GENERATION NETWORKS BASED ON SEQUENCE DISCRIMINATION

Edward Daoud Ibrahim Daoud

A Thesis

in

The Faculty

of

Engineering

Presented in Partial Fulfillment of the Requirement of

The Degree of Doctor of Philosophy at

Concordia University

Montreal, Quebec

Canada

March, 1979

ABSTRACT

QUADRATURE SIGNAL GENERATION NETWORKS BASED ON SEQUENCE DISCRIMINATION

Edward D.I. Daoud, Ph.D.
Concordia University, 1979

This thesis is concerned with the theoretical and experimental investigations concerning a new class of active polyphase networks for quadrature signal generation. The theoretical analysis is based on the representation of the actual applied input signals into their positive and negative sequence equivalence. Three different types of active polyphase networks are introduced:

i) Networks with no feedback
ii) Networks with feedback
iii) Sampled data switched capacitor network

The first two classes of networks make use of resistors and capacitors as the passive components and the operational amplifier as the only active element.

A new configuration of analog sampled data phase splitting sequence discriminator is presented, which yields a frequency response comparable to that of its analog counterpart. The design technique makes use of the equivalence between a resistor and a circuit element

consisting of a capacitor and two switches. The coefficients of the filter transfer function being ratios of capacitors, can be made less sensitive to manufacturing processes.

Theoretical analysis shows that sensitivity reduction can be achieved by applying feedback between the input and the output terminals. From the experimental set-up using a sequence discriminator consisting of two sections in cascade, a minimum stopband attenuation of 25 dB is achieved while in the tranmission band a ripple of less than 0.04 dB over the specified bandwidth of the realization is also achieved. However for a given bandwidth and component values, the network with positive feedback between the input and the output terminals, shows the superior sensitivity performance.

Feasibility of the proposed networks is evaluated through Laboratory experiments. Special emphasis is placed on the generation of single-sideband signals. Experimental results are presented and the design limitations are discussed.

ACKNOWLEDGEMENTS

The author would like to express his deep appreciation to Dr. M.N.S. Swamy and Dr. W.B. Mikhael for their guidance and encouragement throughout the course of this work.

Appreciation is also extended to Dr. V. Ramachandran for reading through the manuscript. Fruitful discussions with the faculty members and fellow graduate students in Electrical Engineering Department is greatly appreciated. Thanks are also due to Mr. G. Jutras of Bell-Northern research for his remarks.

The author deeply acknowledges the understanding and various sacrificies made by his wife Mrs. Odette Daoud throughout the period of this study. Thanks must go to the typing staff at Bell-Northern Research, Montreal, for their efficiency in typing this manuscript, and to the technical relation staff for their assistance in plotting the graphs.

Financial support from Concordia University and the National Research Council of Canada through grants A7739 and A3924 is also appreciated.

TO MY BELOVED PARENTS

WHO DEVOTED THEIR LIVES

TO MAKE LIFE BRIGHTER FOR

THEIR CHILDREN

TABLE OF CONTENTS

LIST OF TABLES

LIST OF FIGURES

LIST OF ABBREVIATIONS AND SYMBOLS

A	Operational amplifier gain
A_o	D.C. gain of the operational amplifier
AP	All-Pass
C	Capacitor
CCITT	International Telegraph and Telephone Consultative Committee
CMOS	Complementary metal oxide semiconductor
C_s	Switched Capacitor
C_x	Equivalent Capacitor
D	Denominator
D_i	Demodulated Signal
dB	Decibels
Exp	Exponential
f_c	Carrier Frequency
H_n	Negative sequence transfer function
H_p	Positive Sequence transfer function
I	Current
i	Instantaneous Current
j	Imaginary quantity, $j = \sqrt{-1}$
L	Integrated resistor length
LSB	Lower sideband
M_i	Modulated Carrier Signal
N	Number of sections
OA	Operational amplifier
P	Modulated function
P_m	Fourier Coefficients
Q	Charge

R	Resistor
r	Average resistance of the switch
s	Complex frequency variable
Sa	Sampling function
S_e^x	Sensitivity of x due to small variations in e
S_i	Switch i
SSB	Single Sideband
SSSD	Single stage sequence discriminator
T_n	Negative sequence transfer function
T_p	Positive sequence transfer function
T_s	Switching period
t_o	Pulse width
USB	Upper Sideband
V	Voltage
V_f	Error voltage
V_{on}	Negative sequence output voltage
V_{op}	Positive sequence output voltage
V_p	Passband Voltage
V_{pn}	Passband of the negative feedback network
V_{pp}	Passband of the positive feedback network
V_s	Stopband voltage
V_{SN}	Stopband of the negative feedback network
V_{SP}	Stopband of the positive feedback network
W	Integrated resistor width
Z	Complex variable
α	closed loop gain
α_1	ratio of capacitors C_s and C
$\alpha(\omega)$	Gain
Δ	Incremental variation

ζ_i	Ratio, $\zeta_i = \omega/\omega_i$
ϕ	Phase angle
ω	Angular velocity
ω_c	Carrier frequency
ω_i	Resonant frequency = $1/R_iC_i$
ω_s	Signal frequency

CHAPTER I

INTRODUCTION

1.1 GENERAL

The transmission and processing of an audio frequency information often requires a 90-degree relative phase shift over a wide frequency range. Continued interest in the design and development of phase splitting networks has generated an immense amount of research over the last few decades [1-13]. These networks have been used in many applications that require single-sideband modulation such as;

1) Carrier telephony

2) Polyphase radio system

3) Elimination of image frequency interference in heterodyne modulators (such as the superheterodyne radio receiver and conventional wave analyzer).

Several basic contributions have been reported for the generation and detection of single-sideband signals [14-26].

The filter method [24], still one of the most popular methods used for direct amplitude modulation, is shown in Figure 1.1. The input signal (e.g. a speech waveform) is applied to a balanced modulator along with the first carrier frequency. The two normal sidebands appear in the

output of the balanced modulator, while the carrier frequency is balanced out. A band-pass filter is used to select one sideband and reject the other. Because of the stringent requirement imposed on the suppression of the unwanted sideband, the band-pass filter may become uneconomical.

The second method, known as the quadrature modulation method, is shown in Figure 1.2 [15,19]. The input signal is split into two signals using a wideband 90-degree phase splitting network. These quadrature signals are applied to two balanced modulators with carriers 90-degree apart. When the output signals from the modulators are added, one set of sidebands will add in phase, generating the desired signal, while the other sideband is canceled out. The quadrature modulation method requires the use of a 90-degree phase difference network operating over a specified frequency band and it is here that most of the difficulties arise. Orchard [9] suggested the use of two all-pass networks as a solution for this problem. The quadrature modulation has been successfully used in many applications in communications and instrumentation area. The method has sensitivity problems in applications with stringent requirements, leading to tight component tolerances. This is because the quadrature signals are obtained from two independant all-pass paths.

A third method was introduced by Weaver [21] and others [24]. This method, sometimes known as the N-path filter method, is shown in Figure 1.3. It depends on double modulation and filtering. This approach is similar to the quadrature modulation method except that the 90-degree phase difference network is replaced by the first set of modulators. However, if one uses this method for the implementation of a high quality transmission system, considerable practical difficulties

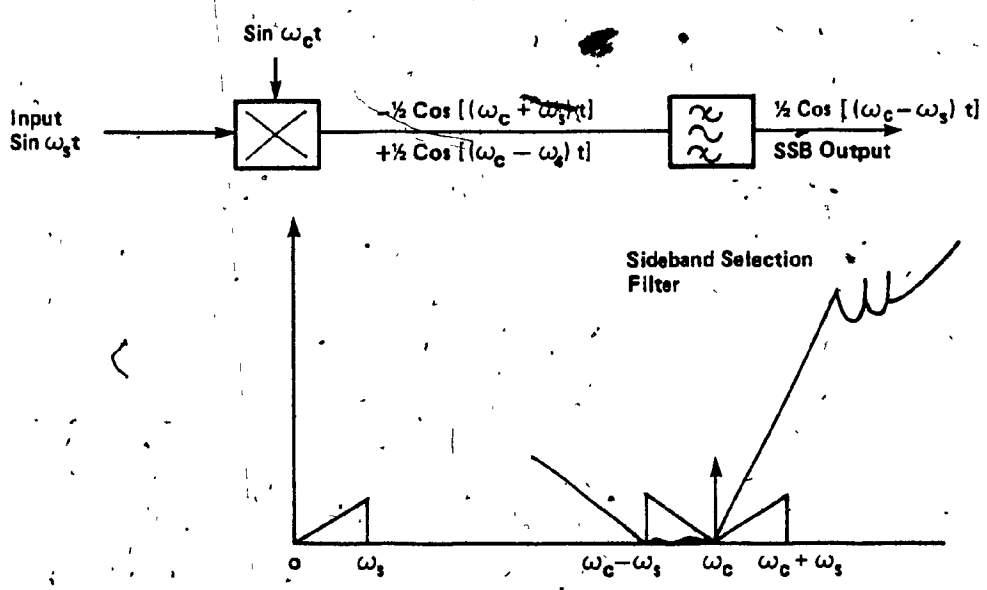

Figure 1.1 Filter Method for Generating SSB Signal

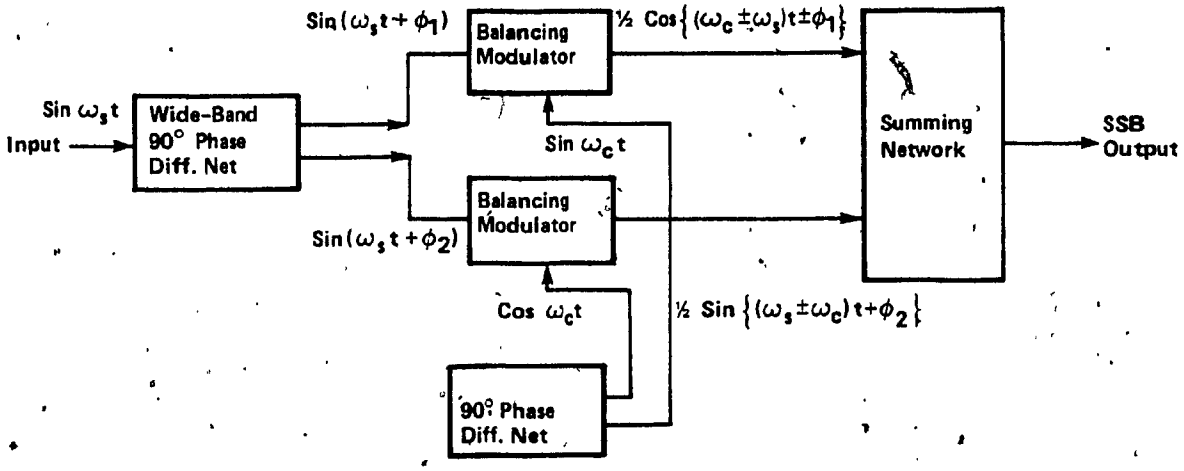

Figure 1.2 Quadrature Modulation Method

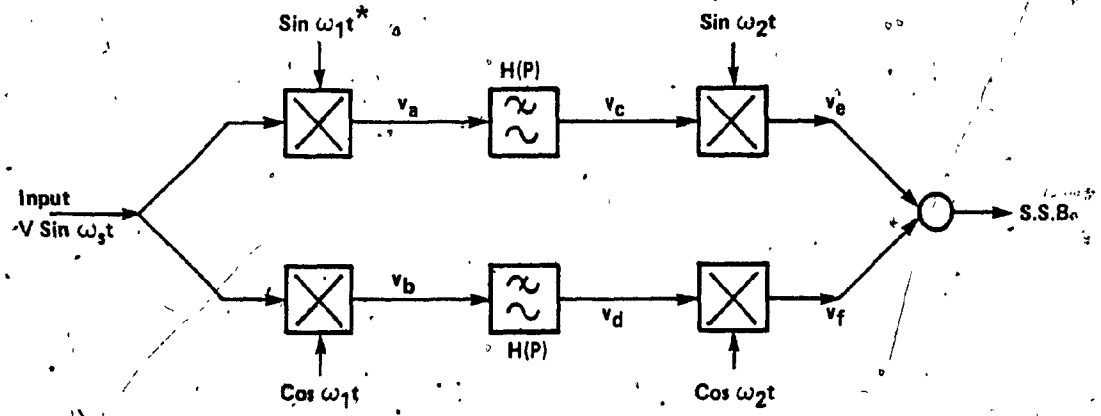

Figure 1.3 Weaver Method

$V_a = \frac{1}{2} V. \quad \text{Cos}\,(\omega_1-\omega_s)\,t - \text{Cos}\,(\omega_1+\omega_s)\,t$

$V_b = \frac{1}{2} V. \quad \text{Sin}\,(\omega_1+\omega_s)\,t - \text{Sin}\,(\omega_1-\omega_s)\,t$

$V_c = \frac{1}{2} V. \quad \text{Cos}\,[(\omega_1-\omega_s)+\theta] \;.\; |H(P-P_1)|$

$V_d = \frac{1}{2} V. \quad \text{Sin}\,[(\omega_s-\omega_1)\,t+\theta] \;.\; |H(P-P_2)|$

$V_e = \frac{1}{4} V. \quad \text{Sin}\,[\omega_2 \pm (\omega_1-\omega_s)]\,t \pm \theta] \;.\; |H(P-P_1)|$

$V_f = \frac{1}{4} V. \quad \text{Sin}\,[\omega_2 \mp (\omega_2 \mp (\omega_1-\omega_s)]\,t \mp \theta] \;.\; |H(P-P_1)|$

* The first carrier frequency ω_1 lies in the center of the baseband signal.

arise [3,14]. This is because the modulators operate with carrier frequencies in the center of the transmission band and any carrier leak (e.g. due to modulator imbalance) appears as a steady tone at a frequency where it is most objectionable.

1.2 RECENT DEVELOPMENTS IN THE DESIGN OF PHASE-SPLITTING NETWORKS

Generation of single-sideband signals with the required channel bandwidth, modulation frequency cut-off and unwanted sideband suppression presents a problem in the design of phase splitting networks. Recent developments in the design of these networks have introduced a new class of polyphase networks [3,14,27]. These polyphase networks can discriminate between different types of the applied polyphase input signals. Some interesting studies were made on the applicability of the polyphase modulation as part of the frequency changing process. It was found that this approach can be used with great advantage to eliminate the need for difficult or inconvenient filter designs. The advantage of polyphase modulation is that polyphase signals possess an identifying property called sequence. By using circuits which distinguish between signals of identical frequency but opposite sequence, it is possible, without any preliminary filtering, to separate - after modulation - signals which originally lie in the same frequency band. Such circuits can be designed to transmit one sequence and reject the other within the same frequency band, but it is very difficult to realize that over a wide-band of frequencies [20]. Before proceeding to discuss the different design considerations of the polyphase networks, it is worthwhile to define the different terms that will be used frequently in the remainder of this thesis.

1.2.1 Polyphase Signals and Symmetric Sequences

In general, an alternating voltage, with respect to ground, of magnitude V volts and frequency ω radians/second is represented by a phasor rotating anti-clockwise with angular velocity ω and length V in the manner shown in Figure 1.4.

A polyphase signal is a set of two or more vectors (e.g. voltages or currents) of the same frequency. This polyphase signal is said to be symmetric if the vectors are equal in magnitude and equally spaced in phase. The case of a symmetric polyphase signal with 4 vectors is shown in Figure 1.5.

1.2.2 Positive and Negative Sequences

The sequence of Figure 1.5(a) is defined as a positive sequence because the phase order from 1 to 4 is clockwise (i.e. $V, -jV, -V, +jV$). If the phase order is reversed as shown in Figure 1.5(b) then the sequence is defined as a negative sequence. It is to be noted that the polarity of a sequence is determined by the phase order of the sequence and not by the direction of rotation (which is always anticlockwise) since the sequence, whether it is positive or negative, is always composed of a set of vectors rotating anticlockwise with an angular velocity ω rad/sec [28].

The network in Figure 1.6 is a simple RC circuit for a quadrature system, proposed in [14,27] as a sequence discriminator. Let the input voltages V_1 to V_4, forming the positive sequence, be applied to the input terminals 1 to 4, respectively. It can be shown that the chain

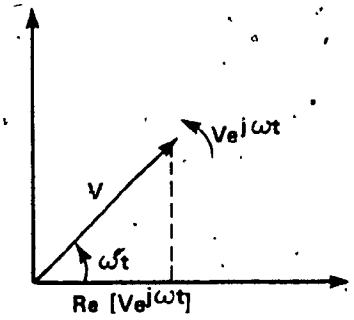

Figure 1.4 Representation of a Rotating Vector

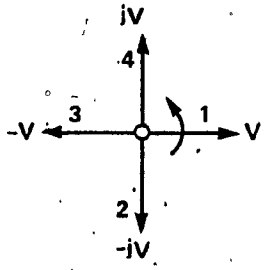

a — Positive Sequence

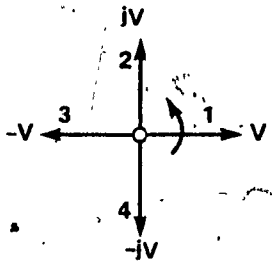

b — Negative Sequence

Figure 1.5 Representation of Symmetric Sequences

matrix of one path, for example, 1 to ground as an input port and 5 to ground as an output port is given by;

$$\begin{bmatrix} V_1 \\ I_1 \end{bmatrix} = \frac{1}{G_1 - \omega C_1} \begin{bmatrix} G_1 + j\omega C_1 & 1 \\ 2(j\omega C_1 G_1) & G_1 + j\omega C_1 \end{bmatrix} \begin{bmatrix} V_5 \\ -I_5 \end{bmatrix} \qquad (1\text{-}1)$$

The open-circuit voltage transfer function $T_{51p}(j\omega)$ is

$$T_{51p}(j\omega) = \frac{V_5}{V_1}\bigg|_{I_5 = 0} = \frac{1 - \omega/\omega_1}{1 + j\omega/\omega_1} \qquad (1\text{-}2)$$

where $\omega_1 = 1/R_1C_1$

If the negative sequence, shown in Figure 1.5.(b), is now applied to the input terminals of the network, then the chain matrix becomes

$$\begin{bmatrix} V_1 \\ I_1 \end{bmatrix} = \frac{1}{G_1 + \omega C_1} \begin{bmatrix} G_1 + j\omega C_1 & 1 \\ 2(j\omega C_1 G_1) & G_1 + j\omega C_1 \end{bmatrix} \begin{bmatrix} V_5 \\ -I_5 \end{bmatrix} \qquad (1\text{-}3)$$

and the open-circuit voltage transfer function $T_{51n}(j\omega)$ is:

$$T_{51n}(j\omega) = \frac{V_5}{V_1}\bigg|_{I_5 = 0} = \frac{1 + \omega/\omega_1}{1 + j\omega/\omega_1} \qquad (1\text{-}4)$$

The frequency response for both the positive sequence (1-2) and the negative sequence (1-4) are shown in Figure 1.7. It can be seen from (1-2) and (1-4) that the response is ideal only at one frequency, $\omega = 1/R_1C_1$, and approximates an ideal response over a narrow frequency range around $\omega = 1/R_1C_1$.

It is important to point out [25] that the network response to positive and negative sequences can be interchanged simply by

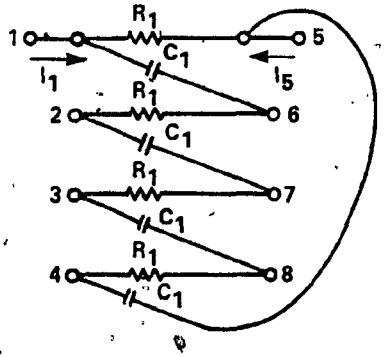

Figure 1.6 Single Stage Passive Sequence Discriminator

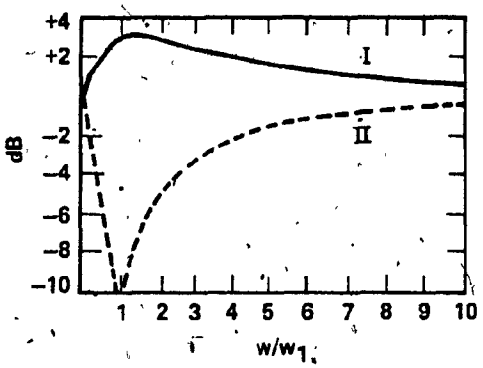

Figure 1.7 Frequency Response of a Passive Sequence Discriminator Network

I Response to a Negative Sequence

II Response to a Positive Sequence

interchanging the inputs to 1 and 3 or 2 and 4, or by interchanging resistors and capacitors in the network. This first sequence discriminator can be made to quite easily reject a particular frequency of a certain sequence, while transmitting the same frequency in the other sequence, but it is more difficult to realize the rejection over a wide band of frequencies. Recently, Gingell [14] suggested a solution to this problem by cascading 'N' sections of different resonant frequencies $\omega_1, \omega_2 \ldots, \omega_N$. Thus the unwanted sequence is nulled completely at those N notch frequencies. This network is shown in Figure 1.8.

A successful approach to improve the network performance and achieve sensitivity reduction at the same time was introduced by Mikhael [27]. It was found that by applying feedback in the manner shown in Figure 1.9 the coupling between adjacent channels is increased and the nominal response exceeds the CCITT requirements [29].

In the present era of microelectronic systems, it is very likely to realize active networks in integrated form of one kind or another. Linear active RC networks certainly represent one of the most practical and economical methods of designing inductorless networks. Hybrid integrated circuit (HIC) technology, i.e. the combination of film resistors and capacitors with silicon integrated active devices, has been singled out as the technology most suited to the design of integrated linear active networks [30]. The passive components may be thick or thin film, although in general, performance will be superior with the latter type, since it is difficult to achieve good temperature coefficients and the tolerances are high for thick film. The analytical simplification resulting from the condition of closely tracking resistor and capacitor values is more accurate with thin film implementation. The main advantages of integrated circuit fabrication are [31,32].

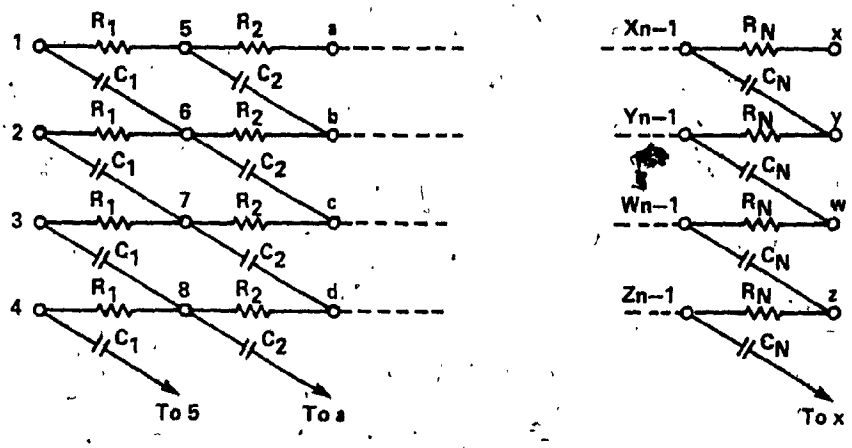

Figure 1.8 Passive RC Sequence Discriminator Consisting of N Sections in Cascade

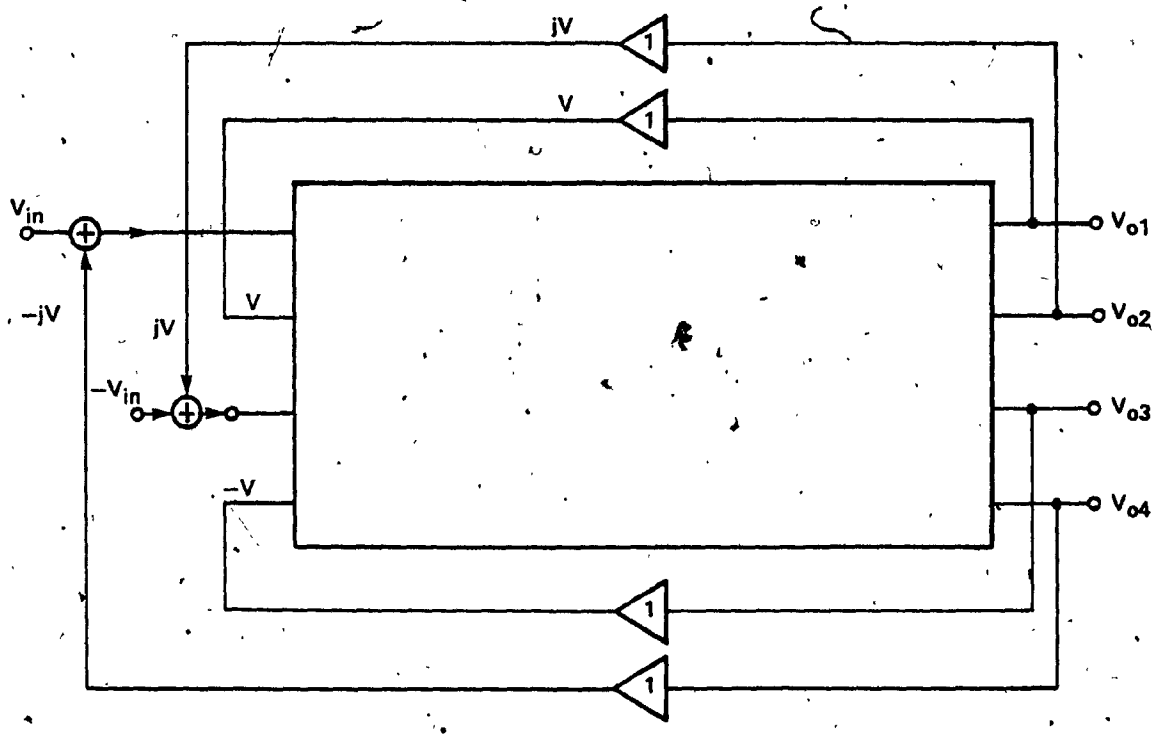

Figure 1.9 Sequence Discriminator with Feedback [25]

1) Increased system reliability.
2) Reduction of size and weight, and an increased equipment density obtained by reducing the packaging levels.
3) Increased operating speed due to the absence of parasitics and decreased propagation delay.
4) Reduction in power consumption.

For the realization with active RC networks to be suitable for available micro electronic technology, attention should be given to the total resistance and, more significantly, to the total capacitance values required as well as the spread in the values of the resistors and capacitors in the circuit. Ideally, for integrated circuit implementation, these values should be as low as possible, failing which, minimization of the total capacitance in the circuit assumes importance.

As large scale integration (LSI) techniques are being used in integrated systems, conventional active circuits using HIC's, while being a significant advance over discrete-component passive circuits, are becoming increasingly important to develop new techniques to efficiently implement such circuits. Since most applications require a large number of circuits on a single integrated chip, it is desirable that these circuits be fully integrated, require no trimming and use as little silicon area as possible. A new technique for analog sampled data filtering had been introduced [33,34] which can be fully integrated using MOS technology. The advantages of this approach are:

1) Reduced circuit complexity.
2) Low coefficient Variation.
3) Efficient utilization of silicon area.

The sampled data technique makes use of switches, capacitors and operational amplifiers. It was pointed out [32] that the MOS technology is particularly suited for implementing these filters. The filter coefficients, being ratios of capacitor, could be made less sensitive to the manufacturing process.

1.3 SCOPE OF THE THESIS

This thesis is mainly concerned with the structure, design and properties of a new class of polyphase networks for quadrature signal generation. These networks use resistors and capacitors as passive elements and the μA 741 operational amplifier as the basic active device. With a proper choice of feedback, these networks compare favorably with the presently available quadrature modulation approach and those in [3,27], especially in terms of simplicity and gain and phase sensitivity to component variations. Chapter 2 is mainly concerned with the study of the general characteristics of a single stage sequence discriminator, SSSD. The result obtained is then generalized by cascading N number of such sections. The voltage transfer ratio (V_{out}/V_{in}), as well as the gain and phase sensitivities to the RC product in each individual section are derived.

In Chapter 3, it is shown that by introducing coupling between adjacent sections, and particularly between the input of the first section and the output of the second section a reduction in both gain and phase sensitivities to component variations is achieved and better characteristics are obtained.

A new configuration of analog sampled data filters that makes use of capacitors, switches and operational amplifiers is introduced in

Chapter 4. The principle of the switched capacitor "resistor" is adopted in this thesis for the following reasons:

1) Resistors (and hence, the need for trimming) are eliminated.

2) The filter's frequency response sensitivity to passive component variations is very low.

3) Tuning can be easily achieved by controlling the capacitor ratios.

4) The circuit can be fully integrated using as little silicon area as possible.

5) Filter coefficients can be derived with a high precision and stability, using the capacitor ratios only, and thus makes it well suited for large scale integration techniques.

One of the most useful areas of application for these networks is the generation of single-sideband (SSB) signals, which is considered in Chapter 5. The modulation scheme is proposed and the general properties of the modulator and demodulator (MODEM) are also discussed in this chapter. It is shown that either the upper-sideband (USB), or lower-sideband (LSB), can be produced by simply interchanging any two signals (out of the four generated signals) that are 180° apart.

Finally, Chapter 6 summarizes the results and the conclusions of this thesis. Suggestions for further studies are also given in this chapter.

CHAPTER II

DESIGN OF ACTIVE RC PHASE SPLITTING NETWORKS

2.1 INTRODUCTION

The purpose of this chapter is to investigate the general properties of a new class of active phase splitting networks [14,27], and to develop a design procedure for realizing such networks. The sequence discriminator consists of two sections in cascade with different resonant frequencies. This class of networks is designed to provide, from the polyphase input signals, two output signals V_o and V_o' which are ideally equal in magnitude and in phase quadrature over the frequency range of interest. A single stage sequence discriminator, SSSD, is first analyzed using the concept of sequence discrimination [14,27,28]. The general principle of analysis outlined can be extended to cascaded sections of different RC product in each section.

2.2 SINGLE STAGE SEQUENCE DISCRIMINATOR - SSSD

The objective of this section is to study and formulate the general characteristics of a single stage sequence discriminator, SSSD, using vectorial notation. The SSSD is shown in Figure 2.1. This network is designed to pass one type of sequence and attenuate the other over a specified frequency range.

Referring to Figure 2.1, let the RC product $R_1C_1 \neq R_1'C_1'$. Starting from the input side, the applied input signal, chosen to be $\pm 2V$

volts for convenience, is resolved to its positive and negative sequences as shown in Figure 2.2, where node 4 is hypothetical and the net signal applied to it is zero.

Consider first the positive sequence (V , -jV, -V, +jV), then

$$\frac{V - V_{op}}{R_1} = \{V_{op} - (-jV)\}\ j\omega C_1 \qquad (2\text{-}1)$$

and

$$\frac{(-jV) - V'_{op}}{R'_1} = \{V'_{op} - (-V)\}\ j\omega C'_1 \qquad (2\text{-}2)$$

From (2-1) and (2-2) the two output signals V_{op} and V'_{op} can be written as:

$$V_{op} = \frac{1 + \omega/\omega_1}{1 + j\omega/\omega_1}\ (V) \qquad (2\text{-}3)$$

and

$$V'_{op} = \frac{1 + \omega/\omega'_1}{1 + j\omega/\omega'_1}\ (-jV) \qquad (2\text{-}4)$$

where

$$\omega_1 = 1/R_1C_1$$

and

$$\omega'_1 = 1/R'_1C'_1$$

For nominal component values and in the ideal case where $\omega_1 = \omega'_1$ then

$$V_{op} = \frac{1 + \omega/\omega_1}{1 + j\omega/\omega_1}\ (V) \qquad (2\text{-}5)$$

and

$$V'_{op} = \frac{1 + \omega/\omega_1}{1 + j\omega/\omega_1}\ (-jV) \qquad (2\text{-}6)$$

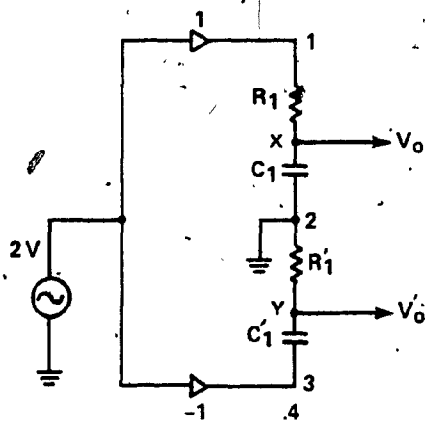

Figure 2.1 Active RC Single Stage Sequence Discriminator

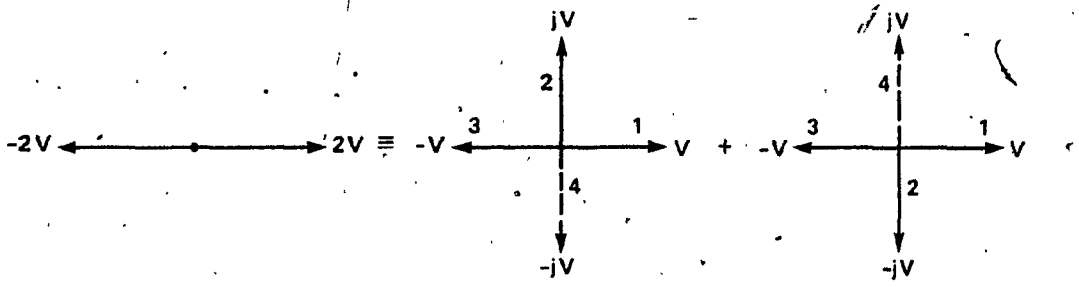

A. Actual Input B. Negative Sequence C. Positive Sequence

Figure 2.2 Input Signals and their Positive and Negative Sequence Equivalence

From (2-5) and (2-6) it is easy to conclude that

$$V'_{op} = -jV_{op} \qquad (2\text{-}7)$$

i.e. The two output signals V_{op} and V'_{op} as given by (2-5) and (2-6) are equal in magnitude and are in phase quadrature, where V_{op} is leading V'_{op}.

By applying the negative sequence (V, jV, -V, -jV) shown in Figure 2.2.(b) to the input terminals of the SSSD, then the two output signals, denoted by V_{on} and V'_{on}, can be derived in a similar way to those in (2-3) and (2-4) as:

$$V_{on} = \frac{1 - \omega/\omega_1}{1 + j\omega/\omega_1} \ (V) \qquad (2\text{-}8)$$

and

$$V'_{on} = \frac{1 - \omega/\omega'_1}{1 + j\omega/\omega'_1} \ (jV) \qquad (2\text{-}9)$$

Again, in the ideal case where $\omega_1 = \omega'_1$, the two output signals V_{on} and V'_{on} are related by

$$V'_{on} = jV_{on} \qquad (2\text{-}10)$$

Here, too, V_{on} and V'_{on} are equal in magnitude and different in phase from one another by 90 degrees, where, in this case V'_{on} is leading V_{on}.

From the previous analysis it is seen that the network has the special property of being able to discriminate between the positive and negative input sequence in the frequency domain. The frequency response of the SSSD is shown in Figure 2.3. It can be seen that the negative sequence has a null at $\omega = \omega_1$.

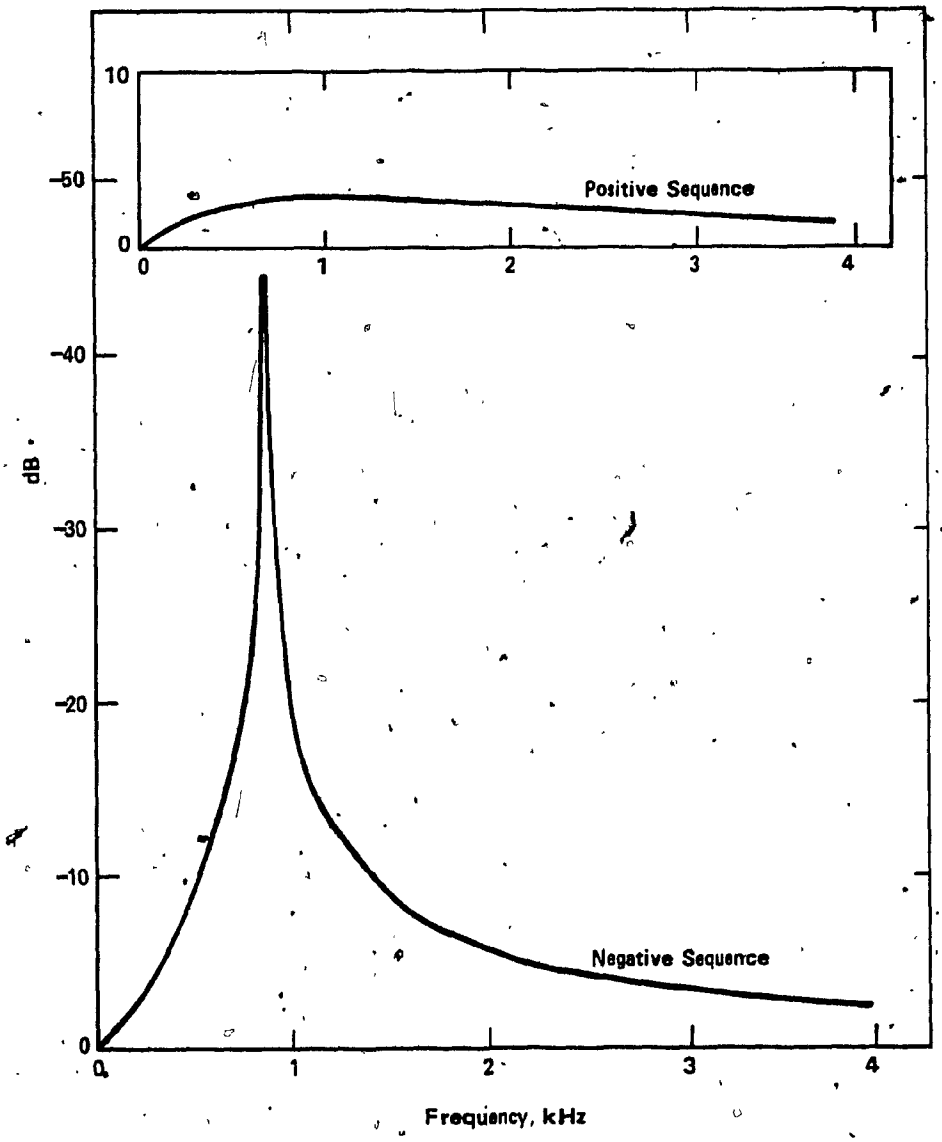

Figure 2.3 Frequency Response to Positive and Negative Sequences

So far we have been able to obtain the response due to positive and negative sequences. In practice there is no symmetric sequence but this is actually what we want to achieve in the ideal case. Since the possible input signals are of asymmetric nature, they can be formed only by adding at least two symmetric sequence of opposite polarity. Applying superposition, the measurable outputs, considering the ideal case, are obtained as:

$$V_o = V_{op} + V_{on} \quad , \tag{2-11}$$

and

$$V'_o = V'_{op} + V'_{on} \tag{2-12}$$

Substituting (2-5), (2-6), (2-8) and (2-9) into (2-11) and (2-12), the actual output signals are:

$$V_o = \frac{1}{1 + j\omega/\omega_1} \quad (2V) \quad , \tag{2-13}$$

and

$$V'_o = \frac{\omega/\omega_1}{1 + j\omega/\omega_1} \quad (-2jV) \quad , \tag{2.14}$$

It can be seen from (2-13) and (2-14) that V_o and V'_o are obtained in terms of the actual input signals ($\pm 2V$). The two signals V_o and V'_o are 90 degrees out of phase at all frequencies and

$$|V_o|_{\omega = \omega_1} = |V'_o|_{\omega = \omega_1} \tag{2-15}$$

A vectorial representation of the output signals as given by (2-5), (2-6), (2-8), (2-9), (2-13) and (2-14) is shown in Figure 2.4. Using (2-5), (2-6), (2-8) and (2-9), the output sequence is ideal at one

frequency $\omega_1 = 1/R_1C_1$ and approximates an ideal sequence over a narrow frequency range.

2.3 PRACTICAL POLYPHASE SEQUENCE DISCRIMINATORS

2.3.1 Grounded Network

To extend the bandwidth of the realization more than one section has to be considered. The two stage sequence discriminator is shown in Figure 2.5. Let the resonant frequencies be ω_i and ω_i' $(i = 1, 2)$ and consider the non-ideal case first where $\omega_i \neq \omega_i'$. The two output signals from the first section, denoted by V_x and V_y, due to both the positive and negative sequences can be obtained from (2-3), (2-4), (2-8) and (2-9) by interchanging $V_{op}(V_{on})$ and $V'_{op}(V'_{on})$ by V_x and V_y respectively. Following the same procedure as in SSSD, the actual output signals V_o and V_o', as given in Appendix A, are:

$$V_o = \frac{\dfrac{1}{1 + j\zeta_1} + \dfrac{\zeta_1'\zeta_2}{1 + j\zeta_1'}}{(1 + j\zeta_2)} \cdot (2V) , \qquad (2\text{-}16)$$

and

$$V_o' = \frac{\dfrac{j\zeta_1'}{(1 + j\zeta_1')} + \dfrac{j\zeta_2'}{(1 + j\zeta_1)}}{(1 + j\zeta_2')} \cdot (-2V) \qquad (2\text{-}17)$$

where $\zeta_i = \omega/\omega_i$ and $\zeta_i' = \omega/\omega_i'$ $(i = 1, 2)$

It will be shown later in Chapter 5 that the quadrature modulation process results in rotating V_o by $\pi/2(-\pi/2)$ with respect to V_o' and summing the modulated outputs to produce the passband (stopband). Thus the two equations governing the passband and stopband are:

$$V_p = \tfrac{1}{2}(V_o + jV_o') , \qquad (2\text{-}18)$$

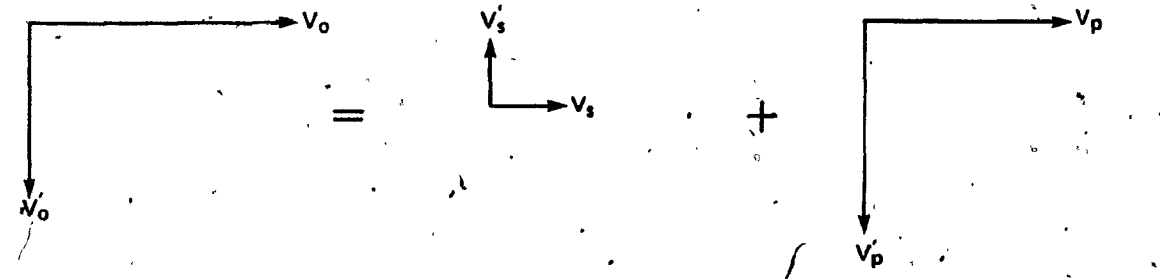

C. Total Output B. Attenuated Sequence A. Non-Attenuated Sequence

Figure 2.4 Vectorial Representation of the Output Sequences

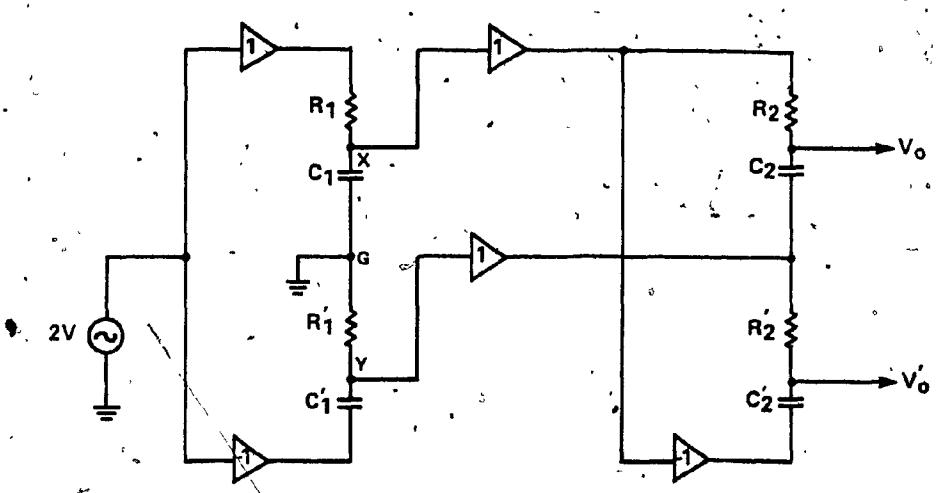

Figure 2.5 Sequence Discriminator Consisting of Two Section in Cascade (Grounded Network)

and

$$V_s = \tfrac{1}{2}(V_o - JV'_o) \qquad (2\text{-}19)$$

The explicit expressions for the passband (V_p) and the stopband (V_s) are:

$$V_p = \left[\frac{\dfrac{1}{(1 + j\zeta_1)} + \dfrac{\zeta'_1\zeta_2}{(1 + j\zeta'_1)}}{(1 + j\zeta_2)} + \frac{\dfrac{\zeta'_1}{(1 + j\zeta'_1)} + \dfrac{\zeta'_2}{(1 + j\zeta_1)}}{(1 + j\zeta'_2)} \right] (V) \qquad (2\text{-}20)$$

and

$$V_s = \left[\frac{\dfrac{1}{(1 + j\zeta_1)} + \dfrac{\zeta'_1\zeta_2}{(1 + j\zeta'_1)}}{(1 + j\zeta_2)} - \frac{\dfrac{\zeta'_1}{(1 + j\zeta'_1)} + \dfrac{\zeta'_2}{(1 + j\zeta_1)}}{(1 + j\zeta'_2)} \right] (V) \qquad (2\text{-}21)$$

Equations (2-20) and (2-21) will be used, in the next section, to derive the sensitivity expressions of both the passband and stopband to the component variations.

Now, for nominal component values, i.e. $\omega_i = \omega'_i$ then (2-16), (2-17), (2-20) and (2-21) are simplified to:

$$V_o = \frac{1 + \omega^2/\omega_1\omega_2}{\prod_{i=1}^{i=2} (1 + j\omega/\omega_i)} (2V) \qquad (2\text{-}22)$$

$$V'_o = \frac{j(\omega/\omega_1 + \omega/\omega_2)}{\prod_{i=1}^{i=2} (1 + j\omega/\omega_i)} (-2V) \qquad (2\text{-}23)$$

$$V_p = \frac{\prod_{i=1}^{i=2} (1 + \omega/\omega_i)}{\prod_{i=1}^{i=2} (1 + j\omega/\omega'_i)} (V) \qquad (2\text{-}24)$$

and

$$V_s = \frac{\prod_{i=1}^{i=2} (1 - \omega/\omega_i)}{\prod_{i=1}^{i=2} (1 + j\omega/\omega_i)} (V) \qquad (2\text{-}25)$$

The frequency response of the two stage sequence discriminator is shown in Figure 2.6, where the stopband has nulls at $\omega = \omega_i$, $(i = 1, 2)$ and a minimum attenuation of 25 dB has been achieved. From (2-22) and (2-23) the voltage transfer ratios are:

$$V_o/2V = \frac{1 - s^2/\omega_1\omega_2}{(1 + s/\omega_1)(1 + s/\omega_2)} , \qquad (2\text{-}26)$$

and

$$V'_o/2V = \frac{(s/\omega_1 + s/\omega_2)}{(1 + s/\omega_1)(1 + s/\omega_2)} \qquad (2\text{-}27)$$

The voltage transfer ratios given in (2-26) and (2-27) have real transmission zeros at $s = 0$ and $s = \pm 1/\sqrt{\omega_1\omega_2}$, and the poles are on the negative real axis at $s = -\omega_i$ $(i = 1, 2)$.

The general expressions of the passband and stopband for N cascaded sections of different resonant frequencies ω_i $(i = 1, \ldots, N)$ can be obtained by generalizing (2-24) and (2-25). Then

$$V_p = \frac{\prod_{i=1}^{i=N} (1 + \omega/\omega_i)}{\prod_{i=1}^{i=N} (1 + j\omega/\omega_i)} \text{ (V)} , \qquad (2\text{-}28)$$

and

$$V_s = \frac{\prod_{i=1}^{i=N} (1 - \omega/\omega_i)}{\prod_{i=1}^{i=N} (1 + j\omega/\omega_i)} \text{ (V)} \qquad (2\text{-}29)$$

As can be seen from (2-29) the stopband has null at N frequencies. Figure 2.7 shows the frequency response of a sequence discriminator consisting of 4 sections in cascade where a stopband rejection of 60 dB has been achieved.

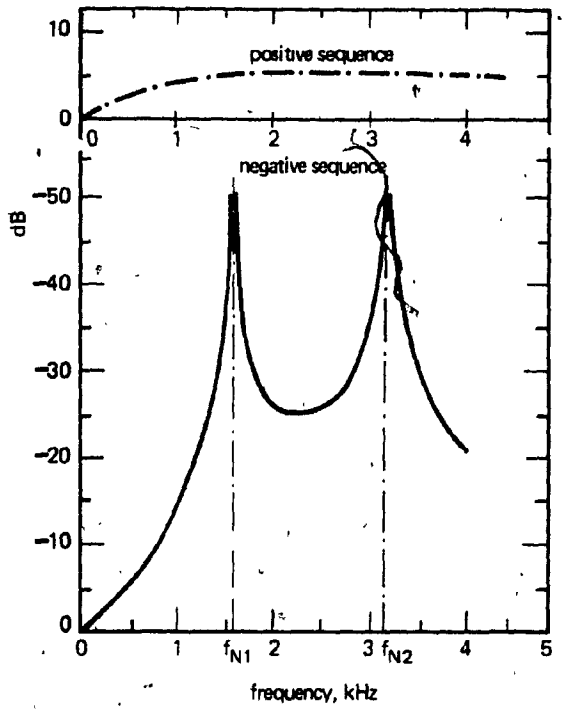

Figure 2.6 Frequency Response of the Active Design — Two Sections in Cascade (Nulls at f_{N1} = 1.59 and f_{N2} = 3.2 kHz)

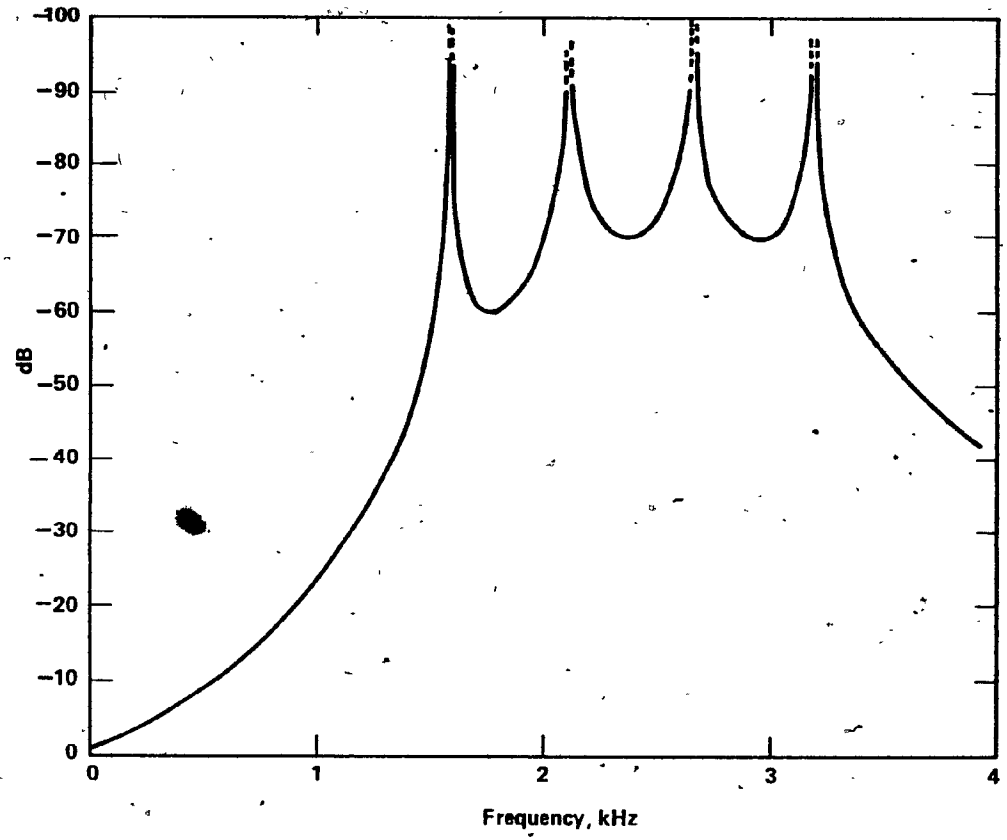

a) Stopband Response

Figure 2.7 Frequency Response of a Sequence Discriminator Consisting of Four Sections in Cascade

a) Stopband Response

b) Passband Response

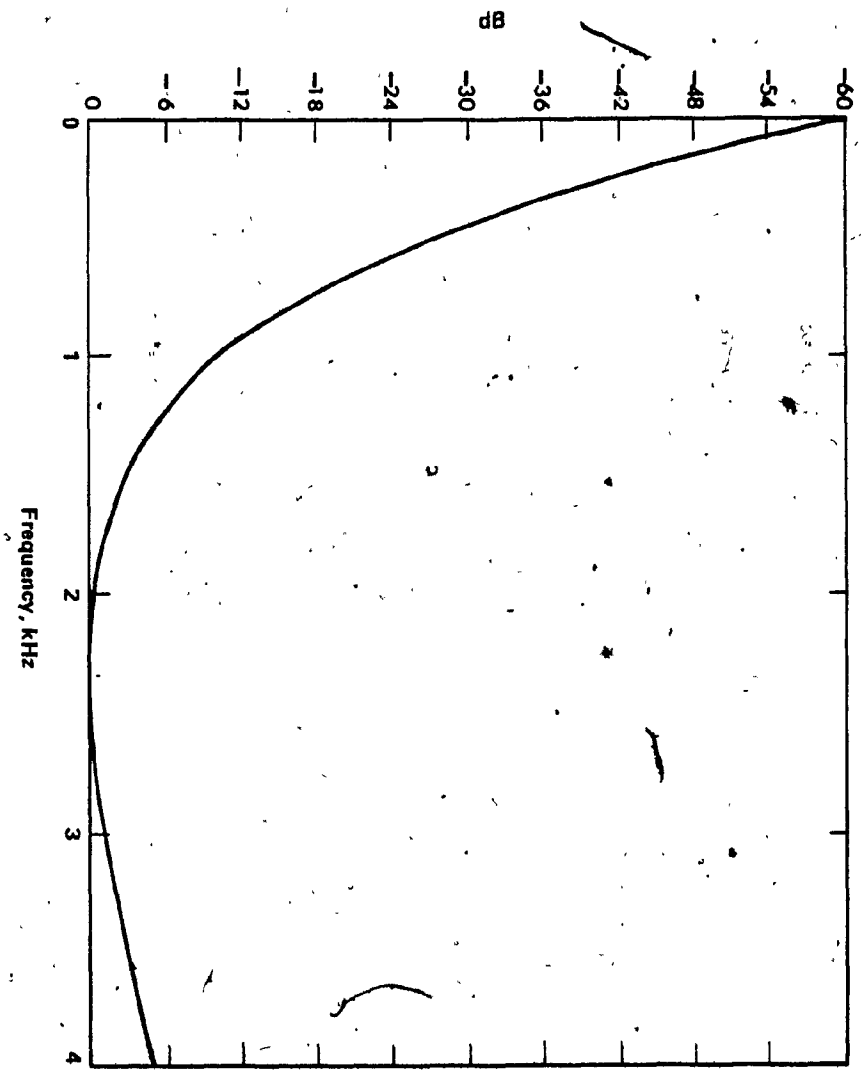

b) Passband Response

2.3.2 Non-Grounded Network

The nongrounded network is shown in Figure 2.8. This network is driven from a single input connected to its terminals as shown. The first section of this network consists only of one RC product as shown, while the second section is identical to that of the grounded configuration of Figure 2.5. By considering the first section acting as a voltage divider, then the output voltage, V_x, from this section is:

$$V_x = \frac{(1 - j\frac{\omega}{\omega_1})}{(1 + j\frac{\omega}{\omega_1})} (2V) \qquad (2\text{-}30)$$

where

$$\omega_1 = 1/R_1C_1$$

Following the same approach discussed for the case of grounded configuration, the two output signals, V_o and V_o', are:

$$V_o = \frac{(1 + s/\omega_1) + (s/\omega_2)(1 - s/\omega_1)}{(1 + s/\omega_1)(1 + s/\omega_2)} (2V) \quad , \qquad (2\text{-}31)$$

and

$$V_o' = \frac{(1 - s/\omega_1) - (s/\omega_2')(1 + s/\omega_1)}{(1 + s/\omega_1)(1 + s/\omega_2')} (2V) \qquad (2\text{-}32)$$

The two equations governing the passband, V_p, and the stopband, V_s, are obtained as:

$$V_p = \frac{1}{(1 + j\omega/\omega_1)} \left[\frac{(1 + j\omega/\omega_1) + (j\omega/\omega_2)(1 - j\omega/\omega_1)}{(1 + j\omega/\omega_2)} \right.$$

$$\left. + j \frac{(1 - j\omega/\omega_1) - (j\omega/\omega_2')(1 + j\omega/\omega_1)}{(1 + j\omega/\omega_2')} \right] (2V) \qquad (2\text{-}33)$$

and

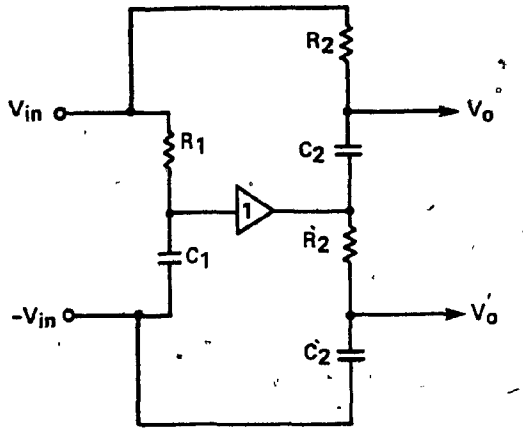

Figure 2.8 Sequence Discriminator Consisting of Two Sections In Cascade (Non–Grounded Network)

$$V_s = \frac{1}{(1 + j\omega/\omega)} \left[\frac{(1 + j\omega/\omega_1) + (j\omega/\omega_2)(1 - j\omega/\omega_1)}{(1 + j\omega/\omega_2)} \right.$$

$$\left. - j \frac{(1 - j\omega/\omega_1) - (j\omega/\omega_2')(1 + j\omega/\omega_1)}{(1 + j\omega/\omega_2')} \right] \quad (2V) \qquad (2\text{-}34)$$

The above expressions for both the passband, (2-33), and stopband (2-34), will be used in Appendix B to derive the sensitivity to the component variations for this network.

For nominal component values and in the ideal case where $\omega_i = \omega_i'$, the above expressions are simplified to:

$$V_p = (1 + j) \left[\frac{(1 + \omega/\omega_1)(1 + \omega/\omega_2)}{(1 + j\omega/\omega_1)(1 + j\omega/\omega_2)} \right] (2V), \qquad (2\text{-}35)$$

and

$$V_s = (1 - j) \left[\frac{(1 - \omega/\omega_1)(1 - \omega/\omega_2)}{(1 + j\omega/\omega_1)(1 + j\omega/\omega_2)} \right] (2V) \qquad (2\text{-}36)$$

The passband and stopband expressions as given by (2-35) and (2-36) are identical to those given by (2-24) and (2-25) except for the multiplication factor which represents the dc gain of the network. As can be seen from (2-35) the stopband is nulled at the positions of the two notch frequencies ω_1 and ω_2.

2.4 SENSITIVITY ANALYSIS

In this section, the magnitude and phase sensitivities of the grounded network* to component variations are derived for both the pass and stop bands. The sensitivity performance criteria to the variation, caused either by perturbation effects (such as temperature) or by the

---

* The sensitivity analysis of the non-grounded network is given in Appendix B.

variation in parameter tolerances, can be considered to be adequate measure for the success or failure of any practical design. In the analysis to follow we consider the variation in the network response caused by a small perturbation in component values in any section of the network which may cause an imbalance between the two resonant frequencies ω_i and ω_i' in such a section. For the sake of completeness, the magnitude and phase sensitivities of the actual output signals, V_o and V_o', from the two-section sequence discriminator are also analyzed using the circuit analysis program, MODNOD, [36].

Consider first the passband expression given in (2-20). Separating the effects of the variations of the individual components, assume first:

$$\omega_1' = \omega_1 \pm \Delta\omega_1 \tag{2-37}$$

and

$$\omega_2' = \omega_2 \tag{2-38}$$

Substituting (2-37) and (2-38) into (2-20) and for first degree approximation with some manipulation, then:

$$V_p' = \left[\frac{(1 + \omega/\omega_1)(1 + \omega/\omega_2)}{(1 + j\omega/\omega_1)(1 + j\omega/\omega_2)} \mp \frac{(\omega/\omega_1)(1 + \omega/\omega_2)}{(1 + j\omega/\omega_1)^2(1 + j\omega/\omega_2)} \frac{\Delta\omega_1}{\omega_1} \right] (V) \tag{2-39}$$

or

$$V_p' = V_p \mp \frac{(\omega/\omega_1)(1 + \omega/\omega_2)}{(1 + j\omega/\omega_1)^2(1 + j\omega/\omega_2)} \frac{\Delta\omega_1}{\omega_1} (V) \tag{2-40}$$

The relative variation in the passband $(\Delta V_p/V_p)$ due to variation of $\pm\Delta\omega_1$ in ω_1 is:

$$\Delta V_p/V_p = (V_p' - V_p)/V_p \qquad (2\text{-}41)$$

$$\Delta V_p/V_p = \mp \frac{\omega/\omega_1}{(1 + j\omega/\omega_1)\ (1 + \omega/\omega_1)} \quad \frac{\Delta\omega_1}{\omega_1} \qquad (2\text{-}42)$$

The sensitivity of the transfer function $T(j\omega)$ of a network to an element e in this network is defined as [29]:

$$S_e^{T(j\omega)} = \frac{d[\text{Ln } T(j\omega)]}{d[\text{Ln } e]} \qquad (2\text{-}43)$$

or

$$S_e^{T(j\omega)} = S_e^{\alpha(\omega)} + jS_e^{\phi(\omega)} \qquad (2\text{-}44)$$

where $\alpha(\omega)$ and $\phi(\omega)$ are the gain and phase functions of $T(j\omega)$, $S_x^{\alpha(\omega)}$ and $S_x^{\phi(\omega)}$ are the respective gain and phase sensitivities. From (2-35) the passband sensitivity is given by:

$$S_{\omega_1}^{V_p} = \mp \frac{\omega/\omega_1}{(1 + \omega/\omega_1)\ (1 + j\omega/\omega_1)} \qquad (2\text{-}45)$$

Separating (2-45) into its real and imaginary parts, then the gain and phase sensitivities of the passband to ω_1 are obtained, after dropping the signs, as:

$$S_{\omega_1}^{|V_p|} = \frac{(\omega/\omega_1)}{(1 + \omega/\omega_1)\ \{1 + (\omega/\omega_1)^2\}} \qquad (2\text{-}46)$$

and

$$S_{\omega_1}^{\phi_p} = \frac{(\omega/\omega_1)^2}{(1 + \omega/\omega_1)\ \{1 + (\omega/\omega_1)^2\}} \qquad (2\text{-}47)$$

The above analysis was considered for a small variation in the RC- products* of the first section with respect to one another while those of the second section are kept at their nominal values.

By considering the opposite situation where the RC-products in the second section are changed with respect to one another while those of the first section are kept at their nominal values, i.e.

$$\omega_1' = \omega_1 \quad , \tag{2-48}$$

and

$$\omega_2' = \omega_2 \pm \Delta\omega_2 \tag{2-49}$$

Following the same approach in driving the passband sensitivities to ω_1, then the gain and phase sensitivities to ω_2 are:

$$S_{\omega_2}^{|V_p|} = \frac{(\omega/\omega_2)\ (1 - \omega^2/\omega_1\omega_2)}{(1 + \omega/\omega_1)\ (1 + \omega/\omega_2)\cdot\{1 + (\omega/\omega_2)^2\}} \quad , \tag{2-50}$$

and

$$S_{\omega_2}^{\phi_p} = \frac{(\omega/\omega_2)\ (\omega/\omega_1 + \omega/\omega_2)}{(1 + \omega/\omega_1)\ (1 + \omega/\omega_2)\cdot\{1 + (\omega/\omega_2)^2\}} \quad . \tag{2-51}$$

Similar results for the stopband sensitivities to ω_1 and ω_2 can be obtained, by substituting (2-37), (2-38), (2-48) and (2-49) into (2-21), as:

---

* Since $\omega_i = 1/R_iC_i$ then $d\omega_i/\omega_i = dR_i/R_i$ and $d\omega_i/\omega_i = dC_i/C_i$ taking into account the variation in either R_i or C_i one at a time. $d\omega_i/\omega_i$ was given the value $\pm$ 5% which corresponds to $\mp$ 5% in dR_i/R_i or dC_i/C_i

$$S_{\omega_1}^{V_s} = \frac{\omega/\omega_1}{(1 - \omega/\omega_1)\ (1 + j\omega/\omega_1)} \qquad (2\text{-}52)$$

and

$$S_{\omega_2}^{V_s} = \frac{(\omega/\omega_2)\ (1 - j\omega/\omega_1)}{(1 - \omega/\omega_1)\ (1 - \omega/\omega_2)\ (1 + j\omega/\omega_2)} \qquad (2\text{-}53)$$

The gain and phase sensitivities to ω_1 and ω_2 are obtained from (2-52) and (2-53) as:

$$S_{\omega_1}^{|V_s|} = \frac{\omega/\omega_1}{(1 - \omega/\omega_1)\ \{1 + (\omega/\omega_1)^2\}}, \qquad (2\text{-}54)$$

$$S_{\omega_2}^{|V_s|} = \frac{(\omega/\omega_2)\ (1 - \omega^2/\omega_1\omega_2)}{(1 - \omega/\omega_1)\ (1 - \omega/\omega_2)\ \{1 + (\omega/\omega_2)^2\}}, \qquad (2\text{-}55)$$

$$S_{\omega_1}^{\phi_s} = \frac{(\omega/\omega_1)^2}{(1 - \omega/\omega_1)\ \{1 + (\omega/\omega_1)^2\}}, \qquad (2\text{-}56)$$

and

$$S_{\omega_2}^{\phi_s} = \frac{(\omega/\omega_2)\ (\omega/\omega_1 + \omega/\omega_2)}{(1 - \omega/\omega_1)\ (1 - \omega/\omega_2)\ \{1 + (\omega/\omega_2)^2\}} \qquad (2\text{-}57)$$

It can be seen from the above analysis that the sensitivities of the response to the RC-product mismatch is higher as we approach the last section. Figure 2.9 and Table 2.1 show the variation in the position of minimum attenuation as well as the variation in the position of the two notch frequencies as a result of $\pm 5\%$ mismatch in ω_i ($i = 1, 2$). The passband and stopband sensitivity curves are shown in Figure 2.10. The computer program of Appendix C together with the circuit analysis program, MODNOD, [36] are used to study the approximate and exact sensitivities of both the passband and stopband to the component variations. The curves obtained are superimposed on their corresponding approximate ones, and are shown in Figure 2.10 for comparison. MODNOD

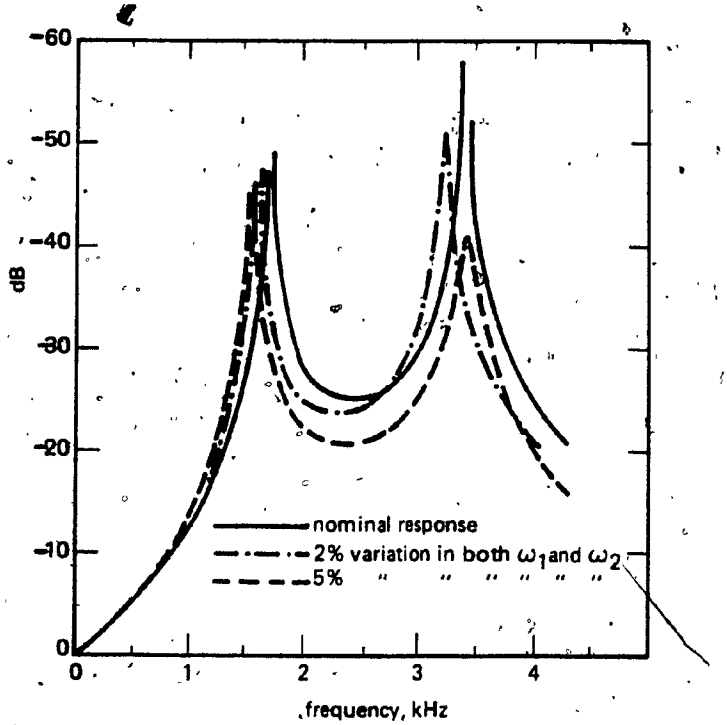

Figure 2.9 Variations of the Minimum Stopband Attenuation with ω_i (i = 1, 2) – Grounded Network

Table 2.1 (a) Variations in the Minimum Attenuation with the Variations in the RC – Products

Types of Networks	Nominal Values		−5% Var. in W_1		+5% Var. in W_1		−5% Var. in W_2		+5% Var. in W_2	
	Min. Atten. (dB)	Position (kHz)	Min. Atten. (dB)	Position (kHz)	Min. Atten. (dB)	Position (kHz)	Min. Atten. (dB)	Position (kHz)	Min. Atten. (dB)	Position (kHz)
Grounded Network*	25.0	2.25	23.7	2.19	26.1	2.31	26.1	2.19	23.7	2.31
Gr. with Positive F.B.	25.0	2.25	24.0	2.21	26.1	2.31	26.1	2.21	23.7	2.31
Gr. with Negative P.B.**	25.0	2.21	23.77	2.15	26.4	2.27	26.34	2.17	23.7	2.27
Non. Grounded Net.**	25.0	2.25	–	–	–	–	26.05	2.19	23.7	2.31
All Pass Network***	24.6	2.21	20.32	2.15	31.17	2.27				

* The Position of Minimum Attenuation Can be Determined as

$$P'_m = P_m \pm (N-2)$$

*** These Values are Due to 5% Variation in the RC – Products of the Path with Higher RC – Product

** The Minimum Stop Band Attenuation has Been Modified to that of the First Two Networks.

Table 2.1 (b) Variations of the Positions of the Notch Frequencies With the Variations in the RC–Products

Types of Network	First Notch			Second Notch		
	Original	−5%	+5%	Original	−5%	+5%
Grounded Network	1.59 kHz	1.51 kHz	1.67 kHz	3.19 kHz	3.03 kHz	3.35 kHz
Gr. with Positive F.B.	1.59	1.51	1.67	3.19	3.03	3.35
Gr. with Negative F.B.	1.59	1.51	1.67	3.19	3.03	3.35
Non. Grounded Network	1.59	–	–	3.19	3.03	3.35
All Pass *	1.55	1.37	1.79	3.13	3.37	2.87

1. The New Location of the First Notch Frequency is Determined by the Relation

$$P'_1 = P_1 \mp 2\,(N-1)$$

2. The New Location of the Second Notch Frequency is Determined by the Relation

$$P'_2 = P_2 \mp 4(N-1)$$

Where P_1 and P_2 are the Original Position of the Two Notches,

and N is the Percentage Variation.

* The Tabulated Values are for 5% Variation in the RC–Product of the Second Section

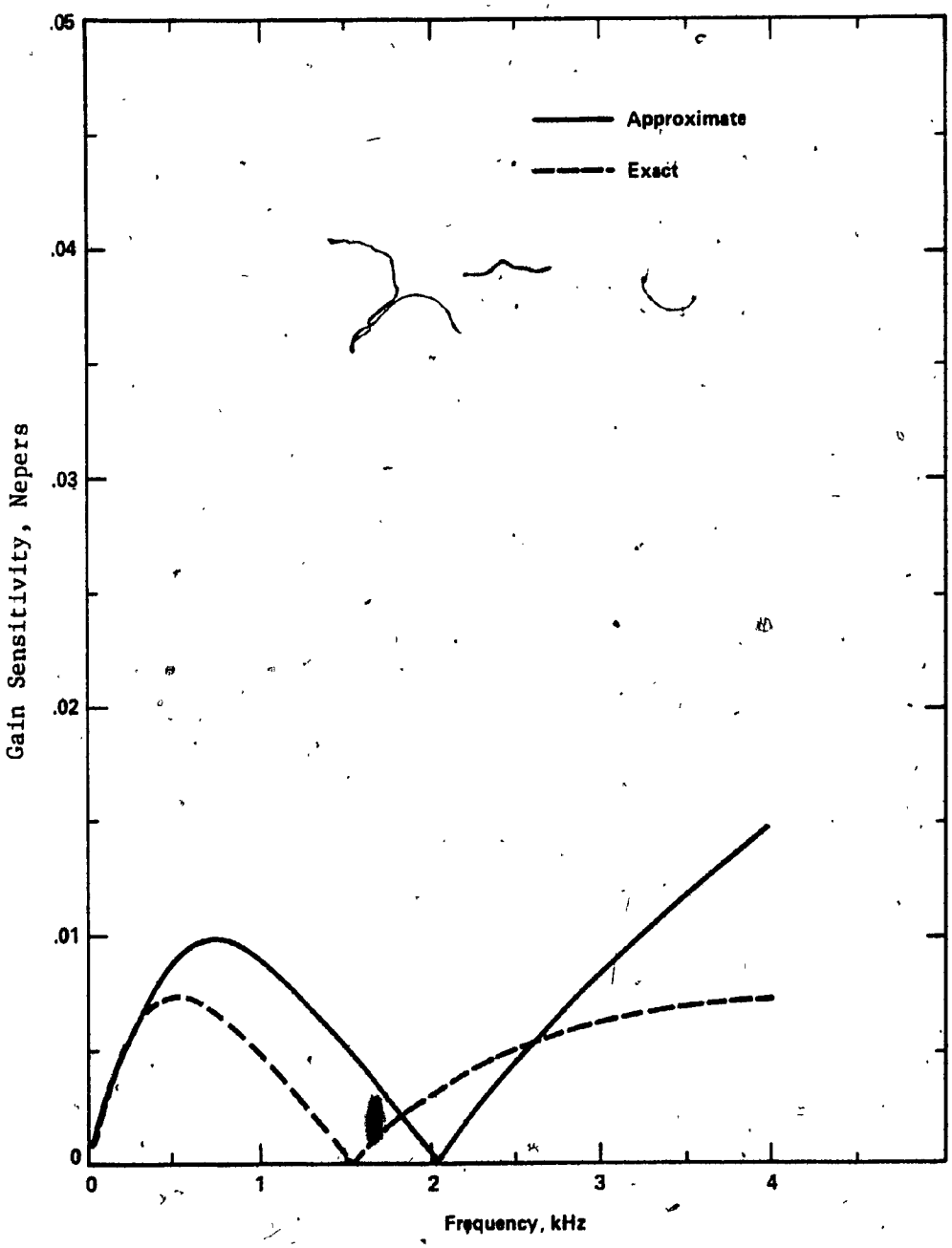

Figure 2.10(a) Passband Sensitivity to 5 % Variation in ω_1

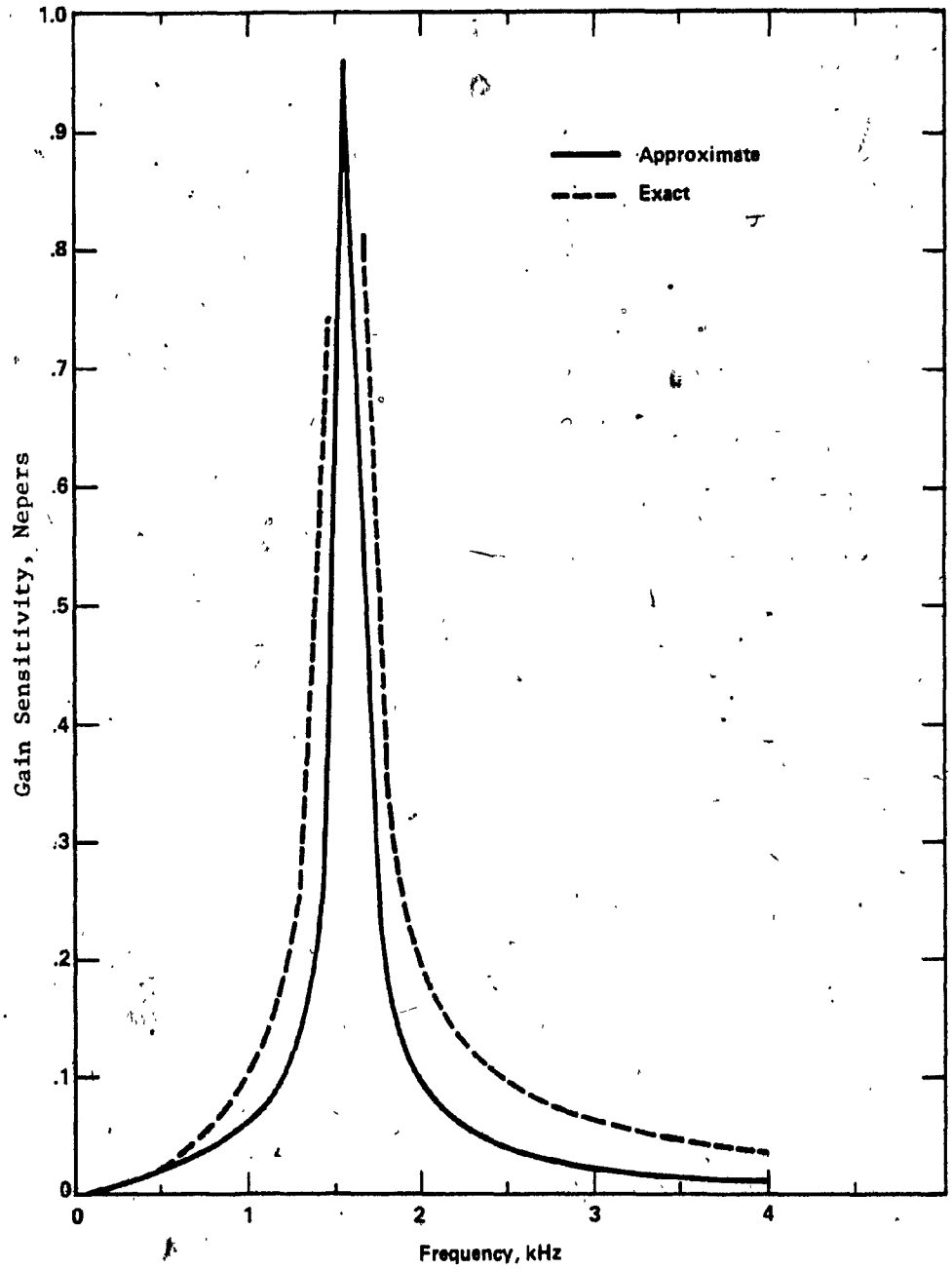

Figure 2.10(b) Stopband Sensitivity to 5 % Variation in ω_1

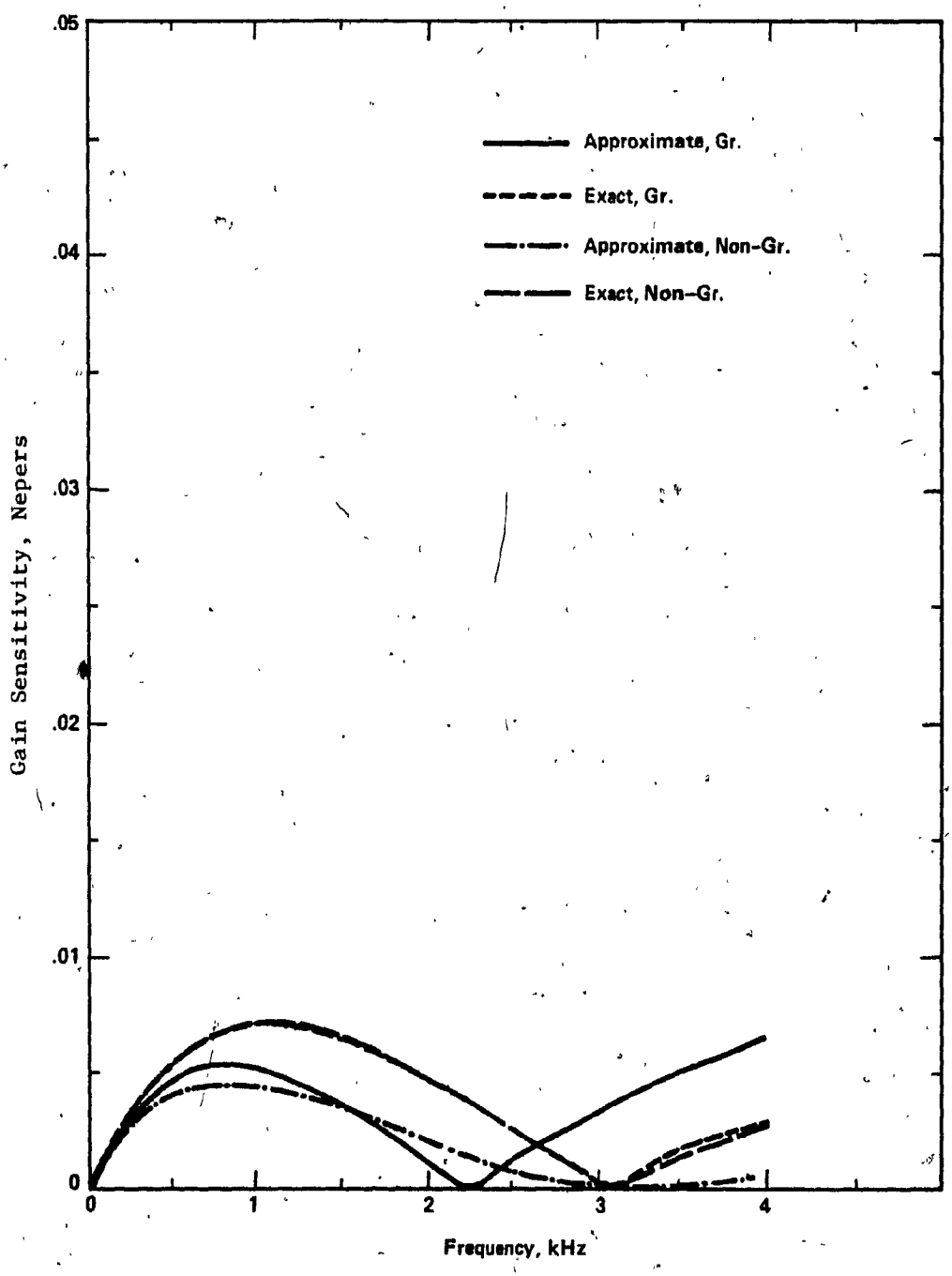

Figure 2.10(c) Passband Sensitivity to 5 % Variation in ω_2

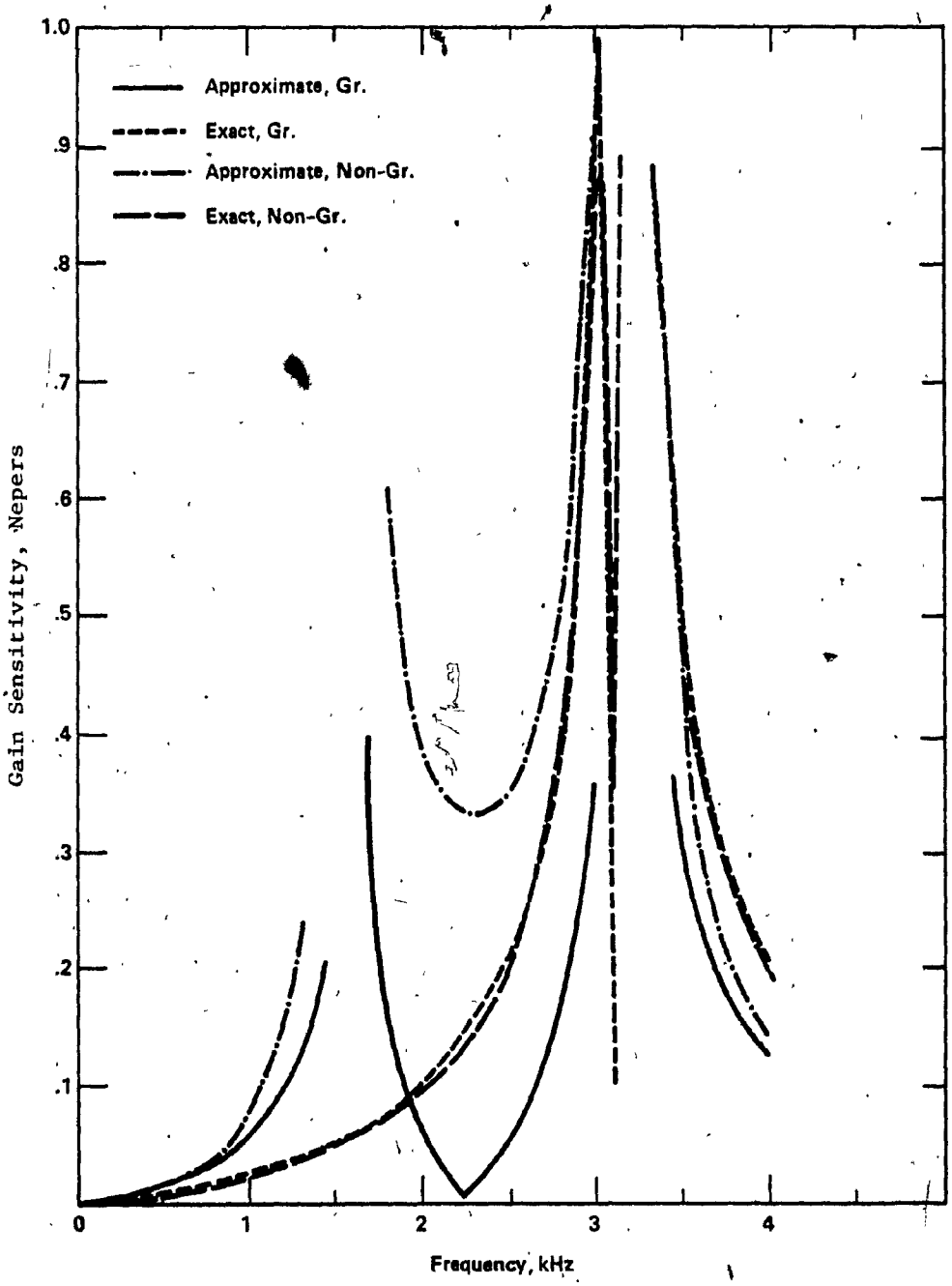

Figure 2.10(d) Stopband Sensitivity to 5% Variation in ω_2

was also used to study the network performance to the variation in component tolerances. The gain and phase sensitivities of the actual output voltages V_o and V_o', as defined in (2-16) and (2-17), to the component variations in either section, are shown in Figure 2.11.

2.5 EXPERIMENTAL RESULTS

The sequence discriminator consisting of 2 sections in cascade is built using discrete resistors and capacitors (with tolerance < 10%) as passive components and the Fairchild μA 741 operational amplifiers as the active devices. The minimax algorithm [38], is used to calculate the values of the resistors and capacitors. These values are chosen such that the RC-product in each section is set to a previously specified value (i.e. additional constraints in the minimax algorithms). The bandwidth of the realization is determined by the difference between the RC-products in the individual sections ($BW = \omega_2 - \omega_1$). The operational amplifiers are used either as buffers between the cascaded sections or as inverters.

The applied input signal is swept over the voice frequency range (4 KHz) and the two output signals V_o and V_o' are measured. It is found that the two output signals are in phase quadrature over the specified bandwidth, and the magnitudes differ depending upon the operating frequency. At the positions of the resonant frequencies the two output signals, V_o and V_o', are identically equal in magnitude, but 90-degrees apart in phase, as shown in Figure 2.12.

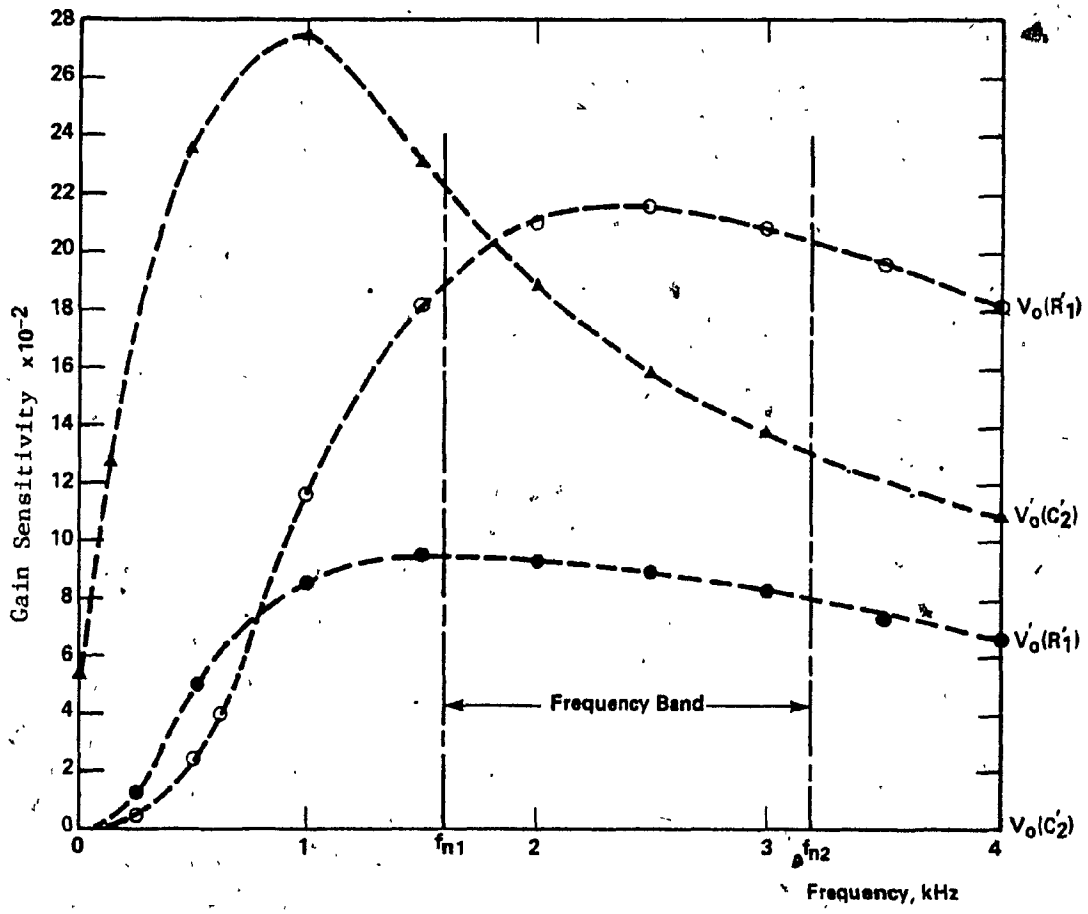

Figure 2.11 (a) V_o and V'_o Sensitivities to 5% Variation in R'_1 and C'_2 Independently

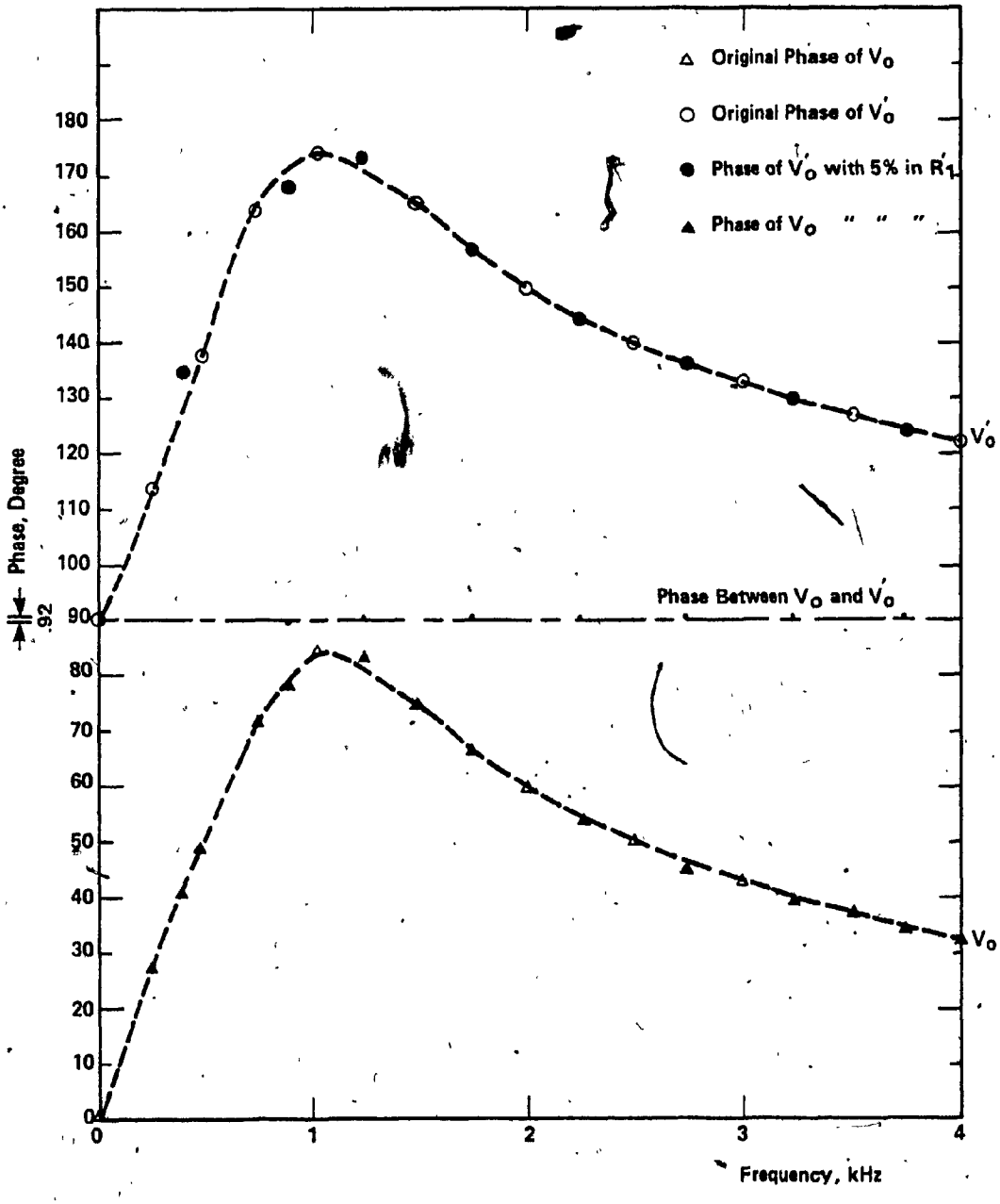

Figure 2.11 (b) Phase Response of the Two Cascaded Sections

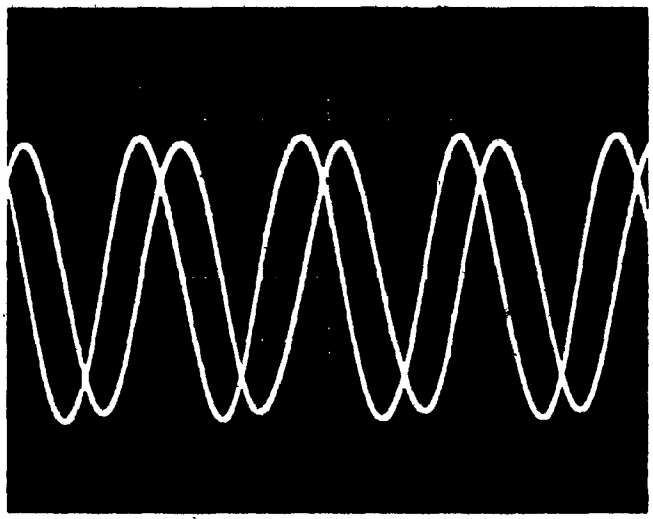

Figure 2.12 The Two Output Waveforms (Vertical Scale, 2 Volts/Division — Horizontal Scale, 0.1 m. Sec/Division)

One of the main reasons for designing such networks is for generation and detection of single-sideband signals. As will be shown in Chapter 5, to generate a single-sideband signal we should have four modulated signals that are 90 degrees apart, in phase with respect to one another. Hence, the two signals V_o and V_o' from the sequence discriminator are inverted, using operational amplifiers in the inverting mode, to generate four signals (V_o, V_o', $-V_o$, $-V_o'$) that are in phase quadrature to one another. Four symmetrical pulse trains are also generated with a clock rate T_c seconds, using CMOS switch and a simple RC network with D-type flip-flop as shown in Figure 5.1. The carrier frequency $f_c (f_c = 1/T_c)$ considered is 64 KHz.

The modulation process was performed in the same way as described in Chapter 5, where each of the four output signals from the sequence discriminator is multiplied by its corresponding pulse modulated signal using CMOS switch as multiplier. Finally, the four modulated output signals, from the multiplier, are summed to produce single-sideband signal.

Either upper side-band (USB) or lower-sideband (LSB) can be produced by simply interchanging any two signals that are in anti-phase (180° apart). Figure 2.13 shows the frequency response of the sequence discriminator of the two section sequence discriminator shown in Figure 2.5.

Minimum stopband rejection of 25 dB has been achieved, while a .04 dB ripple has been obtained in the passband.

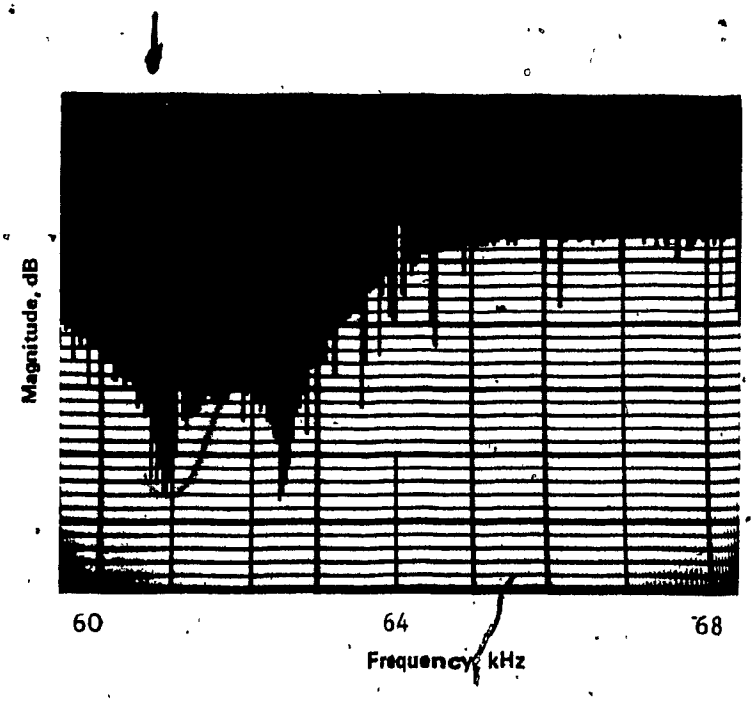

Figure 2.13 Frequency Response of the Active Sequence Discriminator (Vertical Sensitivity 10 dB/D)

2.6 CONCLUSIONS

Two general configurations, i.e. grounded structure and non-grounded structure, are given together with the analysis for the passband and stopband performances. It is shown that both structures perform identically inspite of the variation in the layout of the first section. A careful study of these active networks reveals the following attractive features:

1) Simple structure using only R's, C's and OA's.

2) The cascaded technique is attractive for most post design adjustments as each section is isolated from the other.

3) Tuning can simply be done by varying the RC product in each section separately (i.e. by trimming R's only).

4) LSB or USB can be generated by interchanging any two signals that are out of phase by 180°.

5) Low sensitivity to component variations.

As it was pointed out in Chapter 1, integrated technology offers many attractive advantages to the circuit manufacturers. One is the reduction in cost if these circuits are manufactured in large quantities. This may not be true in some applications where specific transmission characteristics are needed. This problem can be solved by using several

small numbers of universal second order sections in cascade. By using a combination of two or more of these sections the desired transmission characteristics may be obtained. In the next chapter an additional attractive feature is added using the feedback approach.

CHAPTER III

FEEDBACK IMPLEMENTATION IN THE DESIGN OF ACTIVE RC PHASE SPLITTING NETWORKS

3.1 INTRODUCTION

The main objective of this chapter is to introduce a new set of active phase splitting networks with feedback. It was shown in the previous chapter that the poles of the sequence discriminator discussed there are real and on the negative real axis of the S-plane. It is well known that the generation of complex conjugate poles can be achieved by a combination of passive RC networks with active devices and this in turn leads to the feedback configuration [35]. It will be shown that by applying feedback between the input and output terminals of the network of Figure 2.5 and by a proper choice of the feedback path, both the gain and phase sensitivities to component variations are improved and better performance is achieved.

The general principle of analysis outlined in the previous chapter can be extended to this set of networks too. It is important to distinguish two kinds of networks with feedback:

1) Active design with positive feedback.
2) Active design with negative feedback.

Both types of networks will be considered here in detail. For the sake of completeness the all-pass realization approach [8,9] is also given and compared with the proposed ones.

3.2 ACTIVE DESIGN WITH POSITIVE FEEDBACK

A straight forward approach for estimating both the passband and stopband responses is outlined in this section. The network is shown in Figure 3.1, with $\beta = 1$ in the feedback path. This network is driven from a single input connected to its terminals as shown. If the input signals $\pm 2V$ are applied to the network and the resultant output signals, denoted by V_o and V_o', are fed back as indicated, then the actual applied signals to the input terminals of the first section are:

$$V_1 = 2V + V_o \quad , \tag{3-1}$$

$$V_2 = -2V - V_o \quad , \tag{3-2}$$

and

$$V_G = V_o' \quad . \tag{3-3}$$

where point G was originally grounded, but with the feedback its potential has been raised to V_o'.

The main idea behind feedback is that a sequence is constructed from the two output signals, which more closely resemble an ideal wanted sequence, and is fed back to the input terminals.

Consider the network shown in Figure 3.1, with the input signals of the first section given by (3-1), (3-2) and (3-3). The two output signals from the first section are obtained as:

$$V_x = \frac{[2V + V_o + (j\omega/\omega_1)V_o']}{(1 + j\omega/\omega_1)} \tag{3-4}$$

and

$$V_y = \frac{[V_o' - (j\omega/\omega_1')(2V + V_o)]}{(1 + j\omega/\omega_1')} \tag{3-5}$$

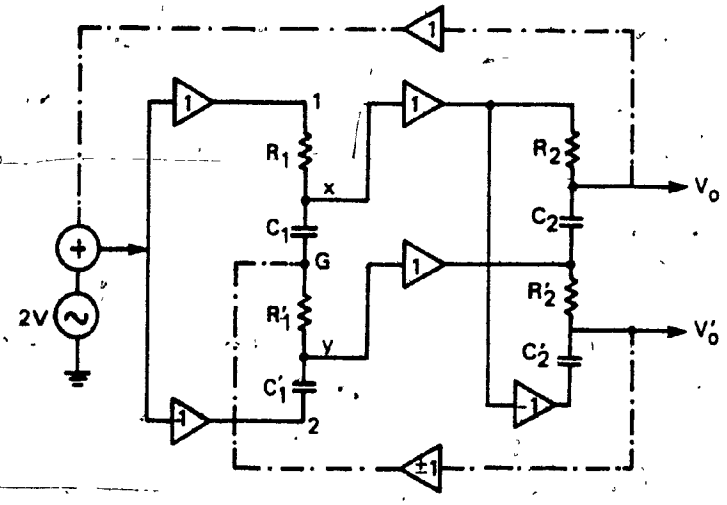

Figure 3.1 Two–stage Sequence Discriminator (broken lines indicate the feedback path between input and output)

where $\omega_1 = 1/R_1C_1$ and $\omega_1' = 1/R_1'C_1'$ are the RC product of the components in the first section.

Now, V_x and V_y together with $(-V_x)$ are applied to the input terminals of the second section to produce the overall ouput signals. The two output signals V_o and V_o' from the two cascaded sections are:

$$V_o = \frac{2V}{D}\left[\left(\frac{1}{1+\zeta_1} - \frac{\zeta_1'\zeta_2}{1+\zeta_1'}\right)\left\{(1+\zeta_2') - \frac{1}{1+\zeta_1'} + \frac{\zeta_1\zeta_2'}{1+\zeta_1}\right\}\right.$$

$$\left. - \left(\frac{\zeta_1'}{1+\zeta_1'} + \frac{\zeta_2'}{1+\zeta_1}\right)\left(\frac{\zeta_1}{1+\zeta_1} + \frac{\zeta_2}{1+\zeta_1'}\right)\right], \qquad (3\text{-}6)$$

and

$$V_o' = \frac{-2V}{D}\left[\left(\frac{\zeta_1}{1+\zeta_1} - \frac{\zeta_1'\zeta_2}{1+\zeta_1'}\right)\left(\frac{\zeta_1'}{1+\zeta_1'} + \frac{\zeta_2'}{1+\zeta_1}\right)\right.$$

$$\left. + \left(\frac{\zeta_1'}{1+\zeta_1'} + \frac{\zeta_2'}{1+\zeta_1}\right)\left\{(1+\zeta_2) - \frac{1}{1+\zeta_1} + \frac{\zeta_1'\zeta_2}{1+\zeta_1'}\right\}\right] \qquad (3\text{-}7)$$

where

$$D = \left[\left\{(1+\zeta_2) - \frac{1}{1+\zeta_1} + \frac{\zeta_1'\zeta_2}{1+\zeta_1'}\right\}\left\{(1+\zeta_2') - \frac{1}{1+\zeta_1'} \quad \frac{\zeta_1\zeta_2'}{1+\zeta_1}\right\}\right.$$

$$\left. + \left(\frac{\zeta_1'}{1+\zeta_1'} + \frac{\zeta_2'}{1+\zeta_1}\right)\left(\frac{\zeta_1}{1+\zeta_1} + \frac{\zeta_2}{1+\zeta_1'}\right)\right] \qquad (3\text{-}8)$$

$$\zeta_i = \omega/\omega_i \quad , \quad \zeta_i' = \omega/\omega_i$$

The general expressions for the two ouput signals V_o and V_o', as given by (3-6) and (3-7), were derived considering $\omega_i \neq \omega_i'$ $(i = 1, 2)$. The expressions will be used in later section to derive the network response sensitivity to component variations.

As it will be seen in Chapter 5, the quadrature modulation process results in rotating V_o by $\pi/2(-\pi/2)$ with respect to V_o' and summing them to produce the passband (stopband). Thus the passband and stopband expressions are given by:

$$V_p = \tfrac{1}{2}\{V_o + jV_o'\}, \tag{3-9}$$

and

$$V_s = \tfrac{1}{2}\{V_o - jV_o'\} \tag{3-10}$$

From (3-6) and (3-7) the explicit expressions for the passband, V_p, and the stopband, V_s, are:

$$V_p = \frac{V}{D}\left[\left(\frac{1}{1+\zeta_1} - \frac{\zeta_1'\zeta_2}{1+\zeta_1'}\right)\left\{\left\{(1+\zeta_2') - \frac{1}{1+\zeta_1'} + \frac{\zeta_1\zeta_2'}{1+\zeta_1}\right\}\right.\right.$$
$$\left. -j\left(\frac{\zeta_1'}{1+\zeta_1'} + \frac{\zeta_2'}{1+\zeta_1}\right)\right\} - \left(\frac{\zeta_1'}{1+\zeta_1'} + \frac{\zeta_2'}{1+\zeta_1}\right)\left\{\left(\frac{\zeta_1}{1+\zeta_1} + \frac{\zeta_2}{1+\zeta_1'}\right)\right.$$
$$\left.\left. + j\left\{(1+\zeta_2) - \frac{1}{1+\zeta_1} + \frac{\zeta_1'\zeta_2}{1+\zeta_1'}\right\}\right] \tag{3-11}$$

$$V_s = \frac{V}{D}\left[\left(\frac{1}{1+\zeta_1} - \frac{\zeta_1'\zeta_2}{1+\zeta_1'}\right)\left\{\left\{(1+\zeta_2') - \frac{1}{1+\zeta_1'} + \frac{\zeta_1\zeta_2'}{1+\zeta_1}\right\}\right.\right.$$
$$\left. + j\left(\frac{\zeta_1'}{1+\zeta_1'} + \frac{\zeta_2'}{1+\zeta_1}\right) - \left(\frac{\zeta_1'}{1+\zeta_1'} + \frac{\zeta_2'}{1+\zeta_1}\right)\right.$$
$$\left.\left.\left\{\left(\frac{\zeta_1}{1+\zeta_1} + \frac{\zeta_2}{1+\zeta_1'}\right) - j\left\{(1+\zeta_2) - \frac{1}{1+\zeta_1} + \frac{\zeta_1'\zeta_2}{1+\zeta_1'}\right)\right\}\right\}\right] \tag{3-12}$$

where D, ζ_1, ζ_1' are defined in (3-8).

Equations (3-11) and (3-12) give the general expressions for both the passband and stopband. These expressions will also be used to derive the

passband and stopband sensitivities to component variations. For nominal component values and in the ideal case where $\omega_i = \omega_i$, the passband and stopband expressions are simplified to:

$$V_{pp} = \frac{V}{D_p}\left[(1 + \omega/\omega_1)(1 + \omega/\omega_2)\{2s^2/\omega_1\omega_2 + (s/\omega_1 + s/\omega_2)(1 - j)\}\right] ,$$

and (3-13)

$$V_{sp} = \frac{V}{D_p}\left[(1 - \omega/\omega_1)(1 - \omega/\omega_2)\{2s^2/\omega_1\omega_2 + (s/\omega_1 + s/\omega_2)(1 + j)\}\right]$$

where (3-14)

$$D_p = (2s^2/\omega_1\omega_2)^2 + (4s^2/\omega_1\omega_2)(s/\omega_1 + s/\omega_2) + 2(s/\omega_1 + s/\omega_2)^2$$

(3-15)

The frequency response is shown in Figure 3.2. It can be seen that the network transmits one type of sequence and attenuates the other over the specified bandwidth. The attenuated signal has nulls at frequencies which are determined by the RC product in each section.

3.3 SENSITIVITY ANALYSIS

The fact that any small perturbation in the component values in any section will cause imbalance between the two resonant frequencies ω_i and ω'_i in such a section. Accordingly, the variation in the network response (equations (3-11) and (3-12)) has to be taken into account and this in turn leads to study the sensitivity of this response to any variation in the component tolerances. Starting first by driving the passband and stopband sensitivities to the variation in the RC product of the first section with that of the second section is kept at its nominal values.

$$\omega'_1 = \omega_1 \pm \Delta\omega_1 \qquad (3\text{-}16)$$

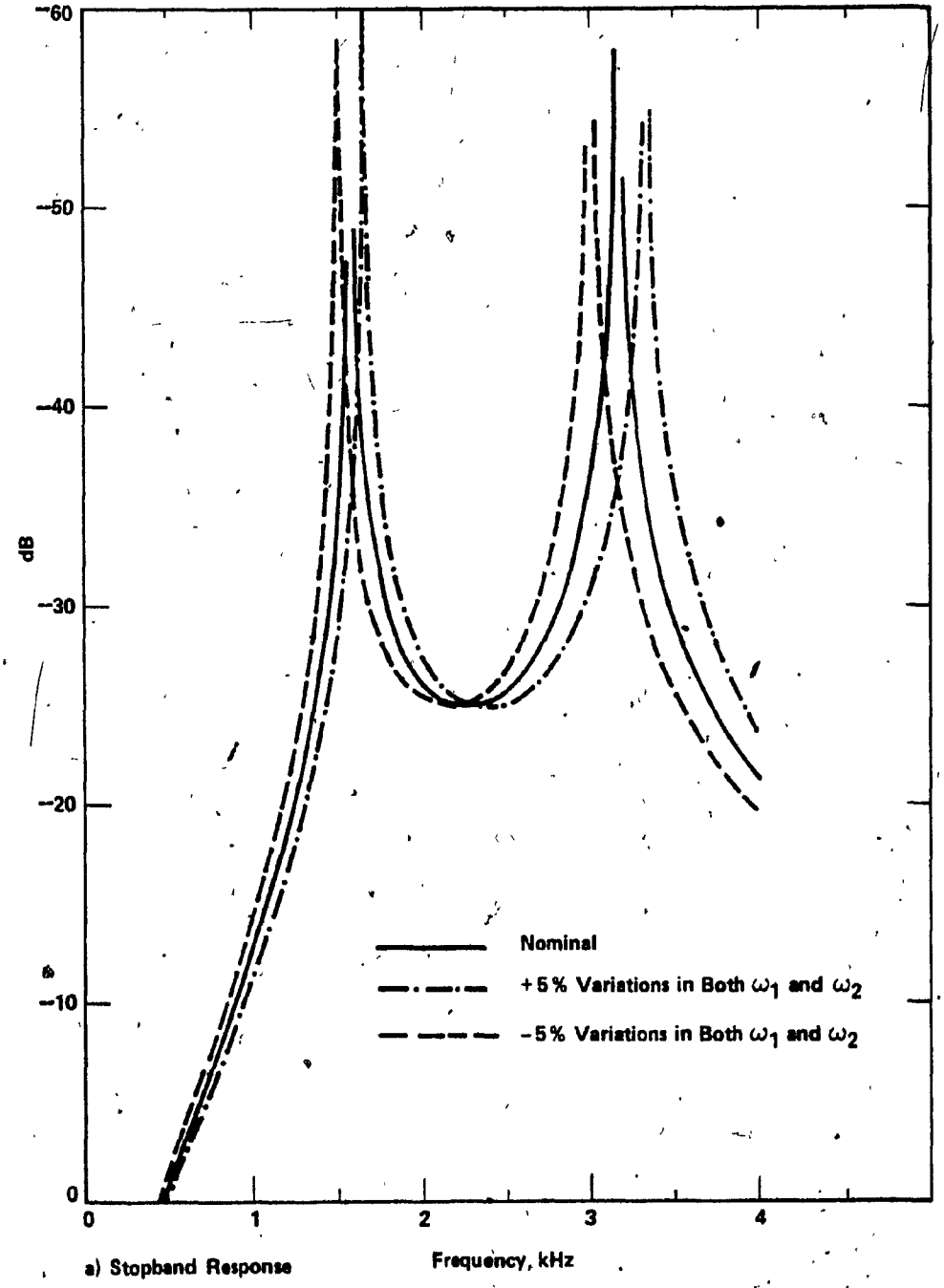

a) Stopband Response

Figure 3.2 Frequency Response of the Positive Feedback Network – ADP

a) Stopband Response

b) Passband Response

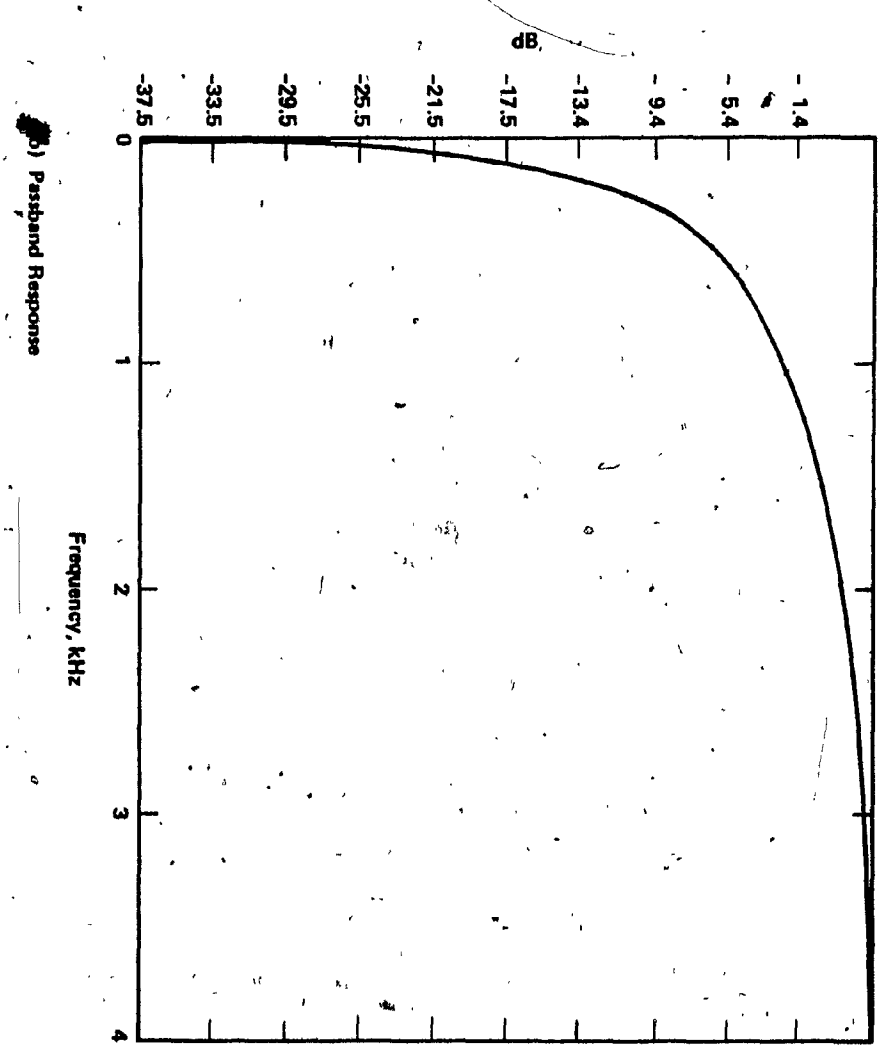

(b) Passband Response

and

$$\omega_2' = \omega_2 \tag{3-17}$$

Substituting (3-16) and (3-17) into (3-11) and (3-12) respectively, then for first degree approximation with some simple manipulation, the passband and stopband sensitivities to ω_1 are:

$$S^{V_{pp}}_{\omega_1} = \frac{(\omega/\omega_1)\ (1 + j\omega/\omega_2)}{(1 + \omega/\omega_1) \cdot D_{p_1}} \tag{3-18}$$

and

$$S^{V_{sp}}_{\omega_1} = \frac{(\omega/\omega_1)\ (1 + j\omega/\omega_2)}{(1 - \omega/\omega_1) \cdot D_{p_1}} \tag{3-19}$$

where

$$D_{p_1} = [(-2\omega^2/\omega_1\omega_2) + j2\omega(1/\omega_1 + 1/\omega_2) + \omega_1\omega_2\ (1/\omega_1 + 1/\omega_2)^2] \tag{3-20}$$

The gain and phase sensitivities to ω_1 can be obtained from (3-18) and (3-19) by separating them to their real and imaginary parts:

$$S^{|V_{pp}|}_{\omega_1} = \frac{(\omega/\omega_1)\ \{2(\omega/\omega_2)^2 + \omega_1\omega_2\ (1/\omega_1 + 1/\omega_2)^2\}}{(1 + \omega/\omega_1)[(2\omega^2/\omega_1\omega_2)^2 + \{\omega_1\omega_2(1/\omega_1 + 1/\omega_2)^2\}^2]} \tag{3-21}$$

$$S^{\phi_{pp}}_{\omega_1} = \frac{(\omega/\omega_1)[(\omega/\omega_2)\ (\omega_1/\omega_2) - (\omega/\omega_1)\ \{1 + 2(\omega/\omega_2)^2\}]}{(1 + \omega/\omega_1)[(2\omega^2/\omega_1\omega_2)^2 + \{\omega_1\omega_2(1/\omega_1 + 1/\omega_2)^2\}^2]} \tag{3-22}$$

$$S^{|V_{sp}|}_{\omega_1} = \frac{(\omega/\omega_1)\ \{2(\omega/\omega_2)^2 + \omega_1\omega_2(1/\omega_1 + 1/\omega_2)\}}{(1 - \omega/\omega_1)\ [(2\omega^2/\omega_1\omega_2)^2 + \{\omega_1\omega_2(1/\omega_1 + 1/\omega_2)^2\}^2]} \tag{3-23}$$

$$S^{\phi_{sp}}_{\omega_1} = \frac{(\omega/\omega_1)[(\omega/\omega_2)\ (\omega_1/\omega_2) - (\omega/\omega_1)\{1 + 2(\omega/\omega_2)^2\}]}{(1 - \omega/\omega_1)\ (2\omega^2/\omega_1\omega_2)^2 + \{\omega_1\omega_2(1/\omega_1 + 1/\omega_2)^2\}^2]} \tag{3-24}$$

The sensitivity curves are shown in Figures (3.3) and (3.4) respectively. Of more interest for this type of this study is the network response

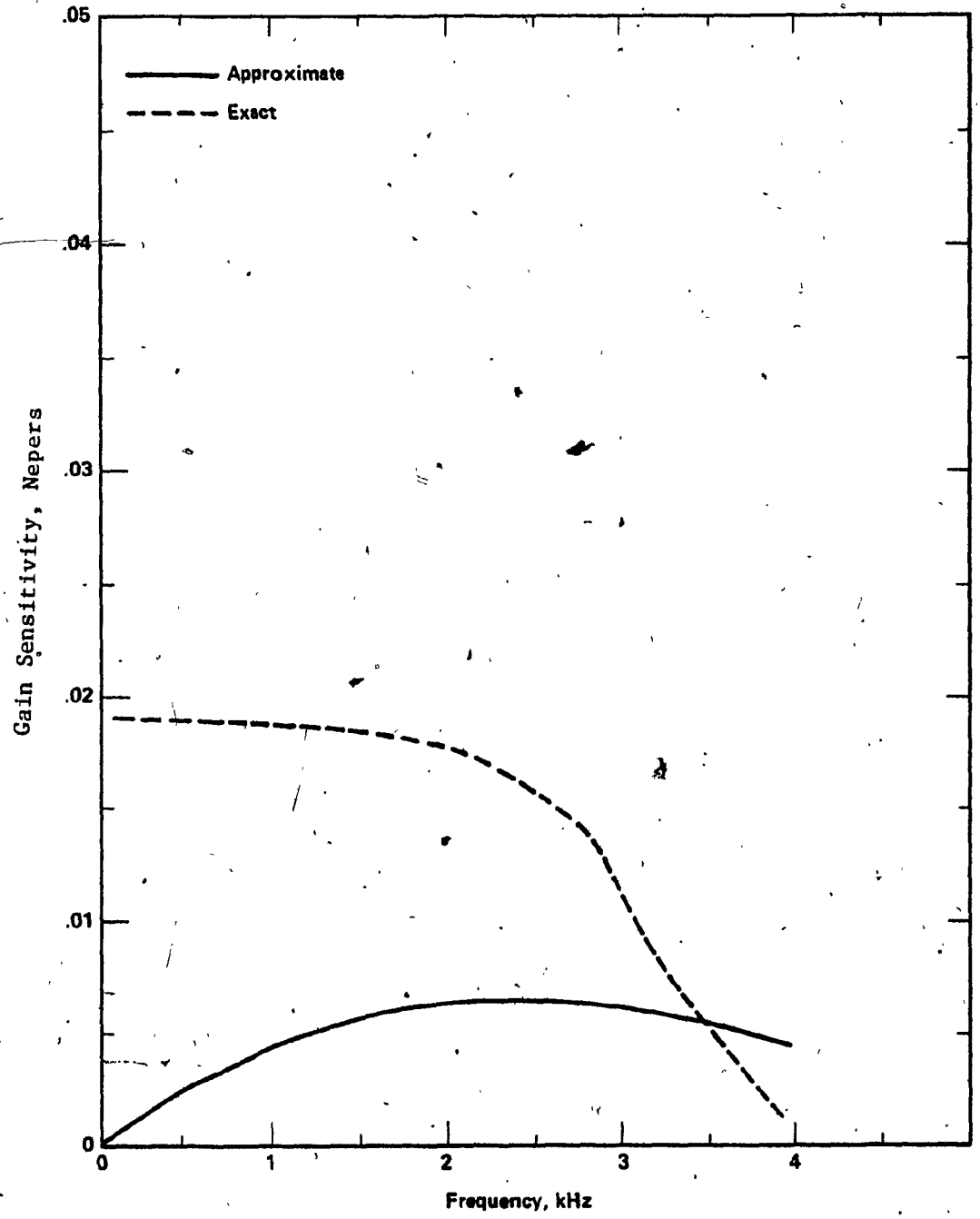

Figure 3.3 Passband Sensitivity of the ADP to 5% Variation in ω_1.

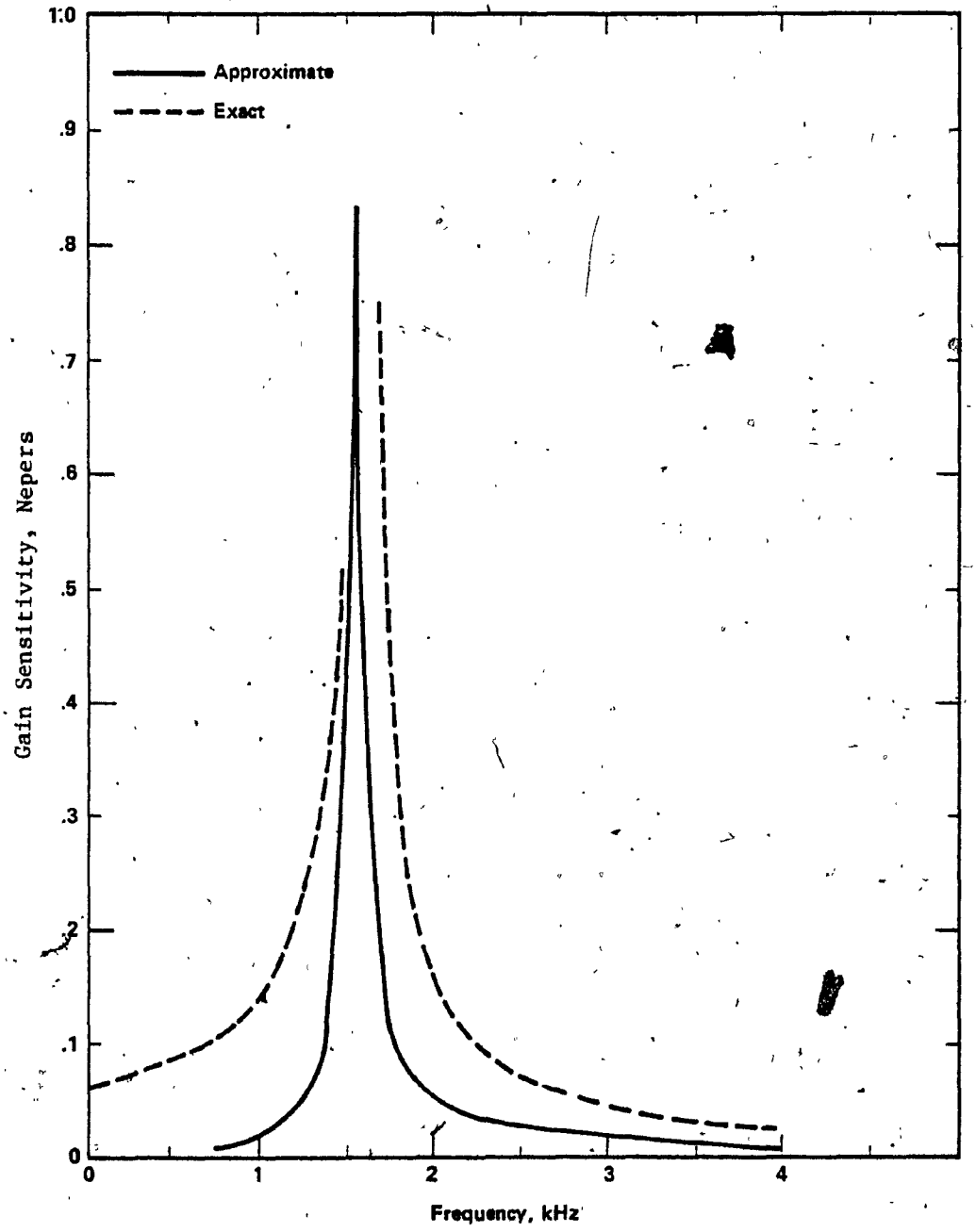

Figure 3.4 Stopband Sensitivity of the ADP to 5 % Variation in ω_1

sensitivity to the variation in the RC product in the second (last) section. In this case let us assume that;

$$\omega_1' = \omega_1 \qquad (3\text{-}25)$$

and

$$\omega_2' = \omega_2 \pm \Delta\omega_2 \qquad (3\text{-}26)$$

Substituting (3-25) and (3-26) into (3-11) and (3-12) respectively, then the sensitivities of both passband and stopband to ω_2 are:

$$S_{\omega_2}^{V_{pp}} = \frac{(\omega/\omega_1)\ (1 + j\omega/\omega_1)\ (1 + j\omega/\omega_2)}{(1 + \omega/\omega_1)\ (1 + \omega/\omega_2)\ .\ D_{P_1}} \qquad (3\text{-}27)$$

and

$$S_{\omega_2}^{V_{sp}} = \frac{(\omega/\omega_1)\ (1 + j\omega/\omega_1)\ (1 + j\omega/\omega_2)}{(1 - \omega/\omega_1)\ (1 - \omega/\omega_2)\ .\ D_{P_1}} \qquad (3\text{-}28)$$

Similar to the gain and phase sensitivities to ω_1, the sensitivities of both the gain and the phase to ω_2 can be obtained from (3-27) and (3-28) by separating the real and imaginary parts of each expression. The sensitivity curves are shown in Figures (3.5) and (3.6) respectively.

It is to be noted that the sensitivity expressions (3-18), (3-19), (3-27) and (3-28) were derived for first degree of approximation. Exact sensitivity studies were done using the circuit analysis program, MODNOD. For comparison the exact sensitivity curve for each particular case is superimposed on the corresponding sensitivity curve obtained by the first order approximation.

3.4 ACTIVE DESIGN WITH NEGATIVE FEEDBACK

The network with negative feedback path between the input and the output terminals is also shown in Figure 3.1 with $\beta = -1$ in the feedback

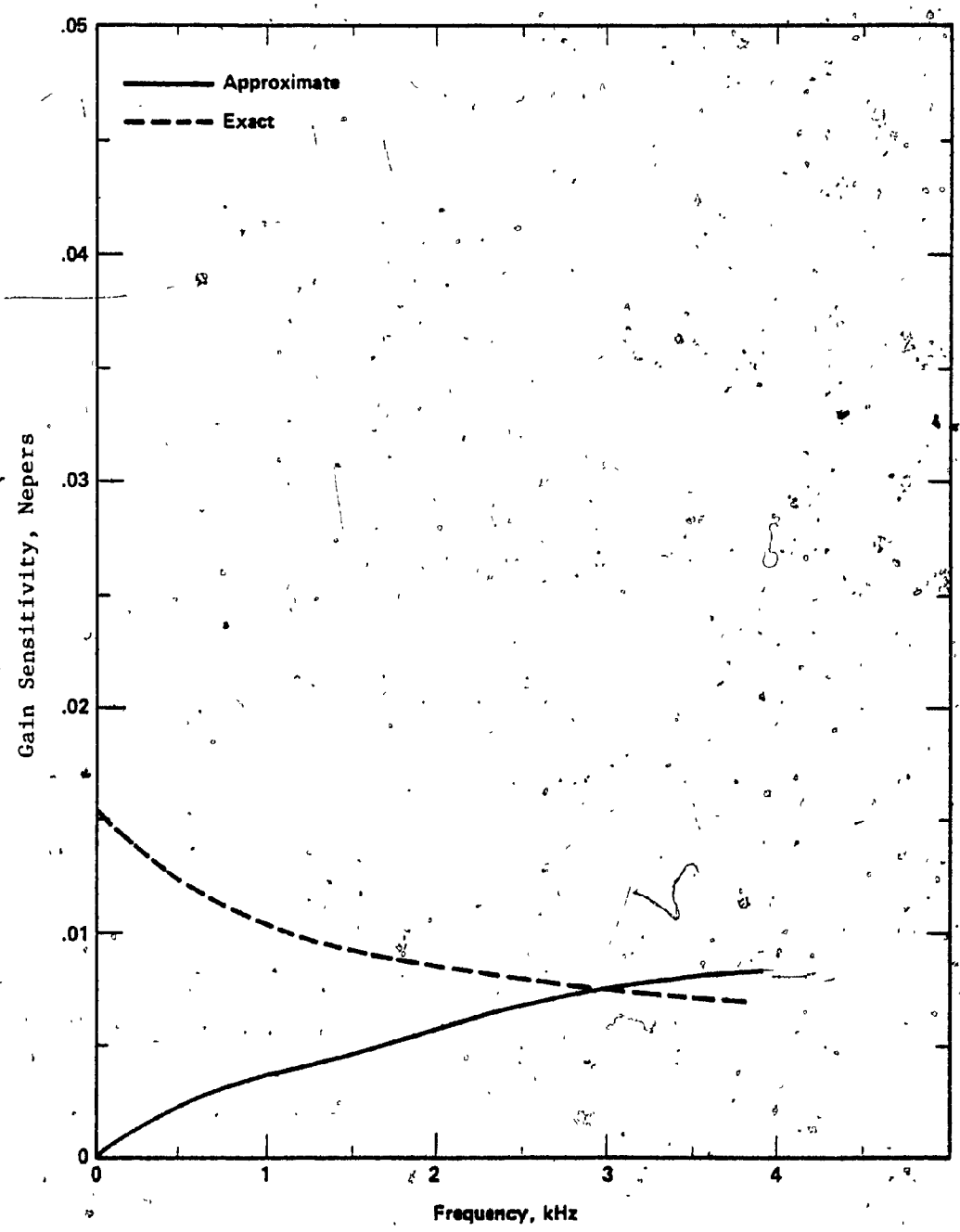

Figure 3.5 Passband Sensitivity of the ADP to 5% Variation in ω_2

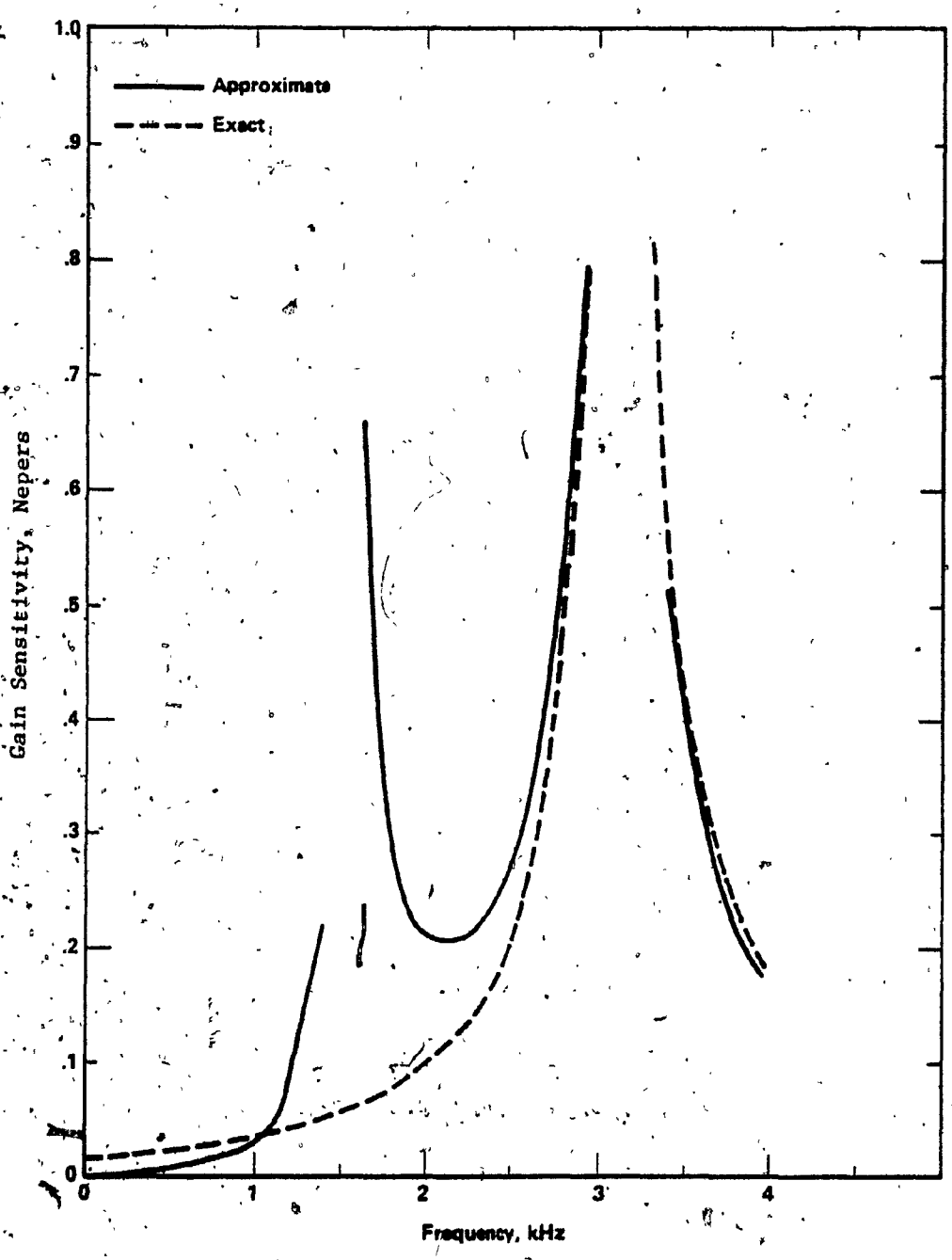

Figure 3.6 Stopband Sensitivity of the ADP to 5 % Variation in ω_2

path between V_o' and point G. In this case the applied input signals to the first section are:

$$V_1 = 2V + V_o \quad , \tag{3-29}$$

$$V_2 = -2V - V_o \quad , \tag{3-30}$$

and

$$V_G = -V_o' \tag{3-31}$$

As previously mentioned in section 3.2, the two voltages V_1 and V_2 are applied to terminals 1 and 2 respectively. The previously grounded point G is raised to the voltage V_G. Following the same procedure as in the positive feedback case, the derived expressions for the two output signals V_o and V_o' are given by:

$$V_o = \frac{V}{D_n}\left[\left(\frac{1}{1+\zeta_1} - \frac{\zeta_1'\zeta_2}{1+\zeta_1'}\right)\left\{(1+\zeta_2) + \frac{1}{1+\zeta_1'} - \frac{\zeta_1\zeta_2'}{1+\zeta_1}\right\}\right.$$

$$\left. + \left(\frac{\zeta_1'}{1+\zeta_1'} + \frac{\zeta_2'}{1+\zeta_1}\right)\left(\frac{\zeta_1}{1+\zeta_1} + \frac{\zeta_2}{1+\zeta_1'}\right)\right] \quad , \tag{3-32}$$

and

$$V_o' = \frac{V}{D_n}\left[\left(\frac{1}{1+\zeta_1} - \frac{\zeta_1'\zeta_2}{1+\zeta_1'}\right)\left(\frac{\zeta_1'}{1+\zeta_1'} + \frac{\zeta_2'}{1+\zeta_1}\right) + \left(\frac{\zeta_1'}{1+\zeta_1'} + \frac{\zeta_2'}{1+\zeta_1}\right)\right.$$

$$\left.\left\{(1+\zeta_2) - \frac{1}{1+\zeta_1} + \frac{\zeta_1'\zeta_2}{1+\zeta_1'}\right\}\right] \tag{3-33}$$

where

$$D_n = \left(\frac{\zeta_1}{1+\zeta_1} + \frac{\zeta_2}{1+\zeta_1'}\right)\left(\frac{\zeta_1'}{1+\zeta_1'} + \frac{\zeta_2'}{1+\zeta_1}\right) -$$

$$\left[(1+\zeta_2) + \frac{1}{1+\zeta_1'} - \frac{\zeta_1\zeta_2'}{1+\zeta_1}\right]\left[(1+\zeta_2) - \frac{1}{1+\zeta_1} + \frac{\zeta_1'\zeta_2}{1+\zeta_1'}\right] \tag{3-34}$$

The general principle of analysis outlined in the previous section, for deriving the passband and stopband expressions for the network with

positive feedback, can be extended to obtain an explicit expression for both the passband and stopband of the negative feedback network. In this case we have

$$V_{pn} = \frac{V}{D_n}\Big[\Big(\frac{1}{1+\zeta_1} - \frac{\zeta_1'\zeta_2}{1+\zeta_1'}\Big)\Big\{\Big\{(1+\zeta_2) + \frac{1}{1+\zeta_1'} - \frac{\zeta_1\zeta_2'}{1+\zeta_1}\Big\} + j\Big(\frac{\zeta_1'}{1+\zeta_1'} + \frac{\zeta_2'}{1+\zeta_1}\Big)\Big\} + \Big(\frac{\zeta_1'}{1+\zeta_1'} + \frac{\zeta_2'}{1+\zeta_1}\Big)\Big\{\Big(\frac{\zeta_1}{1+\zeta_1} + \frac{\zeta_2}{1+\zeta_1'}\Big) + j\Big\{(1+\zeta_2) - \frac{1}{1+\zeta_1} + \frac{\zeta_1'\zeta_2}{1+\zeta_1'}\Big\}\Big\}\Big] \quad (3\text{-}35)$$

and

$$V_{sn} = \frac{V}{D_n}\Big[\Big(\frac{1}{1+\zeta_1} - \frac{\zeta_1'\zeta_2}{1+\zeta_1'}\Big)\Big\{\Big\{(1+\zeta_2) + \frac{1}{1+\zeta_1'} - \frac{\zeta_1\zeta_2'}{1+\zeta_1}\Big\} - j\Big(\frac{\zeta_1'}{1+\zeta_1'} + \frac{\zeta_2'}{1+\zeta_1}\Big)\Big\} + \Big(\frac{\zeta_1'}{1+\zeta_1'} + \frac{\zeta_2'}{1+\zeta_1}\Big)\Big\{\Big(\frac{\zeta_1}{1+\zeta_1} + \frac{\zeta_2}{1+\zeta_1'}\Big) - j\Big\{(1+\zeta_2) - \frac{1}{1+\zeta_1} + \frac{\zeta_1'\zeta_2}{1+\zeta_1'}\Big\}\Big\}\Big] \quad (3\text{-}36)$$

where D_n is defined in (3-34)

For nominal component values and in the ideal case where $\omega_1' = \omega_1$, V_{pn} and V_{sn} expressions are simplified to:

$$V_{pn} = \frac{V}{D_1}\ [(1+\omega/\omega_1)\ (1+\omega/\omega_2)\ \{2 + j\omega(1/\omega_1 + 1/\omega_2)\ (1+j)\}] \quad (3\text{-}37)$$

and

$$V_{sn} = \frac{V}{D_1}\ [(1-\omega/\omega_1)\ (1-\omega/\omega_2)\ \{2 + j\omega(1/\omega_1 + 1/\omega_2)\ (1-j)\}] \quad (3\text{-}38)$$

where

$$D_1 = [(-2\omega^2/\omega_1\omega_2)\ \{j\omega(1/\omega_1 + 1/\omega_2)\} - (4\omega^2/\omega_1\omega_2) + 2j\omega(1/\omega_1 + 1/\omega_2)] \quad (3\text{-}39)$$

From (3-38) it can be seen that the signal is nulled at ω_1 and ω_2 which corresponds to the resonant frequencies of the two cascaded sections sequence discriminator. The frequency response for both the

passband and stopband is shown in Figure 3.7. Again, the bandwidth of the realization is determined by the two notch frequencies.

3.5 SENSITIVITY ANALYSIS

The passband and stopband expressions as given in (3-32) and (3-33) are used to derive the sensitivities to any percentage mismatch in the RC product in one specific section. The analysis is similar to those of the original network and to that with positive feedback. Substituting (3-16), (3-17), (3-25) and (3-26) into (3-32) and (3-37), we get:

Passband

$$V_{\omega_1}^{V_p} = \frac{(j\omega/\omega_1)\ (X_1 + jY_1)}{(1 + j\omega/\omega_1)\ .\ D_x\ .\ N_p} \qquad (3\text{-}40)$$

and

$$S_{\omega_2}^{V_p} = \frac{(j\omega/\omega_2)\ (X_2 - jY_2)}{2\ .\ D_x\ .\ N_p} \qquad (3\text{-}41)$$

where

$$X_1 = \zeta_1\zeta_2^2\ (\zeta_1 + \zeta_2^2) + \zeta_2^2(4\zeta_1^2 + 5\zeta_1\zeta_2 + \zeta_2^2) + (6\zeta_1\zeta_2^2 + 3\zeta_2^2 - \zeta_1^3)$$

$$+ (3\zeta_2^2 + \zeta_1\zeta_2 - 2\zeta_1^2) + (\zeta_2 - \zeta_1)\ , \qquad (3\text{-}42a)$$

$$X_2 = (2\zeta_1^2\zeta_2 + \zeta_1^2 + \zeta_1\zeta_2 + \zeta_1 + \zeta_2)\ (-2\zeta_1^2\zeta_2 - 2\zeta_1\zeta_2^2 + \zeta_1^2 + \zeta_2^2 + \zeta_1 + \zeta_2 + 2)$$

$$+ 2\zeta_2(1 + \zeta_2^2)\ (\zeta_1^2\zeta_2 + \zeta_1\zeta_2^2 + 2\zeta_1\zeta_2 + \zeta_1 + \zeta_2)\ . \qquad (3\text{-}42b)$$

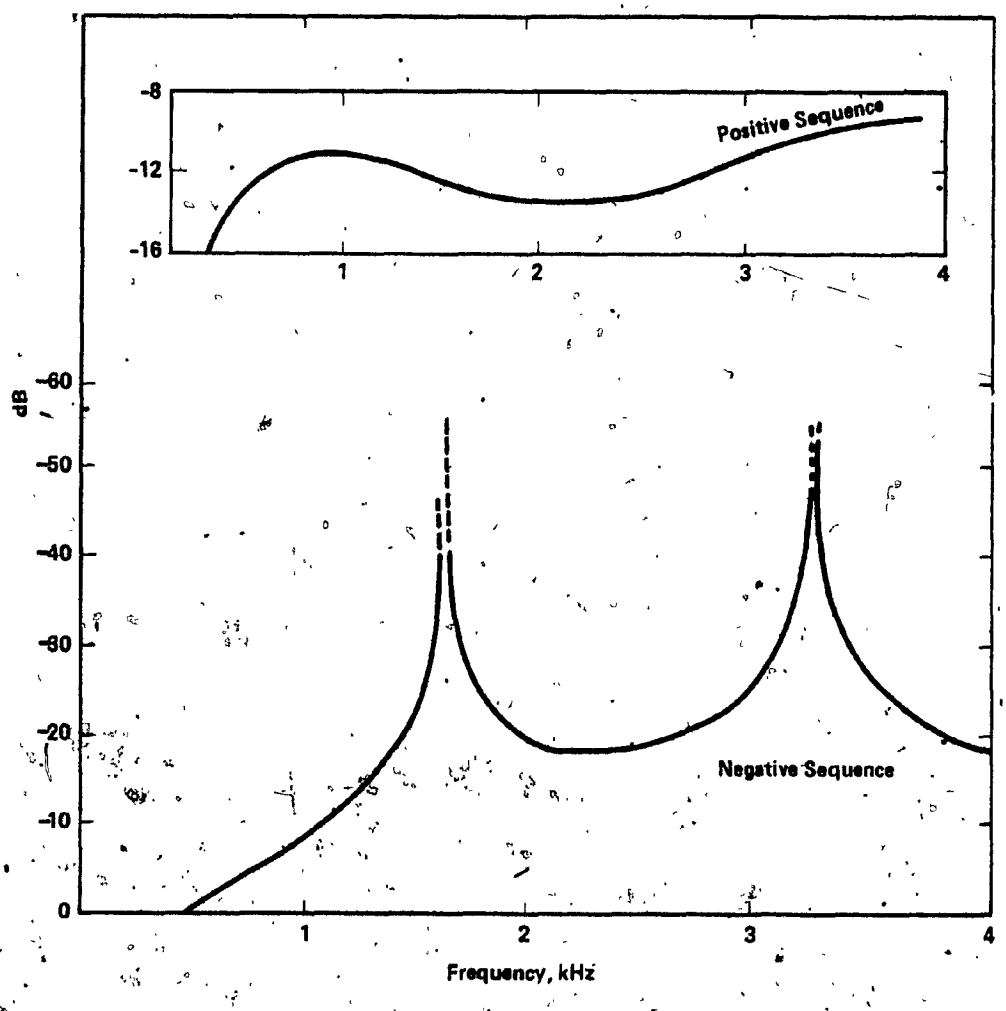

Figure 3.7 Frequency Response of the Negative Feedback Network – ADN

$$Y_1 = \zeta_1\zeta_2^2(\zeta_1^2 - \zeta_2^2) + (2\zeta_1^3\zeta_2 + 4\zeta_1^2\zeta_2^2 - \zeta_1\zeta_2^3 - \zeta_2^4) + (\zeta_1^3 + 5\zeta_1^2\zeta_2$$

$$+ 3\zeta_1\zeta_2^2 - \zeta_2^3) + (2\zeta_1^2 + 3\zeta_1\zeta_2 + \zeta_2^2) \ , \qquad (3\text{-}42c)$$

$$Y_2 = (2\zeta_1^2\zeta_2 + \zeta_1^2 + \zeta_1\zeta_2 + \zeta_1 + \zeta_2)(\zeta_1 + \zeta_2)(\zeta_1^2 + \zeta_2^2 + \zeta_1 + \zeta_2 + 1)$$

$$+ 2D_x\,(\zeta_1\zeta_2 + \zeta_1 + \zeta_2) \ , \qquad (3\text{-}42d)$$

$$D_x = \zeta_1\zeta_2\,(\zeta_1 + \zeta_2) + 2\zeta_1\zeta_2 + (\zeta_1 + \zeta_2) \qquad (3\text{-}42e)$$

and

$$N_p = (1 + \zeta_1)(1 + \zeta_2)\,[2 + (\zeta_1 + \zeta_2)(1 + j)] \qquad (3\text{-}42f)$$

Stopband

$$S^{V_s}_{\omega_1} = \frac{(j\omega/\omega_1)(X_1 + jY_1)}{(1 + j\omega/\omega_1) \cdot D_x \cdot N_p} \ , \qquad (3\text{-}43)$$

and

$$S^{V_s}_{\omega_2} = \frac{(j\omega/\omega_2)(X_2 + jY_2)}{2 \cdot D_x \cdot N_p} \qquad (3\text{-}44)$$

where X_1, Y_1, X_2, Y_2, D_x and N_p were defined in (3-42).

The derived expressions for both the passband and stopband sensitivities to ω_1 and ω_2 as given in (3-40), (3-41), (3-43) and (3-44) may look cumbersome if compared to those in (3-21) through (3-28). But as far as the final output is concerned, the comparison is obvious from the given curves. These curves are shown in figures (3-8), (3-9), (3-10) and (3-11)

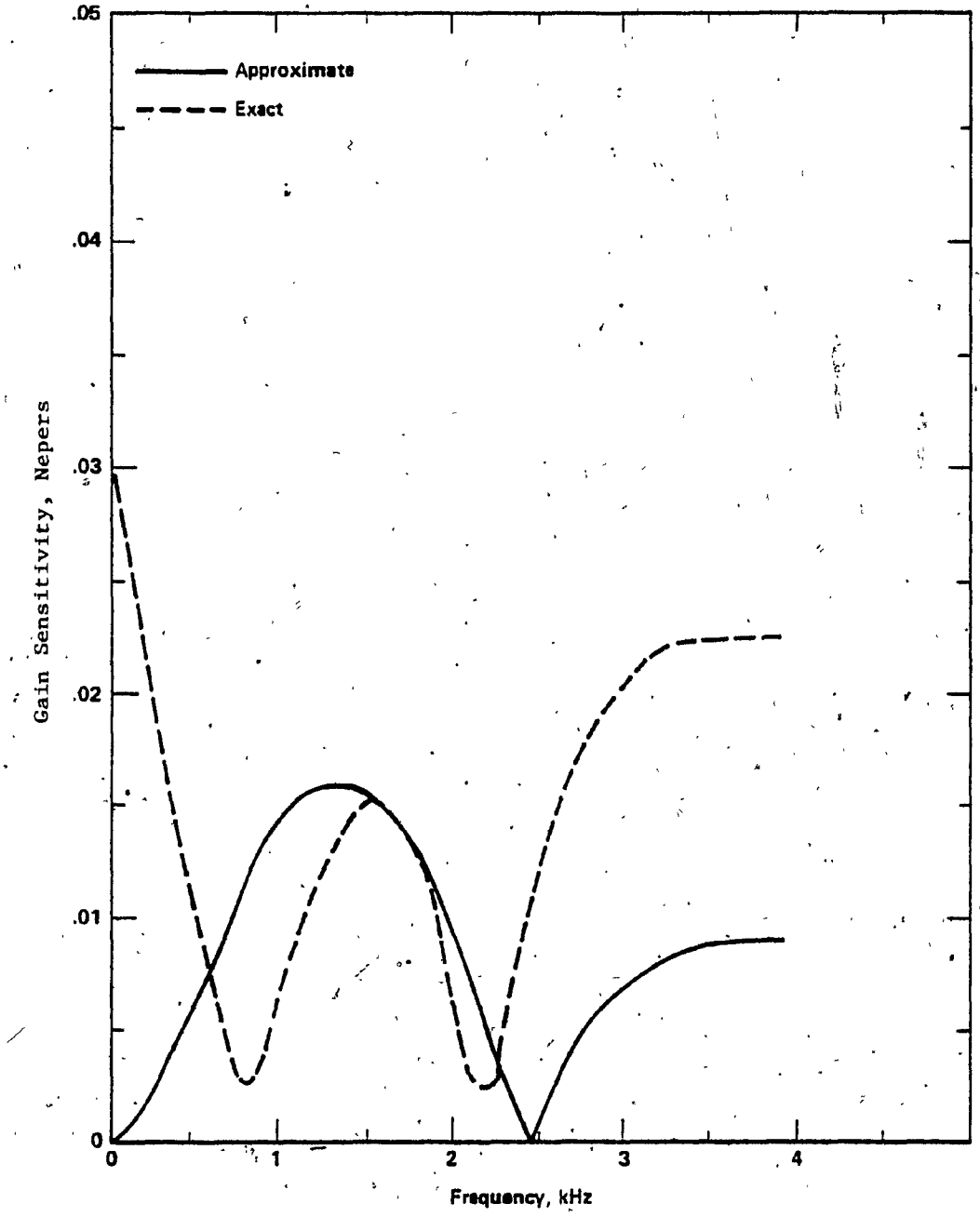

Figure 3.8 Passband Sensitivity of the ADN to 5 % Variation in ω_1

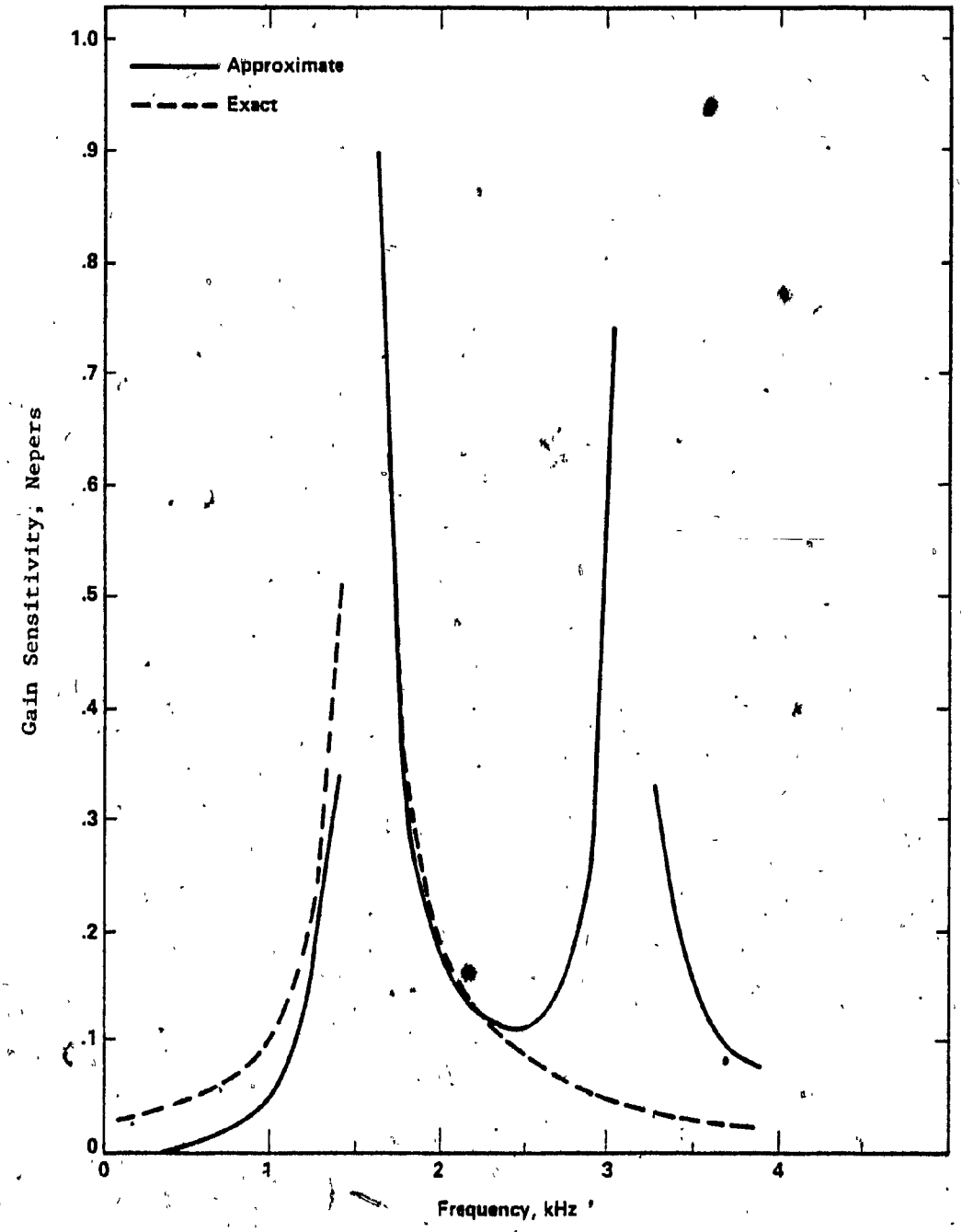

Figure 3.9 Stopband Sensitivity of the ADN to 5% Variation in ω_1

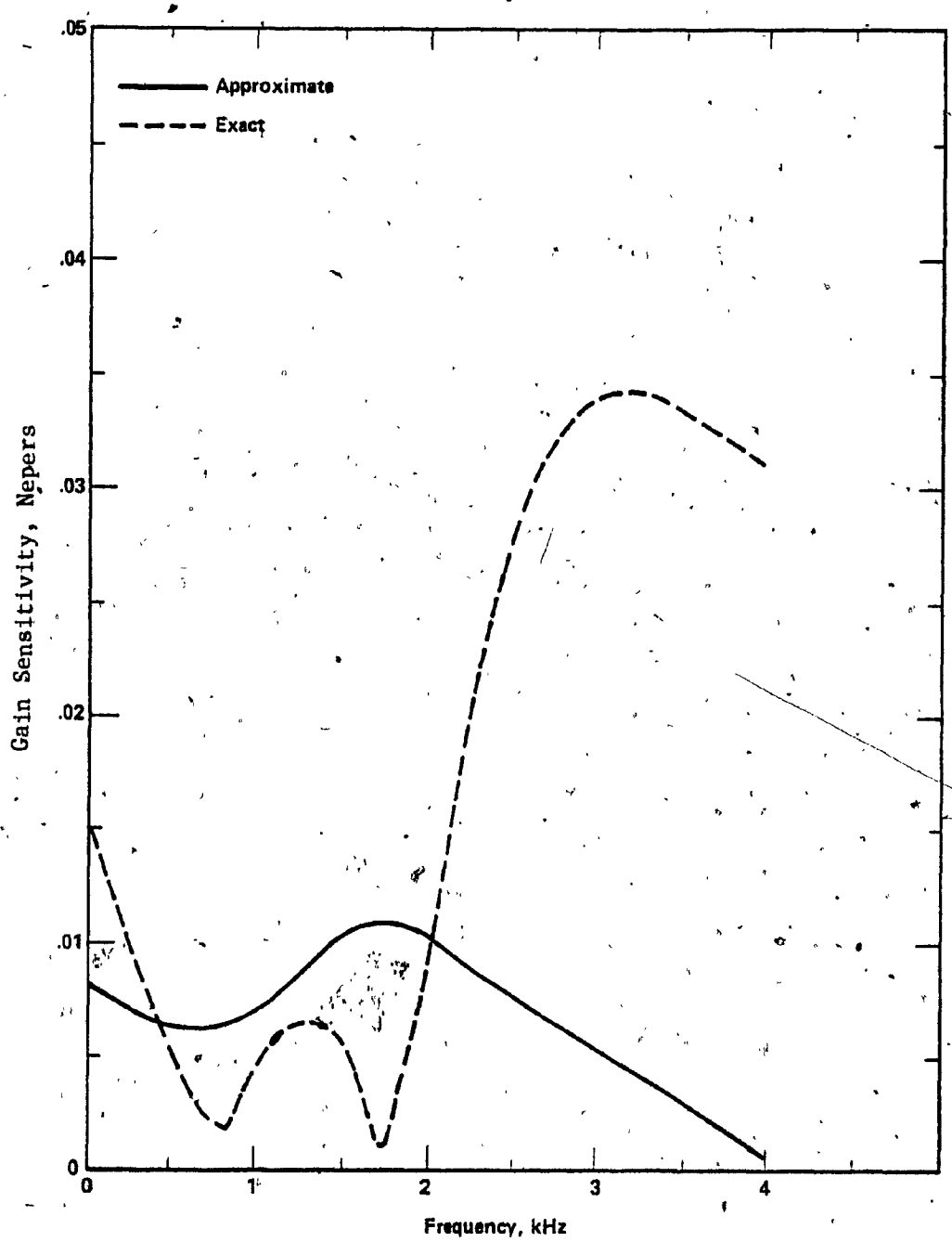

Figure 3.10 Passband Sensitivity of the ADN to 5% Variation in ω_2

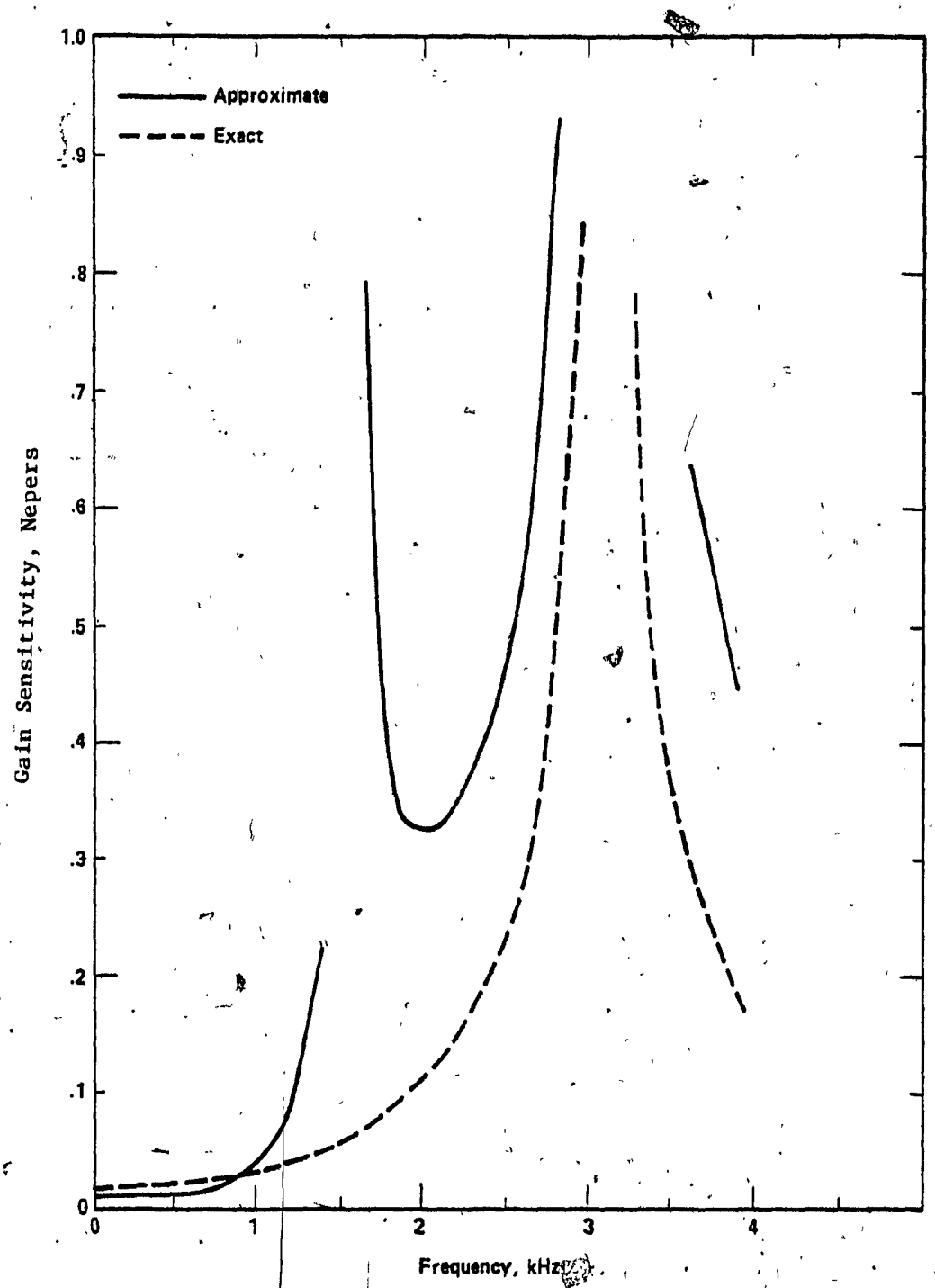

Figure 3.11 Stopband Sensitivity of the ADN to 5% Variation in ω_2

respectively. Also the exact computed sensitivities from MODNOD are superimposed on their corresponding counterparts for comparison.

3.6 ALL-PASS REALIZATION

The 90-degree phase shift realization [8,9] employs two independent all-pass networks to generate two signals V_a and V_b that are equal in magnitude at all frequencies. This realization has a sensitivity problem in applications with stringent specifications leading to tight component tolerances. In this section, two all-pass networks were designed using the same specifications as those in Figure 2.5. Figure 3.12 shows how the two all-pass networks are used to generate two signals V_a and V_b that are in phase quadrature. The transfer functions of the two all-pass networks are [7]:

$$V_a = \frac{1 - j\omega/\omega_a}{1 + j\omega/\omega_a} (V) \quad , \qquad (3\text{-}45)$$

and

$$V_b = \frac{1 - j\omega/\omega_b}{1 + j\omega/\omega_b} (V) \qquad (3\text{-}46)$$

where ω_a^{-1} and ω_b^{-1} are the RC-products in the two independant all-pass paths. As it was given in the previous section, the passband and stopband of these types of networks can be obtained from the two output signals, simply by adding V_a to $\pm jV_b$. For the all-pass case, the passband is given by:

$$V_p = \tfrac{1}{2}\{V_a + jV_b\} \qquad (3\text{-}47a)$$

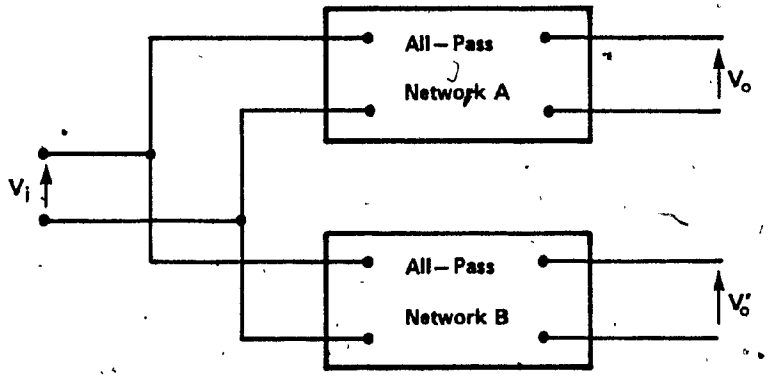

Figure 3.12 All Pass Realization

$$V_p = \tfrac{1}{2}(1 + j)\,\frac{1 - (\omega/\omega_a - \omega/\omega_b) + \omega^2/\omega_a\omega_b}{(1 + j\omega/\omega_a)\,(1 + j\omega/\omega_b)}\ (V) \qquad (3\text{-}47b)$$

and the stopband is given by:

$$V_s = \tfrac{1}{2}\{V_a - jV_b\} \qquad (3\text{-}48a)$$

$$V_s = \tfrac{1}{2}(1 - j)\,\frac{1 + (\omega/\omega_a - \omega/\omega_b) + \omega^2/\omega_a\omega_b}{(1 + j\omega/\omega_a)\,(1 + j\omega/\omega_b)}\ (V) \qquad (3\text{-}48b)$$

It can be seen from (3-47) and (3-48) that the passband and stopband expressions are valid only for $\omega_a > \omega_b$. To compare the performance of the different configurations, the two all-pass networks are designed to give a minimum of 25 dB rejection in the stopband as was obtained originally from the active phase splitting networks introduced in the previous sections.

3.7 SENSITIVITY ANALYSIS OF THE ALL-PASS (AP) REALIZATION

In order to establish the importance of the different types of networks introduced in this thesis, it is necessary to study the sensitivity performance of both the passband and stopband of the all-pass realization. Consider first the passband as given by (3-47). The percentage variation $\Delta V_p/V_p$ in the passband due to a corresponding variation $\Delta\omega_b$ in ω_b is:

$$\Delta V_p/V_p = (-1 + j)\,\frac{(\omega/\omega_b)\,(1 + \omega/\omega_a)}{(1 + j\omega/\omega_b)(1 - \omega/\omega_a + \omega/\omega_b + \omega^2/\omega_a\omega_b)}, \qquad (3\text{-}49)$$

and for the stopband similar relation can be written as:

$$\Delta V_s/V_s = (1 + j)\,\frac{(\omega/\omega_b)\,(1 + j\omega/\omega_a)}{(1 + j\omega/\omega_b)(1 + \omega/\omega_a - \omega/\omega_b + \omega^2/\omega_a\omega_b)} \qquad (3\text{-}50)$$

It is noted that for the all-pass realization, the passband and stopband sensitivities can be derived with respect to the variation in the RC product in either one of the two independant all-pass paths. The sensitivity analysis of both the passband and stopband as given in (3-49) and (3-50) is performed to the variation in the RC product of the second all pass, with $\omega_2 = 1/R_2C_2$ as shown in Figure 3.12. Both the passband and stopband sensitivities to 5% variation in ω_2 are shown in Figures (3-13) and (3-14). Comparison between the approximate passband and stopband sensitivities to ω_2 of the AD, ADP and AP networks is shown in figures 3.15 and 3.16 respectively.

3.8 EXPERIMENTAL RESULTS

The experimental set-up for both the positive and negative feedback networks is similar to that of Chapter 2. The two output signals V_o and V_o' from the original set-up are inverted using 741 OA in the inverting mode. V_o and its inverse are fed back to the input terminals 1 and 2 respectively. The potential of the originally grounded point G is now raised to $V_o'(-V_o')$ for the positive (negative) feedback configuration.

Following the same approach as in the original network, the modulation process is performed to generate single-sideband signal. As previously explained, either upper sideband or lower sideband can be generated simply by inverting any two signals that are out of phase by 180°. The frequency response for both configurations is shown in Figure 3.17. The attractive feature obtained from applying feedback to the original network is that the passband of the feedback network is almost flat, free from ripples within the designed bandwidth.

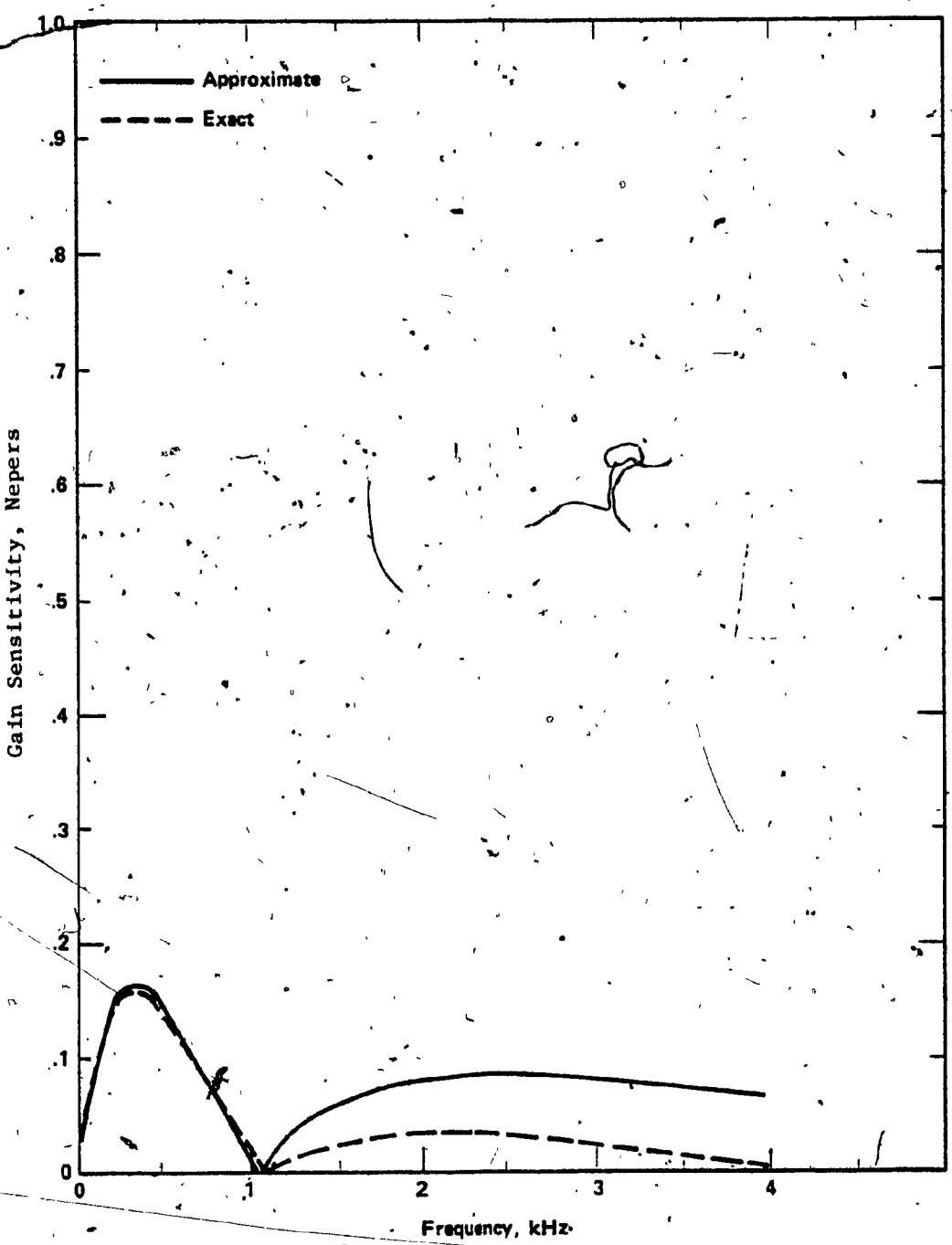

Figure 3.13 Passband Sensitivity of the All-Pass Realization to 5 % Variation in ω_a

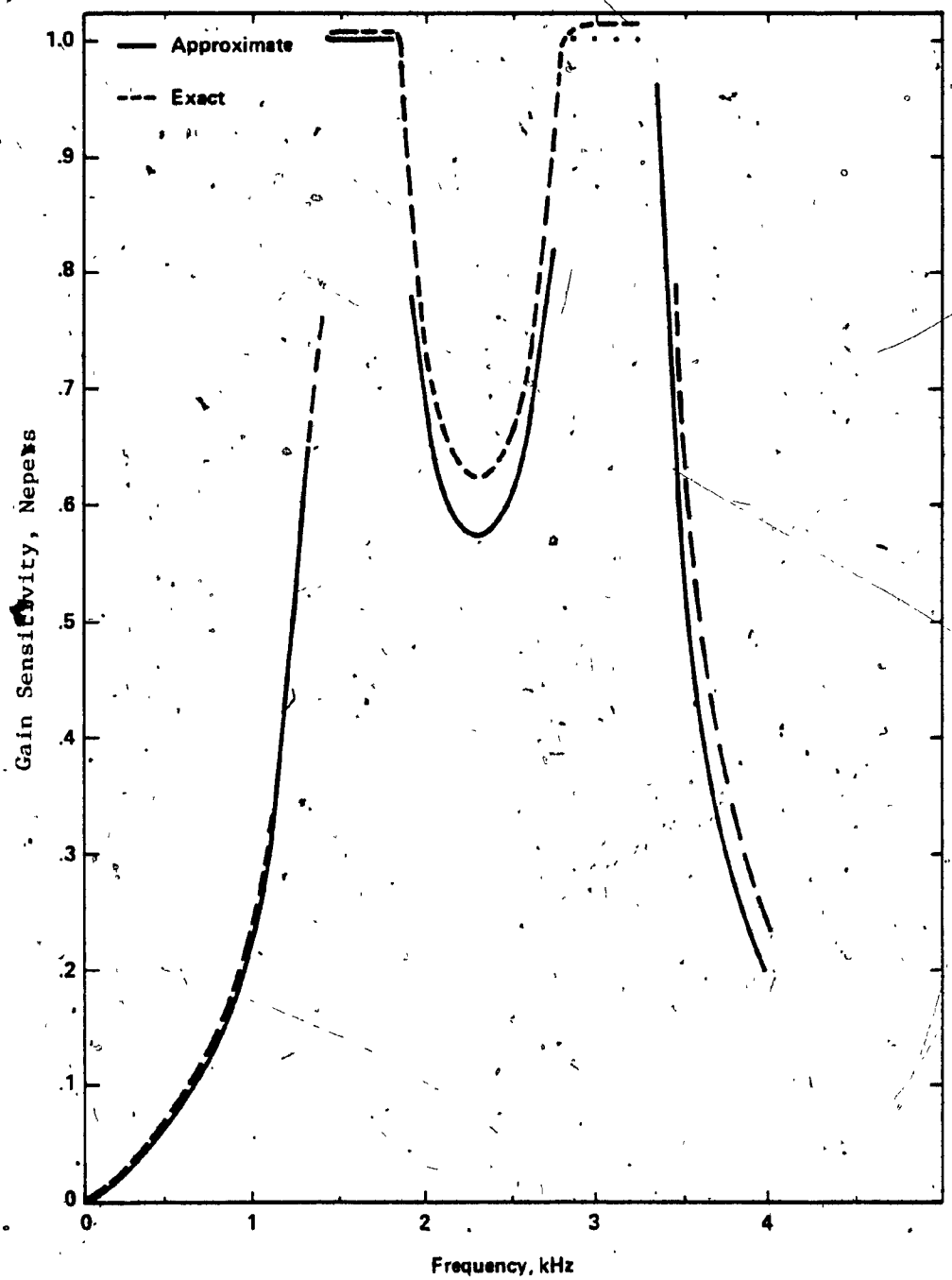

Figure 3.14 Stopband Sensitivity of the All-Pass Realization to 5 % Variation in ω_2

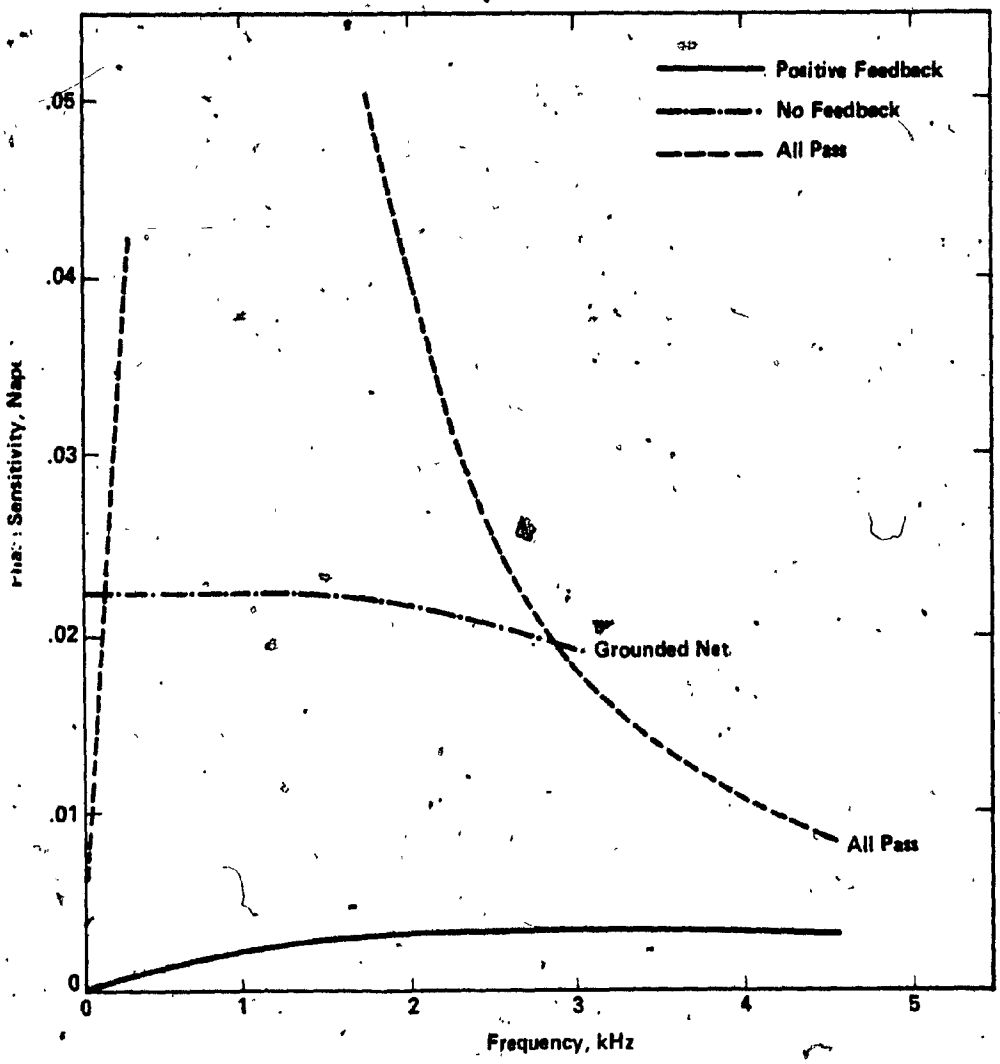

Figure 3.15 Comparison Between the Passband Sensitivities (to ω_2) of the AD, ADP and AP Networks

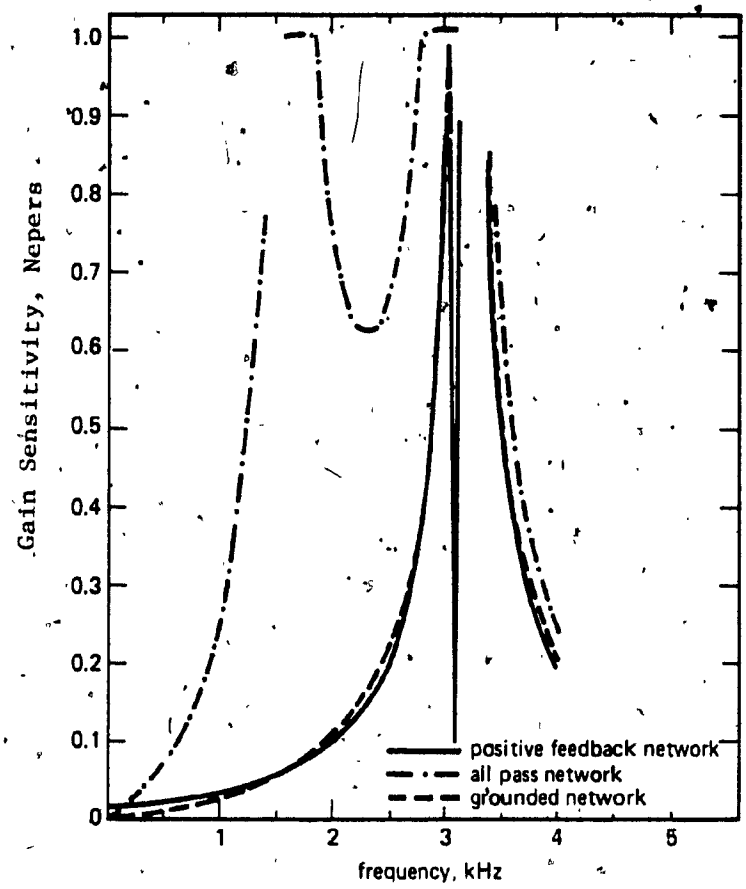

Figure 3.16 Comparison Between the Stopband Sensitivities to ω_2 of the AD, ADP and AP Networks

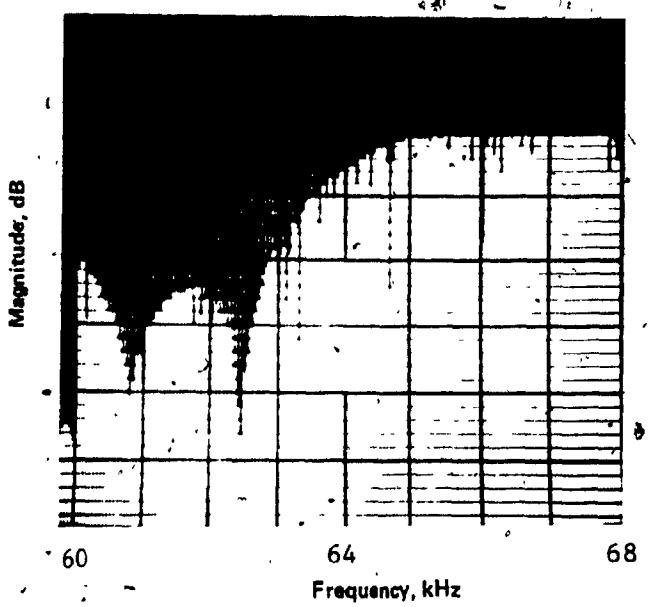

Figure 3.17 (a) Frequency Response of the ADP Network
(Vertical Scale, 10 dB/D)

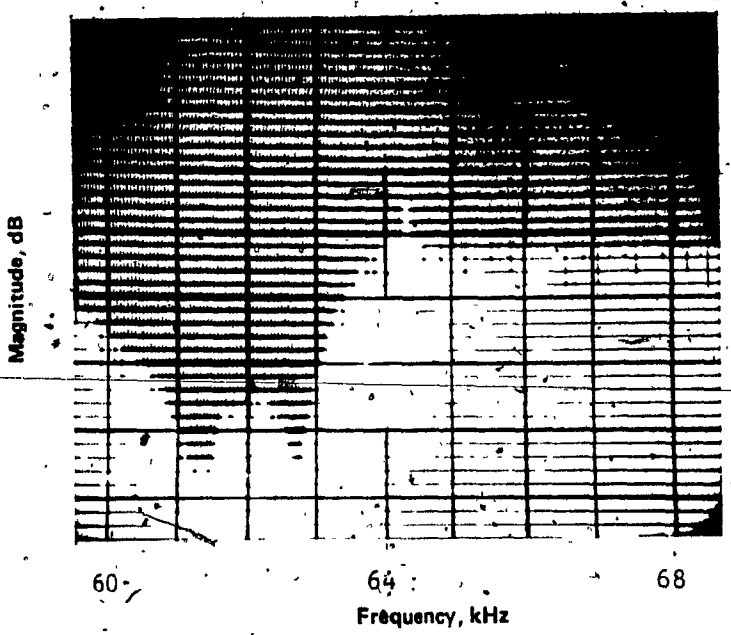

Figure 3.17 (b) Frequency Response of the ADN Network (Vertical Scale 10 dB/D)

While the stopband has not changed from its previously obtained value of 25 dB rejection, the passband has been slightly improved.

3.9 CONCLUSIONS

In this chapter three different types, namely, active design with positive feedback, active design with negative feedback and the all pass realization, used to generate quadrature signals are presented. Separate expressions are derived for both the passband and stopband frequency responses of each configuration for the general non-ideal case where the RC products in each of the sections are assumed to be not equal to (i.e. $\omega_i \neq \omega_i'$). These expressions are used primarily to derive the passband and stopband sensitivities to variations in the component tolerances. Explicit expressions are obtained for both the passband and stopband responses as a function of the nominal component values where $\omega_i = \omega_1'$ was substituted in the general expressions.

The networks with feedback and particularly the positive feedback configuration retain the attractive features of the original design (with no feedback); while improving the sensitivities both in the passband and stopband. In addition to the simplicity of both the structures (with and without feedback), the networks introduced are relatively insensitive to the component variations when compared to the quadrature modulation method for producing SSB which implements the 90 degree phase difference networks by using two independent all pass paths.

CHAPTER IV

SAMPLED DATA SEQUENCE DISCRIMINATOR USING THE PRINCIPLE OF SWITCHED CAPACITOR

4.1 INTRODUCTION

In the present era of microelectronic systems, it is very likely that active networks will be realized in integrated form of one kind or another. Linear active RC networks, represent one of the most practical and economical methods of designing inductorless networks. The hybrid integrated circuit (HIC) fabrication techniques are used to integrate conventional active networks. These techniques can be considered as a significant advance over discrete component networks. However, it is becoming increasingly important to develop new techniques to efficiently integrate such networks for Large Scale Integration (LSI) applications. Since some applications require a large number of circuits on a single integrated chip, it is desirable that these circuits be fully integrated, require no trimming and as little silicon area as possible.

In this chapter a new technique to analog sampled data filtering which applies the principle of the periodic switching of capacitors to obtain the desired analog characteristics is discussed. The basic concept of this technique was introduced by Fried [33]. Other contributions to analog sampled data filtering, such as MOS recursive filters [34, 39], and CCD transversal filters [40] have been recently introduced. McCreary and Gray [41, 42] make use of the sample data technique in designing their analog to digital converter (A/D). The

sampled data technique makes use of the equivalence between a resistor and a combination of two switches and a capacitor. Throughout the present work the name "switched capacitor" will be used to refere to a resistor which has been replaced by a capacitor and two MOS switches.

The sampled data filter introduced in this chapter consists primarly of capacitors, switches and operational amplifiers which can be fully integrated using MOS technology. The filter coefficients, being ratios of capacitors, could be made less sensitive to manufacturing processes.

4.2 ANALOG SAMPLED DATA TECHNIQUE

4.2.1 Principle of Switched Capacitor

The main idea behind the concept of switched capacitor is the transfer of a charge between two points in the network by means of capacitors and switches. Consider the switched capacitor circuit in Figure 4.1 (a), with the switch alternating between the two positions at a switching rate of f_s. Assume first that the switch is in the position shown, then the capacitor is initially charged to the voltage V_{in}. If the switch is then removed from its original position and is connected to the other position then a net charge of $Q = C_s(V_{out}-V_{in})$ is transferred. If the switching period is T_s seconds, then the average current 'i' flowing into V_{out} will be

$$i = \frac{Q}{T_s} \qquad (4-1)$$

or

$$i = \frac{C_s(V_{out} - V_{in})}{T_s} \qquad (4.2)$$

From (4.2), the equivalent resistance can be written as

$$R = \frac{T_s}{C_s} \qquad (4.3)$$

Since $f_s = \frac{1}{T_s}$

Then

$$R = \frac{1}{f_s \cdot C_s} \qquad (4.4)$$

Hence, if the switching rate f_s is much greater than the band of frequencies of interest*, then the circuit of Figure 4.1 simulates a resistor of value $R = 1/f_s C_s$

In the circuit of Figure 4.1 (b) the ideal switches are replaced by MOS switches. These switches are operated by two phase non-overlapping clocks ϕ and $\bar{\phi}$** at a frequency f_s as shown in Figure 4.2. It should be pointed out that if the switching rate is of the same order of magnitude as the signal frequencies, then it is very necessary to bandlimit the input signal to the Nyquist frequency in order to avoid aliasing [43].

---

* If the sampling rate is much greater than the signal highest frequency component then it is practically possible to ignore the time sampling of the signal.

** The two phases ϕ and $\bar{\phi}$ are chosen to be 180° out of phase w.r.t. each other.

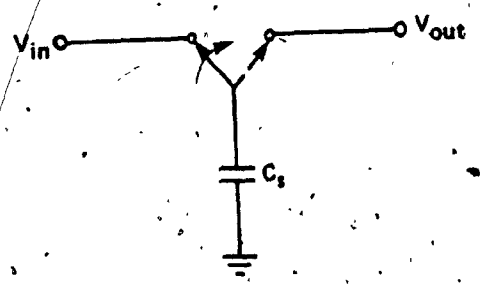

Figure 4.1(a) Resistor Simulation By a Switched Capacitor

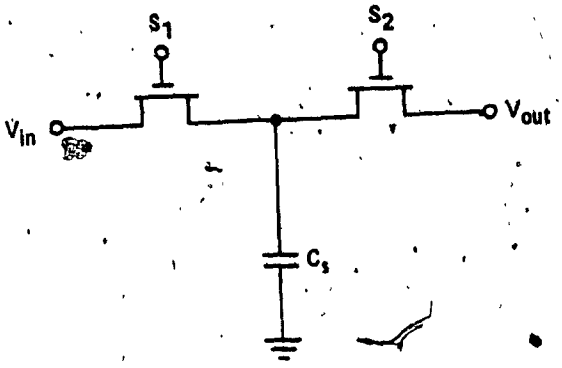

Figure 4.1(b) Implementation Using MOS Switches

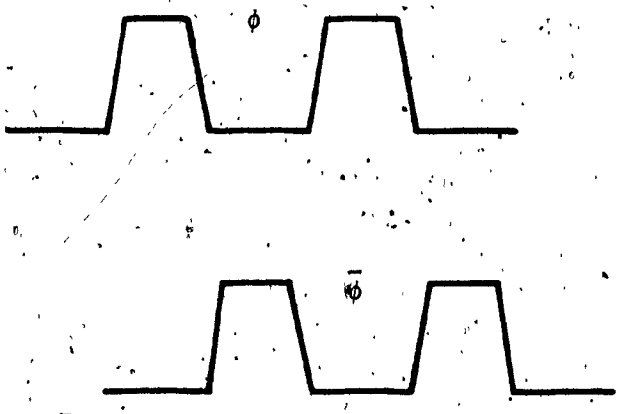

Figure 4.2 Clocking Scheme for the Switched Capacitor

The main advantages of the switched capacitor approach is that the stability and linearity of the equivalent resistor are much better than the integrated (diffused) resistors which have poor temperature and linearity characteristics [41, 42].

4.3 SAMPLED DATA SEQUENCE DISCRIMINATOR USING SWITCHED CAPACITORS

In this section the principle of switched capacitor, discussed in the previous section, is applied to the phase splitting sequence discriminator of chapter 2. New configuration of analog sampled data phase splitting sequence discriminator will be presented, which yields a frequency response comparable to that of its analog counter part using discrete resistors and capacitors. Three cases will be considered for analysis. We start first by anlaysing the case of a single stage sequence discriminator to obtain explicit formulas for both the passband and stopband using the principle of transfer of charge between two points. By applying z-transform technique to the difference equation obtained, both the passband and stopband expressions can be derived. Two-stage sequence discriminator is then considered. Finally, both the passband and stopband expressions for the general N stage* sequence discriminator are considered. The design technique makes use of capacitors, switches and operational amplifiers as the only circuit elements.

---

* Throughout this work, this term will refere to N sections connected in cascade.

4.3.1 Single Stage Sequence Discriminator (SSSD)

Consider the circuit shown in Figure 4.3. The SSSD shown is identical to that shown in Figure 2.1 with all its resistors being replaced by switched capacitors. As previously mentioned, each resistor is replaced by a combination of a capacitor and two MOS switches which are driven by two nonoverlapping phase clocks ϕ and $\bar{\phi}$. Assume that the positions of the switches are as shown. During the 'ON' period of the switch S_1 the capacitor C_x is charged to the voltage V_{in}, and then during the 'ON' period of S_2 (S_1 is OFF), a charge of C_x $(V_{out}-V_{in})$ is transfered to the capacitor C_1. Charge conservation equation yields:

$$C_x [V_o (nT_s) - V_{in}\{(n-1)T_s\}] = -C_1[V_o (nT_s) - V_o\{(n-1)T_s\}] \quad (4.5)$$

and

$$C'_x [V'_o (nT_s)] = -C'_1 [\{V_{in} (nT_s) + V'_o (nT_s)\} - \{V_{in}\{(n-1)T_s\} + V'_o\{(n-1)T_s\}\}] \quad (4.6)$$

where T_s is the clock period.

Applying z-transform technique to the above difference equations yields

$$V_o(z) = \frac{\alpha_1}{1+\alpha_1} \cdot \left\{\frac{1}{z - \frac{1}{1+\alpha_1}}\right\} V_{in}(z) \quad (4.7)$$

and

$$V'_o(z) = \frac{-1}{1+\alpha'_1} \cdot \left\{\frac{z-1}{z - \frac{1}{1+\alpha'_1}}\right\} \cdot V_{in}(z) \quad (4.8)$$

where

$$\alpha_1 = \frac{C_x}{C_1} \quad \text{and} \quad \alpha'_1 = \frac{C'_x}{C'_1}$$

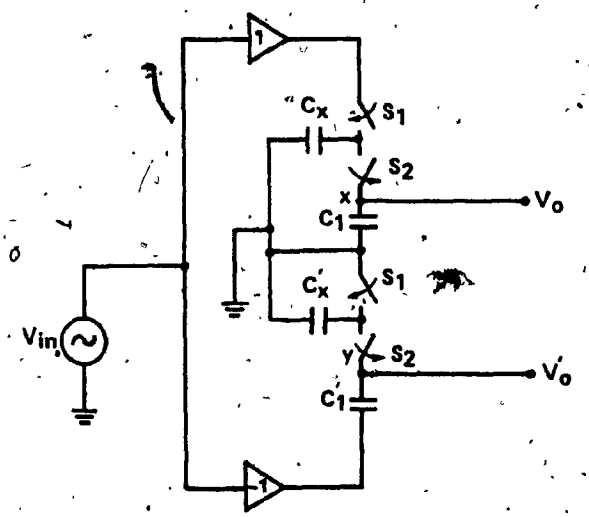

Figure 4.3(a) Single Stage Sequence Discriminator Using Switched Capacitors

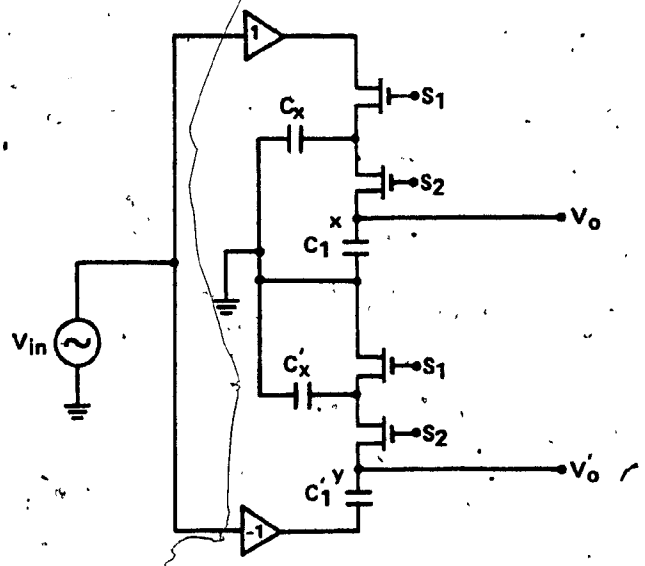

Figure 4.3(b) Implementation Using MOS Switches

As previously mentioned, the passband and stopband equations can be obtained from the two output signals V_o and V_o' simply by adding V_o to $\pm jV_o'$ as;

$$V_p = \tfrac{1}{2}\{V_o + jV_o'\} \tag{4.9}$$

and

$$V_s = \tfrac{1}{2}\{V_o - jV_o'\} \tag{4.10}$$

where V_p and V_s are the passband and stopband respectively. The two capacitors C_1 and C_1' are considered equal which implies that the two switched capacitors C_x and C_x' to be equal.

Hence, for this practical case we have;

$$\alpha_1 = \alpha_1' = \alpha$$

Then

$$V_p(z) = \frac{-j}{1+\alpha} \cdot \frac{z - (1 - j\alpha)}{z - \frac{1}{1+\alpha}} V_{in}(z) \tag{4.11}$$

and

$$V_s(z) = \frac{j}{1+\alpha} \cdot \frac{z - (1 + j\alpha)}{z - \frac{1}{1+\alpha}} \cdot V_{in}(z) \tag{4.12}$$

It should be pointed out here that the value of the switched capacitor is dependent upon the sampling rate of the switching waveforms. The above expressions concerning V_o, V_o', V_p and V_s as given by (4.7), (4.8), (4.11) and (4.12) respectively, can also be obtained using the principle of sequence discrimination. These derivations are given in Appendix D.

One of the main advantages of the switched capacitor design approach is the high accuracy of the RC time constant that can be determined by a ratio of capacitor values which can be designed to a higher degree of accuracy and which makes it less sensitive to most processing variations. Hence, by eliminating the resistors from the active RC design, it now becomes possible to fully integrate active RC networks using MOS technology.

4.3.2 Two Stage Sequence Discriminator

The two stage sequence discriminator of Figure 2.5 is represented here in its sampled data form shown in Figure 4.4 where each resistor is replaced by a combination consisting of a capacitor and 2 MOS switches operated by the two clocks shown in Figure 4.2. In designing such type of filters, two important aspects are to be considered. First, all the MOS switches are controlled by the same clock rate, and the second aspect is that using identical capacitors in the same section which, in turns, leads to the use of identical switched capacitors. The analysis is similar to that of the SSSD.

Recall V_o and V_o' as given by (4.7) and (4.8) to be V_x and V_y respectively. Since the input to the second section is comprised of V_x, V_y and $(-V_x)$ as shown then; by applying the charge conservation equation, the two output signals V_o and V_o', for the general non-ideal case, are given by:

$$V_o(z) = \frac{1 \quad \phi}{(1 + \alpha_2) - z^{-1}} \left[\frac{\alpha_1 \alpha_2' z^{-2}}{(1 + \alpha_1) - z^{-1}} \phi \right. \left. \frac{(1 - z^{-1})^2}{(1 + \alpha_1') - z^{-1}} \right] V_{in}(z) \qquad (4.13)$$

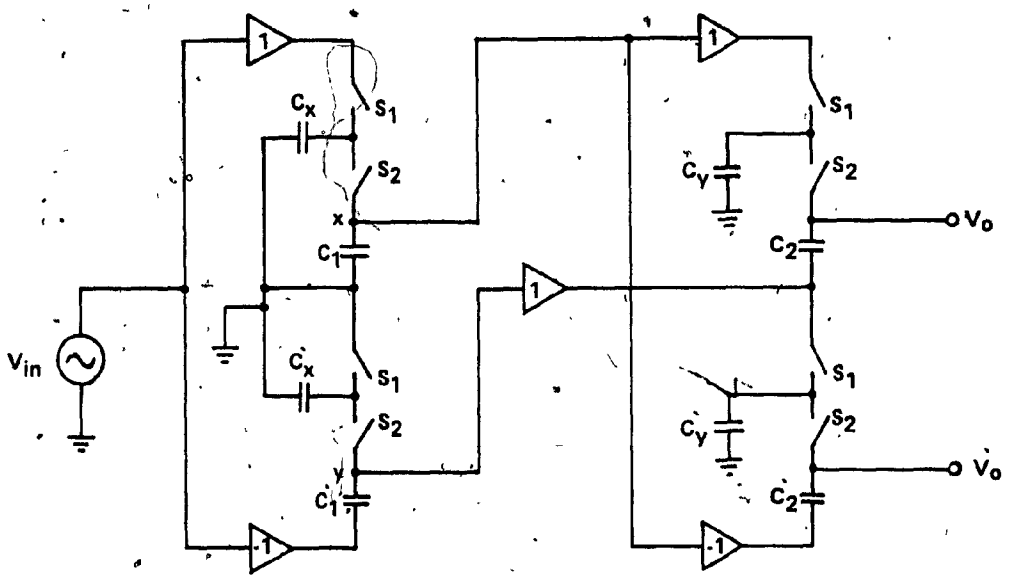

Figure 4.4 Sampled Data Sequence Discriminator Using Switched Capacitors

and

$$W_o(z) = \frac{-1}{(1+\alpha_2')- z^{-1}} \left[\frac{\alpha_1 z^{-1}(1-z^{-1})}{(1+\alpha_1) - z^{-1}} + \frac{\alpha_2' z^{-1}(1-z^{-1})}{(1+\alpha_1') - z^{-1}} \right] V_{in}(z) \quad (4.14)$$

From (4.13) and (4.14) and the expressions given in (4.9) and (4.10), the general expressions for both the passband and stopband can be directly obtained.

For most practical cases, the ratios of the capacitors in each individual section are considered identically equal. Hence, letting these ratios for the two individual sections to be α_1 and α_2 respectively, then, the passband and stopband expressions are:

$$V_p(z) = \frac{-1}{(1+\alpha_1)(1+\alpha_2)} \left[\frac{\{z-(1-j\alpha_1)\}\{z-(1-j\alpha_2)\}}{\{z-\frac{1}{1+\alpha_1}\}\{z-\frac{1}{1+\alpha_2}\}} \right] V_{in}(z) \quad (4.15)$$

and

$$V_s(z) = \frac{-1}{(1+\alpha_1)(1+\alpha_2)} \left[\frac{\{z-(1+j\alpha_1)\}\{z-(1+j\alpha_2)\}}{\{z-\frac{1}{1+\alpha_1}\}\{z-\frac{1}{1+\alpha_2}\}} \right] \quad (4.16)$$

The above results agree with the previously obtained one using the concept of symmetric sequences, where the two output signals are obtained from each input sequence of either polarity. These two outputs are identically equal in magnitude and in phase quadrature as shown in Appendix D. The frequency response of the two stage sampled data sequence discriminator is shown in Figure 4.5. It is to be noted that the position of the notch frequencies is dependent upon the value of the switched capacitor which in turns depends upon the sampling (clock) rate considered.

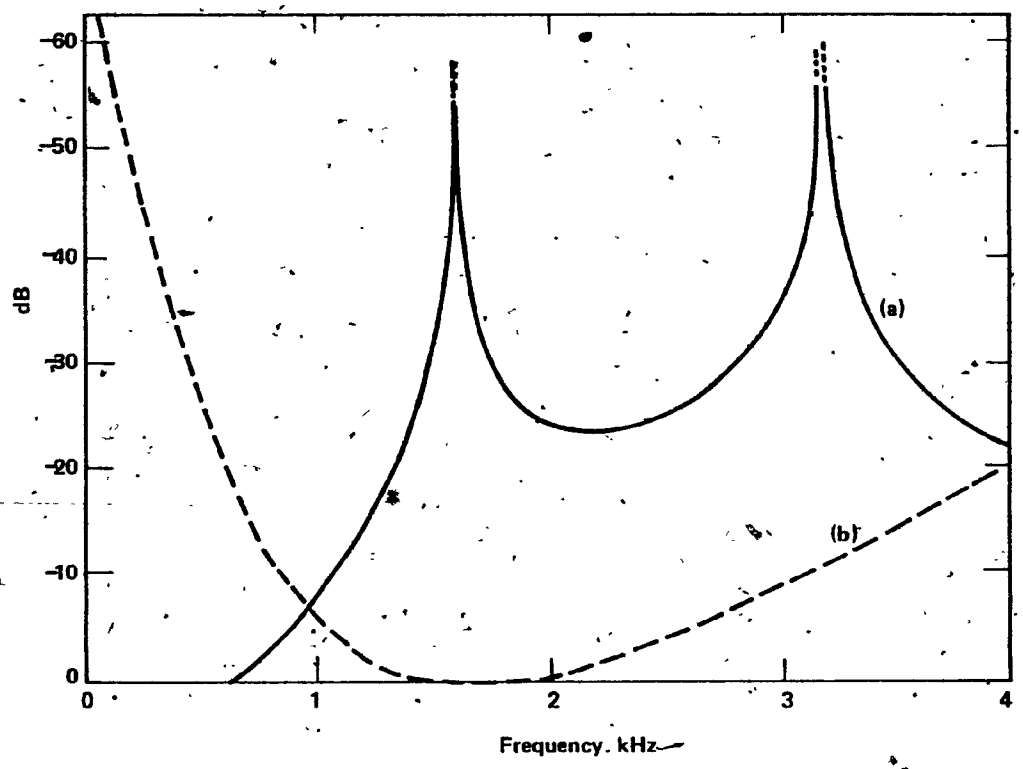

Figure 4.5 Frequency Response of the Switched Capacitor Network
a) Stopband Response (Negative Sequence)
b) Passband Response (Positive Sequence)

4.3.3 N Stage Sampled data sequence discriminator

Analysis was given in the previous section for both the passband and stopband expressions, in both the general non-ideal case and for the case where nominal component values are considered, for single and two stage sampled data sequence discriminators. This analysis is generalized in this section for the N stage case. We start first by recalling V_o and V_o', as given in (4.13) and (4.14) for the two stage sequence discriminator, to be V_x and V_y respectively. If V_x, V_y and $(-V_x)$ are applied to the next section and the output of this section is applied to the subsequent section in the same manner, then, it can easily be proved that the general expressions for V_p and V_s in this N stage sequence discriminator case are:

$$V_p = \frac{(-j)^N}{\prod_{i=1}^{N}(1+\alpha_i)} \left[\frac{\prod_{i=1}^{N}\{z - (1-j\alpha_i)\}}{\prod_{i=1}^{N}\{z - \frac{1}{1+\alpha_i}\}} \right] V_{in}(z) \qquad (4.17)$$

and

$$V_s = \frac{(+j)^N}{\prod_{i=1}^{N}(1+\alpha_i)} \left[\frac{\prod_{i=1}^{N}\{z - (1+j\alpha_i)\}}{\prod_{i=1}^{N}\{z - \frac{1}{1+\alpha_i}\}} \right] V_{in}(z) \qquad (4.18)$$

It is to be pointed out that in all the above cases, the denominator depends upon α which is always positive since it represents a ratio of two capacitors. Hence $1/(1+\alpha)$ is always less than unity and, hence all the poles lie within the unit circle $|z| < 1$, thereby representing a stable realization [43, 44].

4.3.4 ACTIVE RC SEQUENCE DISCRIMINATOR VS. SAMPLED DATA SEQUENCE DISCRIMINATOR THROUGH THE BILINEAR Z-TRANSFORMATION

To compare the active RC sequence discriminator with the sample data active switched capacitor sequence discriminator, the transfer functions of both realizations, for either type of sequences, are related through the bilinear z-transformation. It can be shown that if the clock (sampling) rate $f_s(1/T_s)$ is much higher than the highest frequency of the signal i.e. $f_s >> f$, and since

$$z = \exp(j\omega T_s) \tag{4.19}$$

hence, for first degree of approximation z can be written as:

$$z \cong 1 + j\omega T_s \tag{4.20}$$

Recall the transfer function $H_p(j\omega) = V_{op}(j\omega)/V_{in}(j\omega)$ as given by (2.4) and subistitute (4.20). Then

$$H_p(z) = \frac{1 + \dfrac{z-1}{j\omega_1 T_s}}{1 + \dfrac{z-1}{\omega_1 T_s}} \cdot (-j) \tag{4.21}$$

Since $$\omega_1 = \frac{1}{R_1 C_1}$$

$$\omega_1 = \frac{C_s}{T_s C_1}$$

Then

$$\omega_1 T_s = \frac{C_s}{C_1} = \alpha_1$$

and (4.21) becomes

$$H_p(z) = (\mp j)\ \frac{z - (1 - j\alpha)}{z - (1 - \alpha)}$$

or

$$V_p(z) = (-j)\ \frac{z - (1 - j\alpha)}{z - (1 + \alpha)}\ V_{in}(z)$$

which is identical to that in (4.11) for small value of α (i.e. $\alpha < 1$). Same result can be obtained for the stopband expressions as given in (2.9) and (4.12). This conclusion can be generalized for the N stage discriminator case.

4.4 SENSITIVITY ANALYSIS

It has been shown that the transfer function of the sampled data network as given by (4.17) and (4.18) can be uniquely characterized by the capacitors ratio α_N which is primarly dependant upon the sampling rate f_s of the switches. To study the sensitivity performance of this type of networks, one has to consider the variation in the passband and stopband to an incremental variation in the capacitors ratio α_i in any section of the network.

In this section we consider only the variation in the value of α_i that is caused by the non-ideal operations of the switches which may cause α_i to deviate from its nominal designed value. It can be seen, from (4.17) and (4.18), that α_i is the major design parameter for this class of networks.

The sensitivity analysis can be performed in a similar manner to that of the active RC realization. Recall V_o and V_o' as given by (4.13)

and (4.14), then the general expressions for both the passband and stopband are given by:

$$V_p(z) = \left[\frac{1}{(1+\alpha_2)-z^{-1}} \left\{ \frac{\alpha_1\alpha_2' z^{-2}}{(1+\alpha_1)-z^{-1}} + 1 - \frac{(1-z^{-1})^2}{(1+\alpha_1')-z^{-1}} \right\} \right.$$

$$- \frac{j}{(1+\alpha_2')-z^{-1}} \left\{ \frac{\alpha_1 z^{-1}(1-z^{-1})}{(1+\alpha_1)-z^{-1}} + \right.$$

$$\left. \left. \frac{\alpha_2' z^{-1}(1-z^{-1})}{(1+\alpha_1')-z^{-1}} \right\} \right] V_{in}(z) \qquad (4.22)$$

and

$$V_s(z) = \left[\frac{1}{(1+\alpha_2)-z^{-1}} \left\{ \frac{\alpha_1\alpha_2' z^{-1}}{(1+\alpha_1)-z^{-1}} + 1 - \frac{(1-z^{-1})^2}{(1+\alpha_1')-z^{-1}} \right\} \right.$$

$$+ \frac{j}{(1+\alpha_2')-z^{-1}} \left\{ \frac{\alpha_1 z^{-1}(1-z^{-1})}{(1+\alpha_1)-z^{-1}} + \right.$$

$$\left. \left. \frac{\alpha_2' z^{-1}(1-z^{-1})}{(1+\alpha_1')-z^{-1}} \right\} \right] V_{in}(z) \qquad (4.23)$$

The sensitivity analysis can be performed in two steps:

1) By assuming $\alpha_1' = \alpha_1 \pm \Delta\alpha_1$,

$\alpha_2' = \alpha_2$

Then, the passband and stopband sensitivities to α_1 are given by

$\frac{\partial V_p}{V_p} / \frac{\partial \alpha_1}{\alpha_1}$ and $\frac{\partial V_s}{V_s} / \frac{\partial \alpha_1}{\alpha_1}$ respectively.

2) By assuming $\alpha_1' = \alpha_1$

$\alpha_2' = \alpha_2 \pm \Delta\alpha_2$

Then, the passband and stopband sensitivities to α_2 are given by

$\frac{\partial V_p}{V_p} / \frac{\partial \alpha_2}{\alpha_2}$ and $\frac{\partial V_s}{V_s} / \frac{\partial \alpha_2}{\alpha_2}$ respectively.

The derivations of these expressions are straightforward as was done for the active RC structures of chapters (2) and (3). It can be seen that the ratio of the capacitors plays a major roll in the design and performance of these networks. Since capacitors can be fabricated using metal gate technology, then careful control of the capacitor ratios during the manufacturing process makes this filter less sensitive to most processing variations.

It is important to point out that the frequency response characteristics of the two types of realization are close to each other in the frequency band of interest as can be seen from Figures (2.6) and (4.5). Since it has been proven that the response of the active RC realization has low sensitivity along the $j\omega$-axis, this property can be preserved for the sampled data active switched capacitor realization along the unit circle [44]. Also, since the former realization is stable with all its poles in the left-half of the S-plane, this stability property is transformed into a stable sampled data active switched capacitor network, with all its poles inside the open unit circle.

4.5 PRACTICAL DESIGN CONSIDERATIONS

So far, the discussion has been under ideal conditions and the only deviation, from the ideal operations of the switches, has been the finite accuracy of the capacitor ratio. However, MOS switches and amplifier limitations introduce some secondary effects to the overall performance of the network. These limitations can be summarized as follows:

1) Incomplete transfer of charge: During the process of charging the capacitor C_s, a total charge of $C_s V_{in}$ is stored which has to be transferred completely during the finite pulse width of the clocks. Due to the finite ON resistance of the switches, complete transfer of charge does not occur. At very high clock rates the time constant of the switched capacitor will become important. This time constant is determined by the ON resistance of the switches (typically several kilohms) and the values of the switched capacitor (typically tens of picofarads). The maximum switching rate of the switches sets a limit on the maximum size of the switched capacitor, relative to the size of the switches, and limits the precision (i.e. amplitude and frequency distortion and noise), which will deteriorate with an increase in sampling frequency.

It is important to point out that because the ON resistance of the charging switch S is dependent on the signal (i.e. The channel charge is modulated by the signal), any non-linear behaviour of this switch will cause distortion of the signal for finite pulse width. Similarly, the finite pulse width of the switch S may be approximated, for passive RC circuit, as [45];

$$V_o(nT) = V_o\{(n-1)T\} + \frac{C_s}{C_s + C}\{1 - \exp(-\Delta/rC_x)\}\{V_{in}(nT) - V_o\{(n-1)T\}\}$$

where

Δ is the pulse width;

r is the average resistance of S,

C_x is the equivalent capacitive value of C and C_s in series.

From this equation we can conclude that the effect of finite pulse width is to increase the value of the switched capacitor C_s by the proportion $1/\{1-\exp(-\Delta/rC_x)\}$. Actually, this source of error is not a fundamental limitation on accuracy since it is simply an offset error.

2) Feedthrough: The non-linear capacitance, associated with the MOS transistor switch, including channel charging and discharging, results in a clock feedthrough error voltage. Referring to the circuit in Figure 4.6.a, after application of a pulse to the gate of the transistor, the resulting capacitor voltages are [42]:

$$V_1 = V_2 = \tfrac{1}{2}[V_1(o) + V_2(o)] + V_f$$

The magnitude of the error voltage, V_f, is proportional to the channel capacitance of the MOS switch C_o, and inversely proportional to the sum of charge sharing capacitors, that is;

$$V_f \quad \alpha^{\ell} \frac{C_o}{C_1 + C_2}$$

As discussed in [40] this error can be reduced by reading the capacitor voltages only after the gate voltage has been returned to zero. By this manoeuvre, the negative falltime feedthrough partially cancel the positive risetime feedthrough. Again, the feedthrough error can be minimized by using a charge canceling device* [42] shown in Figure 4.6.b.

3) Leakage current: Between the sampling periods, the leakage current in the switched capacitor will cause an offset error.

---

* It is a dummy device with the drain and source short circuited to block any flow of DC current.

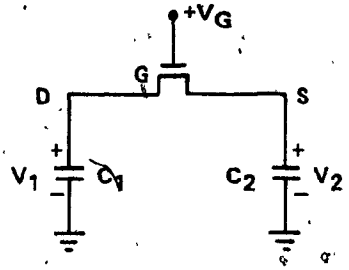

Figure 4.6.a Feed Through Effect

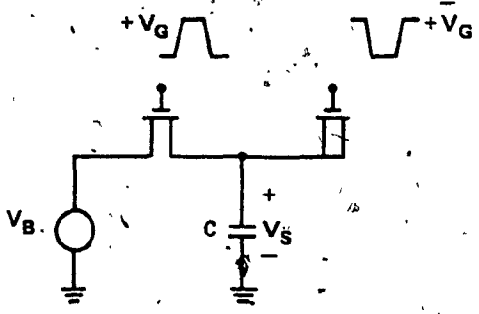

Figure 4.6.b Charge Canceling Device for Feed Through Compensation

4) Noise: Switched capacitor and operational amplifiers are the two major sources of noise in active switched capacitor networks. The switched capacitor noise is mainly thermal* of value (KT/C_s) for each switching operation, where C_s is the switching capacitance and KT is thermal voltage. This noise can be minimized by increasing the size of the switched capacitor.

5) Component matching: The attainable matching accuracy is higher for capacitors than resistors because of the difference between the aspect ratios of diffused resistors of practical values versus those of capacitors. A major source of component mismatches in integrated circuits is the uncertainties in photolithographic edge definition [42]. Table 4.1 lists published matching data on integrated resistors [47] and measured data on MOS capacitors as well as voltage and temperature coefficients on these components. The tabulated data suggest a standard deviation edge uncertainty of approximately 0.1 um.

4.6 EXPERIMENTAL RESULTS

The experimental integrated circuit schematic is shown in Figure 4.7. This experiment was conducted using fixed and switched capacitors as well as μA 741 operational amplifiers. MOS transistors were used as switches.

---

* Thermal noise is a phenonmenon associated with Brownian (random Thermal) motion of electrons in a conductor. The mean square velocity of the electrons is proportional to the absolute temperature.

Table 4.1 Characteristics of Integrated Resistors and Capacitors [44]

Component	Fabrication Technique	Standard Deviation Matching	Derived σ_x (μm)	Temperature Coefficient (ppm/°C)	Voltage Coefficient (ppm/y)
Resistors	Diffused (W=40μm)	± 0.23%	0.1	+1500 [2]	-200
	Ion-Implanted (W=40 μm)	± 0.12%	0.05	+ 400 [2]	-500
Capacitors	MOS (t_{OX} = 0.1 μm L = 10 Mils N^+ Substrate)	±0.06%	0.1	26	-10

L is the Resistor Length
W is the Resistor Width

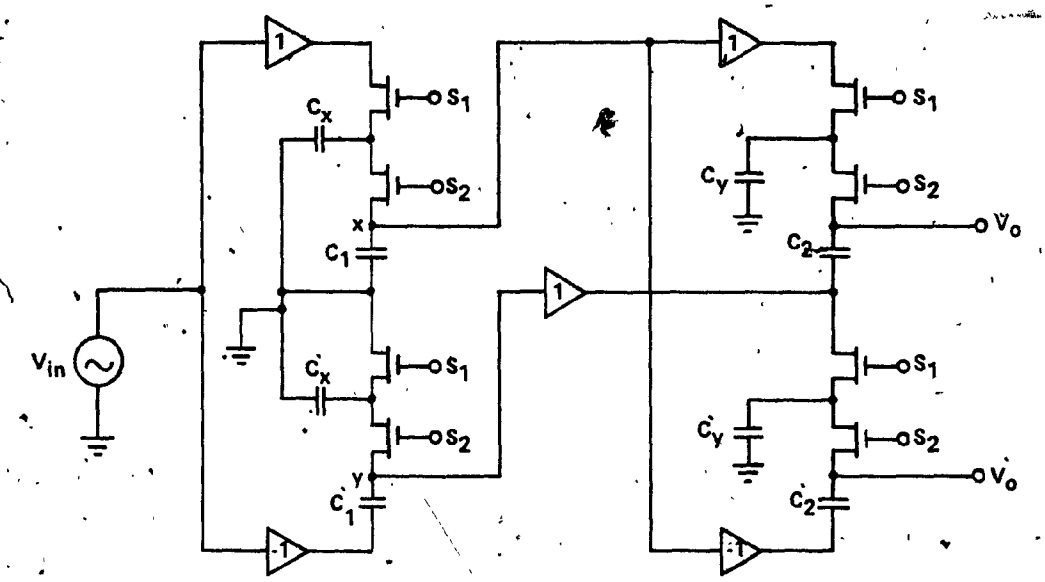

Figure 4.7 Sampled Data Sequence Discriminator Using Switched Capacitor and MOS Switches

The network was driven from a voltage source connected as shown, while the switches were operated with a unified clock rate of 25 KHz (higher clock rate was also considered). It was found experimentally that the 25 kHz rate is the optimum clock rate for simulating the resistive components.

The two output signals, which are in phase quadrature, were used to generate 4 phase sequence (either positive or negative) as previously discussed. The four modulated waveforms shown in Figure 5.6 were used for modulation purposes as in the RC active design.

The experimental result is shown in Figure 4.8. It was found that a slight modification of about 10% was required in the values of the switched capacitors in the second section to obtain the designed value of the second notch frequency with relatively good depth of notch compared with that without modification. This can be explained in terms of the clock feedthrough which is caused by the inherent capacitance of switches as well as the channel charging and discharging capacitance as previously explained. Also, this deviation from the designed values can be explained in terms of the incomplete transfer of charge due to the finite ON resistance of switches.

The experimental result shown in Figure 4.8 confirm the theoretical results as depicted in Figure 4.5. It should be pointed out that the network response was obtained for identical capacitor ratios in each individual section of the two stage sequence discriminator.

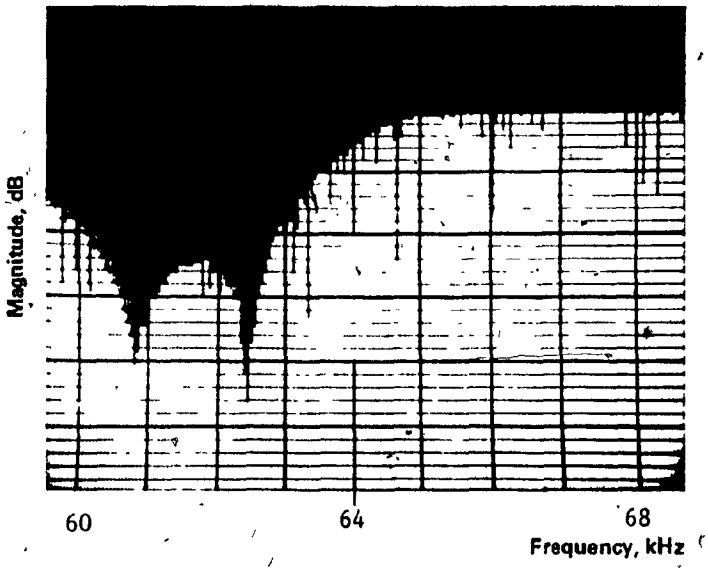

Figure 4.8 Frequency Response of the Switched Capacitor Network
Vertical Scale 10 dB/div.
Sampling Rate 25 kHz

4.7 CONCLUSIONS

The sampled data active phase splitting sequence discriminator discussed in this chapter has demonstrated the possibility of replacing the active RC circuits, of chapters 2 and 3, by a new circuit configuration with all its resistor elements replaced by switched capacitors. The new configuration does not require any trimming operation and can be fully integrated with MOS LSI technology. The characteristics of this filter such as its resonant (notch) frequency and selectivity can be controlled by varying the capacitor ratios in any section or by varying the operating clock rate or both. This new configuration can be used in many applications requiring 90 degree phase difference networks.

The basic concept of the design, of this class of network is the simulation of a resistor element with a combination of a capacitor and two switches. The filter coefficients, being ratio of capacitors, can be made less sensitive to manufacturing processes.

The conventional active-RC filter theory and design may be directly applied, without significant change, in many practical situations, and can also be used as a design procedure along with the exact analysis using z-transform techniques.

CHAPTER V

SINGLE-SIDEBAND SIGNAL GENERATION AND DETECTION

5.1 INTRODUCTION

Generating single-sideband signals having the required amounts of unwanted sideband suppression, and channel bandwidth presents a problem in the design of single-sideband devices. The existing methods of single sideband signal generation may be classified into two types:

1. Successive modulation by performing modulations and filtering for several stages.
2. Cancellation method by applying the phase rotation.

Attention has recently been drawn to the 90 degree phase shift networks as a mean of generating single sideband signals [7-11]. The phase shift method permits simultaneous generation of a two-channel single-sideband signal in which upper and lower sidebands convey different intelligence [17].

In this chapter the concept of frequency translation and single-sideband signal generation is first discussed. A brief analysis of the N-path filter [5] is then given together with Gingell's sequence asymmetric filter [4]. The generation and detection of single-sideband signals using the proposed networks (discussed in the previous chapters) is given together with the difficulties that one may encounter. Finally a complete single sideband modulator/demodulator is suggested.

5.2 FREQUENCY TRANSLATION AND SINGLE-SIDEBAND SIGNAL GENERATION

5.2.1 Frequency Translation

In communication engineering the signals are transmitted from one point to the other through a channel which may be in the form of a pair of wires (such as telephone channel) or merely an open space in which the signals bearing information are radiated (e.g. radio and television broadcasting, satellite communication, etc). Each of these signals has a small finite bandwidth compared to that of the channel itself. It is therefore wasteful to transmit one signal at a time on a channel since the channel will be operated very much below its capacity to transmit information [47]. It is now possible to transmit a large number of signals at the same time on one channel by using modulation techniques, which in effect shifts the frequency spectrum of the desired signal to a higher frequency range. Modulation, therefore, not only allows the simultaneous transmission of several signals without interference, but it also makes it possible to transmit these signals effectively.

In many filtering applications the signals to be dealt with are audio signals which are to be translated to/from higher frequencies (frequency division multiplexing, hetrodyne receivers, etc.). From the modulation theorem [47], the spectrum of any signal can be translated by $\pm \omega_c$ in the frequency domain by multiplying such signal by a periodic signal of frequency ω_c. For frequencies above a few tens of kilohertz, filters reported so far in the literature fail to operate with commerically available operational amplifier of the 741 family or equivalent [37, 48]. Using quadrature modulation for filtering, the

active 90 degree phase splitting networks can be used to operate beyond the audio frequency range since both filtering and frequency translation are achieved in one step. The direct modulation scheme to place a group of 12 voice channels into the prescribed frequency band of 60–108 kHz is shown in Figure 5.1.

5.2.2 N-Path Filters and Single-Sideband Signal Generation

In this section the N-path filter concept is discussed and compared with the polyphase sequence discriminator [3,5] as used for single-sideband signal generation. The N-path filter is shown in Figure 5.2, where there are N identical paths each of which consists of:

1) A modulator with V(t) as an input signal and P(t) as the first modulating function.
2) A bandpass filter with a transfer function h(t).
3) A second modulator with q(t) as the second modulating function.

The band-limited* input signal is applied to the first set of modulators. The outputs from the second set of modulators are summed and passed through another band-limiter as shown in Figure 5.2. It has been shown [3] that, if the modulating signals to any set of modulators have the same waveform but delayed in time with respect to each other by T/N (each

---

* In practice, to minimize the effects of the unwanted products produced by modulation, it is necessary to band-limit this signal to eliminate all the unnecesary products.

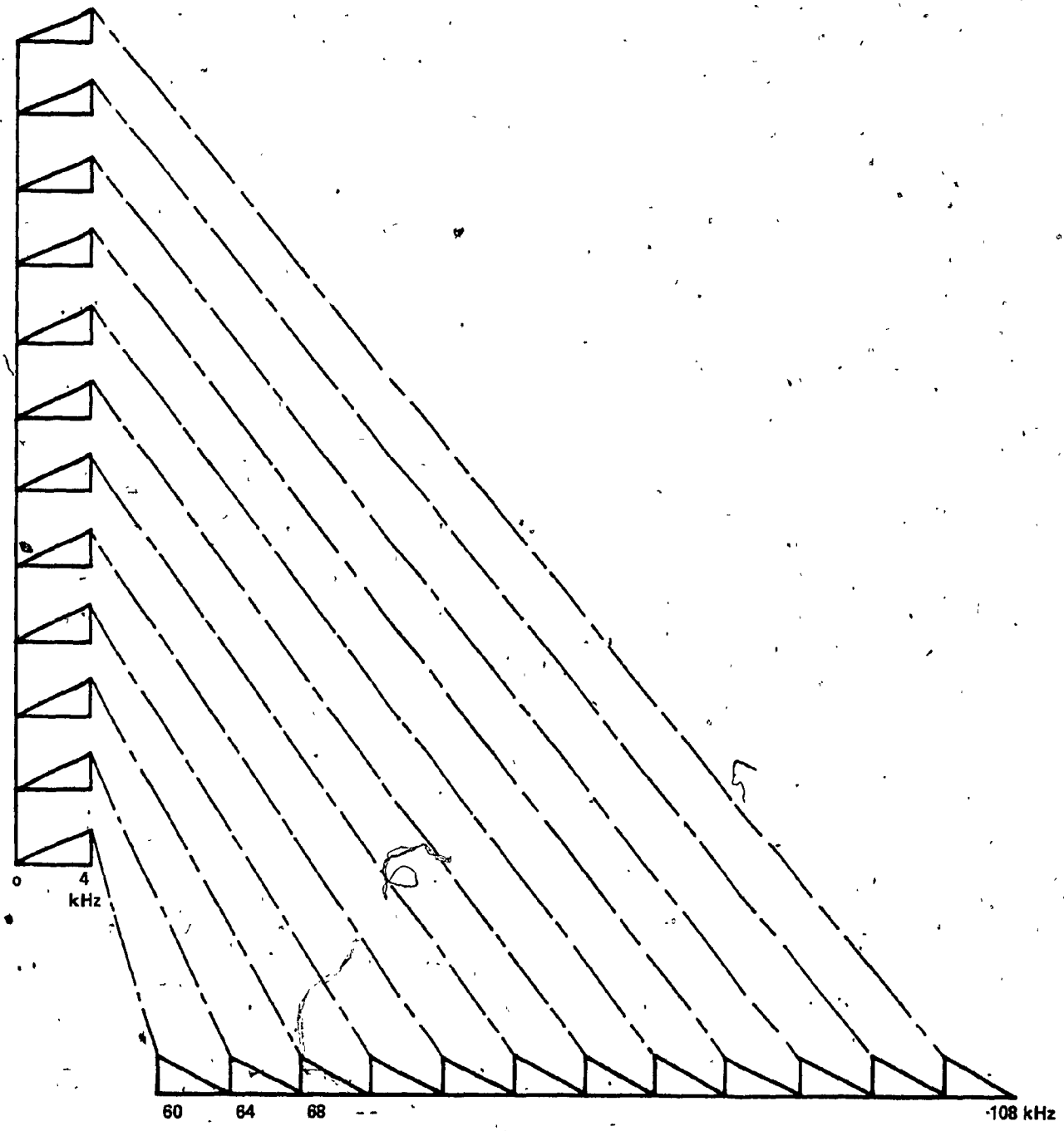

Figure 5.1 Direct Modulation Scheme

path is delayed in time w.r.t. the previous one by T/N) where N is the number of paths, then the summed output $V_o(\omega)$ can be written as [3]:

$$V_o(\omega) = N \sum_{L=-\infty}^{L=+\infty} \sum_{k=-\infty}^{k=+\infty} k_1 \cdot H(\omega - L\omega_1) \cdot V_1(\omega - L\omega_1 - k\omega_2) \qquad (5.1)$$

where

N is the number of paths,

K is a constant,

H( ) is the filter transfer function,

$k_1 = -\frac{1}{2}$ for $L = \pm 1$ and $k = \pm 1$,

and

ω_1 and ω_2 are the two carrier frequencies.

In most cases the terms of interest are mainly those that correspond to $L = \pm 1$ and $K = \pm 1$ while all other terms can be suppressed by suitable choice of modulating waveform or by pre or post filtering.

For L = 1 and K = 1, equation (5.1) is simplied to:

$$V_o(\omega) = N. k_1 H(\omega - \omega_1) \cdot V\{\omega - (\omega_1 + \omega_2)\} \qquad (5.2)$$

It can be seen from (5.2) that the lower sideband signals is produced while the upper sideband is suppressed. The generated lower sideband signal is attenuated by the factor $NK_1H(\omega - \omega_1)$ as shown in (5.2).

Gingle [3,4] had implemented the idea of N-path filter in his design of the sequence asymmetric polyphase filter. He has shown that

the N filters in the above design can be replaced by a single N-phase sequence asymmetric polyphase filter with transfer function H( ) as shown in Figure 5.3. By summing the N-path outputs and by assuming the two carrier to be identical, then;

$$V_o(\omega) = \frac{N}{4}\left[H(\omega - \omega_c) + H(\omega + \omega_c)\right]V_1(\omega) \qquad (5.3)$$

where ω_c is the carrier frequency.

By a proper design of the filter transfer function $H(\omega)$ to pass only negative frequencies and attenuate positive frequencies, a lowpass filter results which has a transfer function of: $V_o/V_1 = \frac{N}{4} H(\omega - \omega_c)$

5.3 MODULATORS AND SINGLE-SIDEBAND SIGNAL GENERATION

The general properties of the modulator/demodulator (MODEM) used in this thesis will be investigated in this section. The characteristics of the analog multipliers impose restrictions on their suitability for our application. CMOS bilateral switch is found to be the most successful candidate. These switches were used to produce symmetrical four-phase waveforms with a clock rate of T seconds. They are characterized by low-power, low-cost, and are commercially available in different forms as a set of matched quad bilateral switches, or as a differential four channel multiplexer/demultiplexer with logic level conversion. In addition to their excellent linearity, the switches possess the following features [48]:

1. Extremely low off switch leakage resulting in very low offset current and high off-resistance.

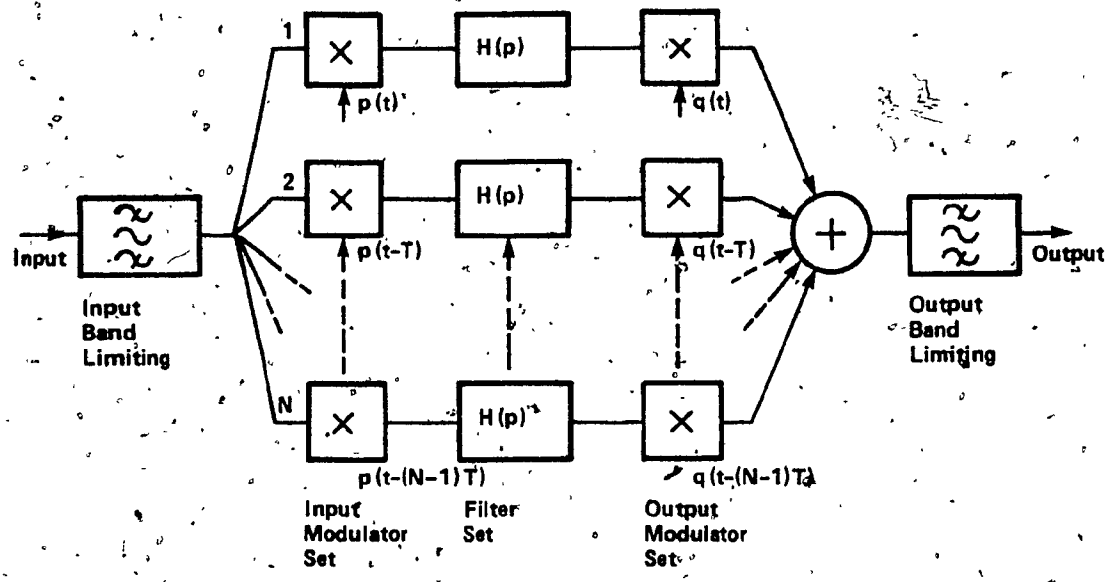

Figure 5.2 The N-Path Configuration

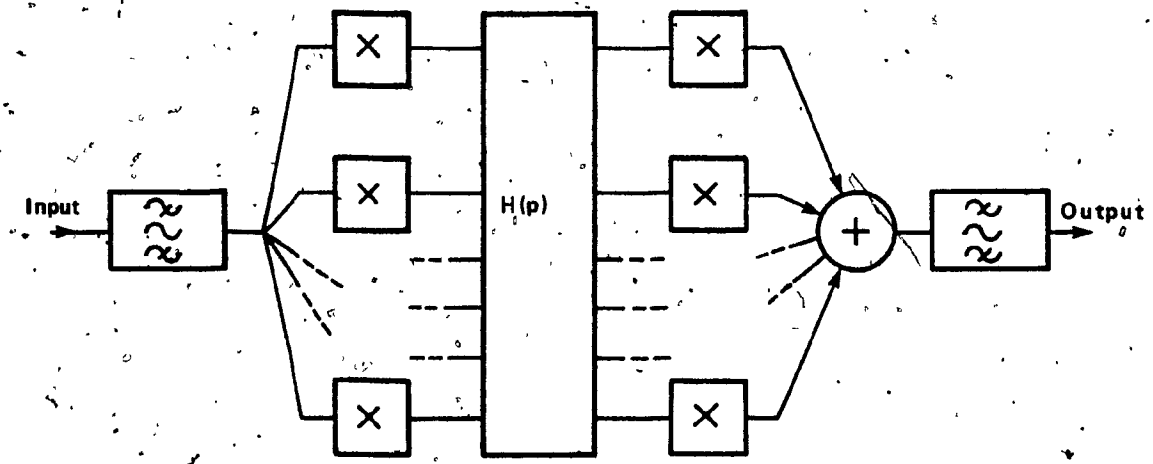

Figure 5.3 N-Path Filter with Sequence Asymmetric Polyphase Filter

2. High on/off output voltage ratio (typically 65 dB, f_{is} = 10 KHz, R = 10 k Ω).

3. Low crosstalk between switches

4. Extremely high control input impedance (control circuit isolated from signal circuit)

5. Low ON resistance.

The modulation scheme is shown in Figure 5.4. The two output signals V_o and V_o' from the sequence discriminator are inverted to generate four signals 90 degree phase apart which constitute a symmetric sequence and are applied to the input of the modulators. The four modulated signals (carrier signals) are generated using a dual D-type flip-flop switch together with the simple circuit shown in Figure 5.5. The input signal to the switch is 4 f_c cycle/second, where f_c is the required carrier frequency, which is converted into the four switching pulse trains each of T clock rate as shown in Figure 5.6.

Let P(t) be the modulated pulse which can be replaced by its Fourier series,

$$\hat{P}(t) = \sum_{m=-\infty}^{m=+\infty} P_m \exp(jm\omega_c t) \qquad (5.4)$$

where

$$\omega_c = 2\Pi f_c = \frac{2\Pi}{T}$$

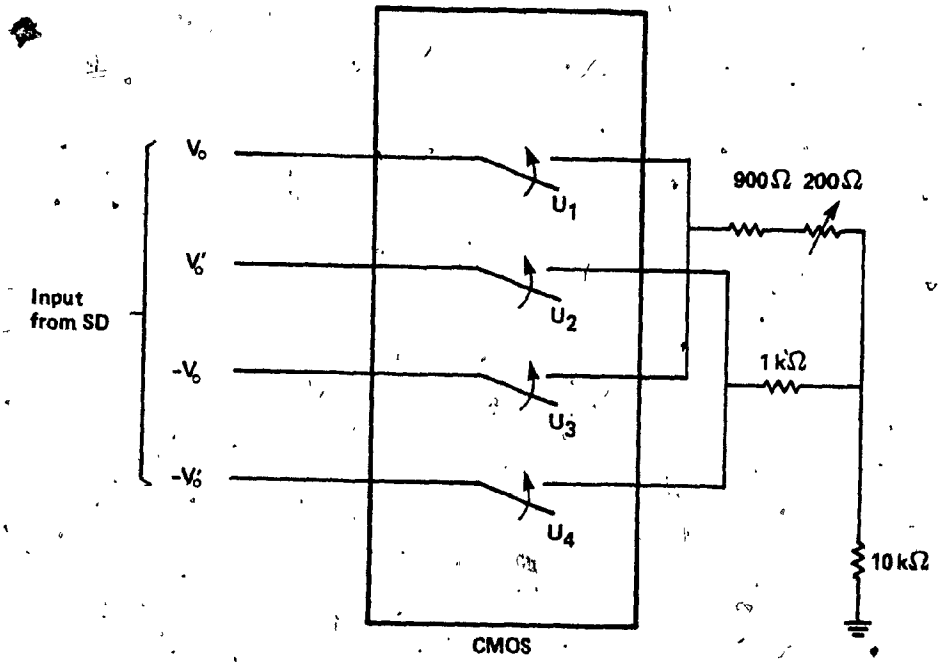

Figure 5.4 Modulation Scheme

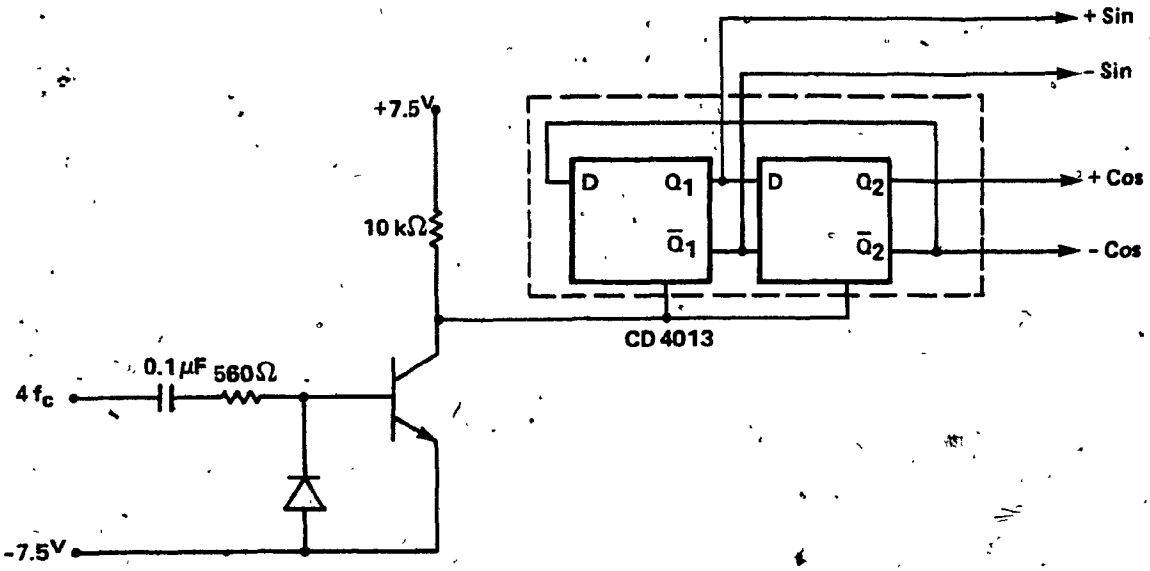

Figure 5.5 Generation of the Four Modulated Signals with Carrier Frequency f_c

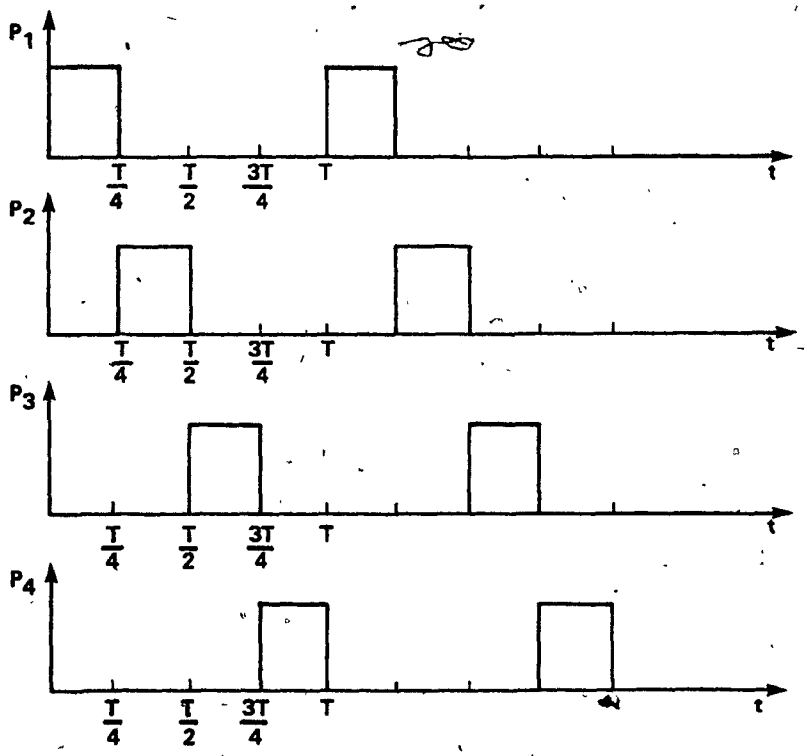

Figure 5.6 (a) Schematic Represention of the Switching Pulses

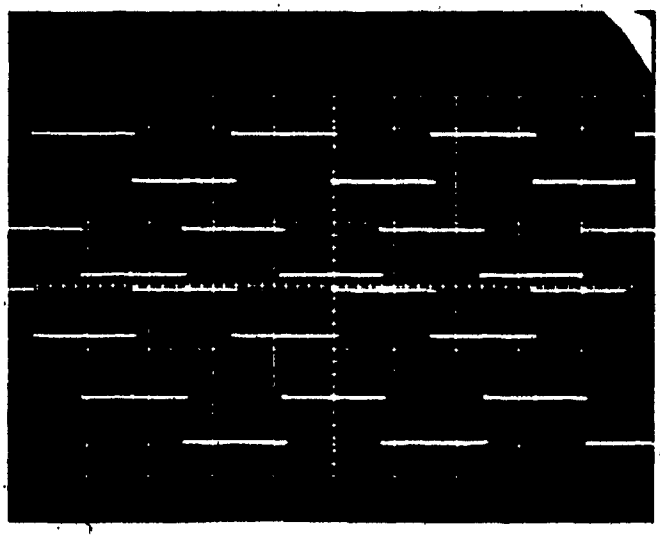

Figure 5.6(b) The Four Switching Pulses

and

$$P_m = \frac{1}{T} \int_{-\frac{T}{2}}^{\frac{T}{2}} P(t).\ \exp(-jm\omega_c t).\ dt \qquad (5.5)$$

For a pulse of width t_o the above integration yields

$$P_m = \frac{1}{T} \int_{o}^{t_o} 1.\ \mathrm{Cos}(m\omega_c t)\ dt \qquad (5.6)$$

$$P_m = k.\ \frac{\mathrm{Sin}(2\Pi mk)}{2\Pi mk} \qquad (5.7)$$

where $t_o = KT$. Back substitution in (5.4) gives

$$P(t) = k.\ \sum_{m=-\infty}^{m=+\infty} \mathrm{Sa}(2\Pi mk).\ \mathrm{Cos}(m\omega_c t) \qquad (5.8)$$

where

$\mathrm{Sa}(2\Pi mk) = P_m$ is the sampling function defined by (5.7)

As shown in Figure 5.6, the modulated signal in the r^{th} path is delayed in time by an amount T/N seconds with respect to that in the $(r-1)^{th}$ path, where N is the number of phases.

For a duty period (1/4), the four modulated functions take the form

$$P_1(t) = \sum_{m=-\infty}^{m=\infty} \mathrm{Sa}\ (2\Pi mk).\ \mathrm{Cos}(m\omega_c t)\ , \qquad (5.9\text{-a})$$

$$P_2(t) = \sum_{m=-\infty}^{m=\infty} \mathrm{Sa}\ (2\Pi mk).\ \mathrm{Cos}\{m\omega_c (t-\tfrac{T}{4})\}\ , \qquad (5.9\text{-b})$$

$$P_3(t) = \sum_{m=-\infty}^{m=\infty} Sa\,(2\Pi mk).\ \mathrm{Cos}\{m\omega_c(t - \frac{T}{2})\} \qquad (5.9\text{-c})$$

$$P_4(t) = \sum_{m=-\infty}^{m=\infty} Sa\,(2\Pi mk).\ \mathrm{Cos}\{m\omega_c(t - \frac{3T}{4})\} \qquad (5.9\text{-d})$$

The four modulating signals from the sequence discriminator for the negative sequence input are:

$$V_1(t) = V_o\ \mathrm{Cos}(\omega_s t + \theta_s) \qquad (5.10\text{-a})$$

$$V_2(t) = V_o\ \mathrm{Cos}(\omega_s t - \frac{\Pi}{2} + \theta_s) \qquad (5.10\text{-b})$$

$$V_3(t) = V_o\ \mathrm{Cos}(\omega_s t - \Pi + \theta_s) \qquad (5.10\text{-c})$$

$$V_4(t) = V_o\ \mathrm{Cos}(\omega_s t - \frac{3\Pi}{2} + \theta_s) \qquad (5.10\text{-d})$$

To perform the modulation process, each one of the modulating functions in (5.10) is multiplied by its corresponding modulated function in (5.9). The output signal M_i from the modulator i, after modulation is given by,

$$M_i = V_i\ P_i$$

Applying the frequency shifting property [49], the Fourier spectrum of a modulated signal $f(t)\ \mathrm{COS}\,\omega_c t$ is given by

$$f(t).\ \mathrm{Cos}\ \omega_c t \leftrightarrow \tfrac{1}{2}\,[F(\omega - \omega_c) + F(\omega + \omega_c)]$$

Hence,

$$M_1(t) \leftrightarrow \Pi kV_o\,[\delta(\omega - \omega_s) + \delta(\omega + \omega_s)] + \frac{\Pi}{2}\,kV_o \sum_{m=1}^{\infty} Sa\,(2\Pi mk).$$

$$[\delta\{\omega - (m\omega_c + \omega_s)\} + \delta\{\omega + (m\omega_c + \omega_s)\}$$

$$+ \delta\{\omega - (m\omega_c - \omega_s)\} + \delta\{\omega + (m\omega_c - \omega_s)\}\,, \qquad (5\text{-}11\text{-}b)$$

$$M_2(t) \leftrightarrow j\Pi kV_o\,[\delta(\omega + \omega_s) - \delta(\omega - \omega_s)] + j\,\frac{\Pi}{2}\,kV_o \sum_{m=1}^{\infty} Sa\,(2\Pi mk).$$

$$[\exp(-j\frac{T}{4}m\omega_c)[\delta\{\omega - (m\omega_c - \omega_s)\} - \delta\{\omega - (m\omega_c + \omega_s)\}]$$

$$+ \exp(j\frac{T}{4}m\omega_c)[\delta\{\omega + (m\omega_c + \omega_s)\} - \delta\{\omega + (m\omega_c - \omega_s)\}]], \qquad (5\text{-}11\text{-}b)$$

$$M_3(t) \leftrightarrow -\Pi kV_o[\delta(\omega - \omega_s) + \delta(\omega + \omega_s)] - \frac{\Pi}{2}\,kV_o \sum_{m=1}^{\infty} Sa\,(2\Pi mk).$$

$$[\exp(-j\frac{T}{2}m\omega_c)[\delta\{\omega - (m\omega_c + \omega_s)\} + \delta\{\omega - (m\omega_c - \omega_s)\}]$$

$$+ \exp(j\frac{T}{2}m\omega_c)[\delta\{\omega + (m\omega_c - \omega_s)\} + \delta\{\omega + (m\omega_c + \omega_s)\}]], \qquad (5\text{-}11\text{-}c)$$

$$M_4(t) \leftrightarrow -j\Pi kV_o[\delta(\omega + \omega_s) - \delta(\omega - \omega_s)] - j\,\frac{\Pi}{2}\,kV_o \sum_{m=1}^{\infty} Sa\,(2\Pi mk).$$

$$[\exp(-j\frac{3T}{4}m\omega_c)[\delta\{\omega - (m\omega_c - \omega_s)\} - \delta\{\omega - (m\omega_c + \omega_s)\}]$$

$$+ \exp(j\frac{3T}{4}m\omega_c)[\delta\{\omega + (m\omega_c + \omega_s)\} - \delta\{\omega + (m\omega_c - \omega_s)\}]] \qquad (5\text{-}11\text{-}d)$$

Table 5.1 gives the exponential values for m = 1, 2

Summing up all the modulated functions as given in (5-11), the summed output M_o is given by,

$$M_o = \sum_{i=1}^{i=4} M_i \qquad (5.12)$$

The four modulated signals and the summed output are sketched in Figure 5.7.

From Figure 5.7 and Table 5.2, it can be seen that for the negative input sequence, the summed output adds at $\omega_c - \omega_s$ and cancels at ω_s, $\omega_c + \omega_s$ and $2\omega_c \pm \omega_s$. It also adds at the higher harmonics $n\omega_c \pm \omega_s$, $n > 2$. Similar conclusions can be reached for the positive input sequence, where in this case, the summed output adds at $\omega_c + \omega_s$ and cancels at ω_s, $\omega_c - \omega_s$

Table 5.1 Numerical Values of $\exp(\pm jm\omega_c t_o)$ for $t_o = kT$, $k = 1/4$ and $m = 1, 2$

m	$\exp(\pm jm\omega_c \frac{T}{4})$	$\exp(\pm jm\omega_c \frac{T}{2})$	$\exp(\pm jm\omega_c \frac{3T}{4})$
1	$\pm j$	-1	$\mp j$
2	-1	$+1$	-1

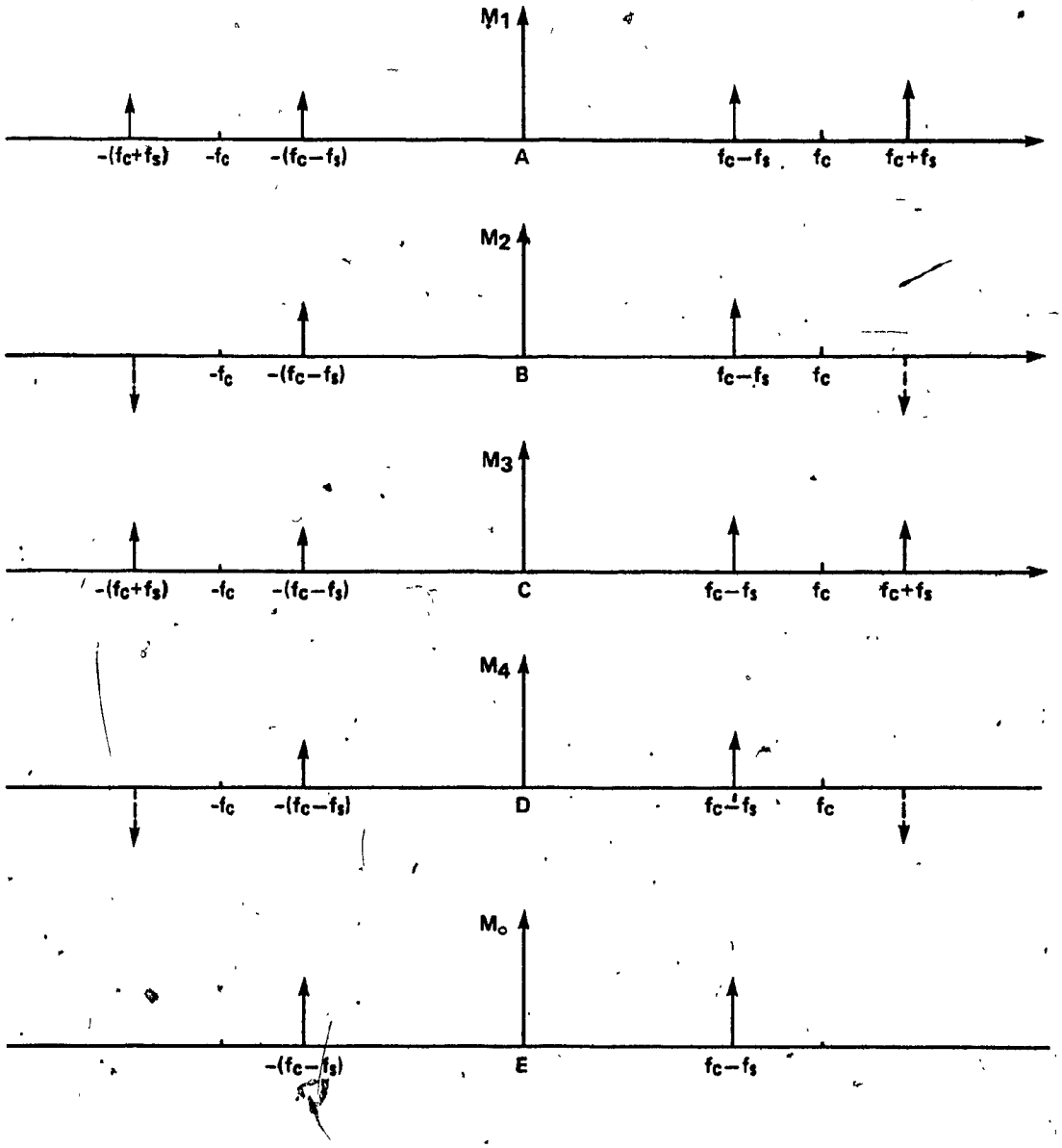

Figure 5.7 Schematic Representation of the Four Modulated Signals (M_1-M_4) and Their Final Sum (M_o)

Table 5.2 Modulated Components for Various Values of m

m	Frequency	Multiplier Constant	Modulated Components	
			Negative Sequence	Positive Sequence
0	ω_s	k	V_o Cos V_o Sin	V_o Cos V_o Sin
			$-V_o$ Cos $-V_o$ Sin	$-V_o$ Cos $-V_o$ Sin
1	$\omega_c - \omega_s$	$k \frac{\text{Sin } 2\,\Pi\, k}{2\,\Pi\, k}$	V_o Cos V_o Cos	V_o Cos $-V_o$ Cos
			V_o Cos V_o Cos	V_o Cos $-V_o$ Cos
	$\omega_c + \omega_s$	$k \frac{\text{Sin } 2\,\Pi\, k}{2\,\Pi\, k}$	V_o Cos $-V_o$ Cos	V_o Cos V_o Cos
			V_o Cos $-V_o$ Cos	V_o Cos V_o Cos
2	$2\omega_c + \omega_s$	$k \frac{\text{Sin } 4\,\Pi\, k}{4\,\Pi\, k}$	V_o Cos $-V_o$ Cos	V_o Cos $\mp V_o$ Sin
			$\pm V_o$ Sin $\mp V_o$ Sin	$-V_o$ Cos $\pm V_o$ Sin

and $2\omega_c \pm \omega_s$ as also shown in Table 5.2.

The summed output M_o is given in terms of its Fourier spectrum as

$$M_o \leftrightarrow 2\Pi k V_o . Sa\ (2\Pi k)\ [\delta\{\omega - (\omega_c - \omega_s)\} + \delta\{\omega + (\omega_c - \omega_s)\}] \quad (5.13)$$

By taking the inverse Fourier transform of (5.13), the summed output is:

$$M_o = 2kV_o \quad \frac{Sin\ 2\Pi k}{2\Pi k} . Cos\{(\omega_c - \omega_s)t\} \quad (5.14)$$

Note that in the above derivations we have assumed $\theta = 0$ for simplicity only. As can be seen from (5.14) the lower sideband is produced while the upper sideband is suppressed. For positive sequence input and frequency $\omega_c + \omega_s$, it can be easily shown that the summed output is give by:

$$M_o = 2kV_o \quad \frac{Sin\ 2\Pi k}{2\Pi k} . Cos\{(\omega_c + \omega_s)t\} \quad (5.15)$$

and the USB is produced, while the LSB is suppressed. Figure 5.8 gives two possible modulation schemes together with summing circuit for two different duty periods, i.e. $k = \frac{1}{2}$ and $k = \frac{1}{4}$

Alternately, the LSB as given by (5.14) or the USB as given by (5.15) can be produced by interchanging the input to the modulators P_1 and P_3. Similar results can be obtained by interchanging the input signals V_1 and V_3 or V_2 and V_4. The above results concerning the generation of single-sideband signals are summarized in Table 5.2.

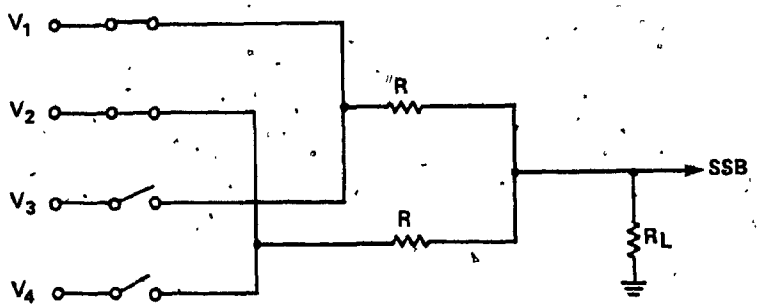

Figure 5.8(a) Modulation Scheme and Summing Circuit for Duty Period k = ½

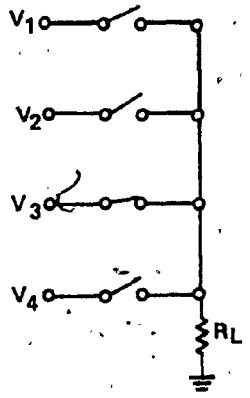

Figure 5.8(b) Modulation Scheme and Summing Circuit for Duty Period k = ¼

5.4 DEMODULATORS AND SINGLE SIDEBAND SIGNAL DETECTION

The spectrum of the modulated waveforms as given by equations (5.11) can be conviently retranslated to obtain the original signal by multiplying the modulated signal by the carrier signal at the receiving end. The four switching signals used for demodulation are identically the same as those in Figure 5.6. If the network is driven from a voltage source, another set of switches which is driven by the complementary logic signals in Figure 5.6, is used to short the input to the reference in the absence of the signal to this input.

Since multiplication in time domain is equivalent to convolving the spectrum in the frequency domain, it is evident that the spectrum of the resultant signal will be obtained by convolving the spectrum of the received signal with that of the carrier signal.

The demodulation scheme is shown in Figure 5.9. The incoming signal (12 channels occupy the frequency range 60-108 kHz) is multiplied by the four carrier signals in figure 5.6. Assuming the input signal to the demodulator as $V_s \sin\omega_s t$, then the four demodulated signals are:

$$D_1 = kV_s \sum_{m=-\infty}^{m=+\infty} Sa(2\Pi mk) \cdot \cos(m\omega_c t) \cdot \sin\omega_s t \qquad (5.16\text{-a})$$

$$D_2 = kV_s \sum_{m=+\infty}^{m=+\infty} Sa(2\Pi mk) \cdot \cos\{m\omega_c (t - \frac{T}{4})\} \cdot \sin\omega_s t \qquad (5.16\text{-b})$$

$$D_3 = kV_s \sum_{m=-\infty}^{m=\infty} Sa(2\Pi mk).\ Cos\{m\omega_c(t-\frac{T}{2})\}.\ Sin\ \omega_s t \qquad (5.16\text{-c})$$

$$D_4 = kV_s \sum_{m=-\infty}^{m=\infty} Sa(2\Pi mk).\ Cos\{m\omega_c(t-\frac{3T}{4})\}.\ Sin\ \omega_s t \qquad (5.16\text{-d})$$

where $Sa(2\Pi mk)$ is the sampling function defined in (5.7). The Fourier spectrum of the four demodulated signals is shown in Appendix E. From this Appendix, the frequency components of the four demodulated signals up to $2\omega_c + \omega_s$ are given in Table 5.3.

It can be shown that the four demodulated outputs form a symmetric sequence which changes polarity as f_s changes from above to below the carrier [25], as shown in Figure 5.10. Therefore, the sequence discriminator, which is able to distinguish between sequences in the voice frequency range can reject the adjacent channel on the other side of the carrier. A low pass filter can be used to reject the remaining channels.

5.5 SINGLE-SIDEBAND SIGNAL GENERATION USING THE SWITCHED CAPACITOR SEQUENCE DISCRIMINATOR

Similar to the RC active design sequence discriminator the switched capacitor sequence discriminator network was used to generate four phase symmetric sequence, of either polarity, which was used as an input to the four modulators as shown in Figure 5.4. These modulated signals were multiplied by their corresponding modulating ones of Figure 5.6 and the final outputs from these multipliers were summed out to

Table 5.3 Frequency Components of the Demodulated Four Outputs

Frequency	Multiplier	Demodulated Components			
ω_s	kV_s	Sin	Sin	Sin	Sin
$\omega_c - \omega_s$	$V_s \frac{\text{Sin } k\pi}{\pi}$	−Sin	Cos	Sin	−Cos
$\omega_c + \omega_s$	$V_s \frac{\text{Sin } k\pi}{k}$	Sin	−Cos	−Sin	Cos
$2\omega_c - \omega_s$	$V_s \frac{\text{Sin } 2k\pi}{2\pi}$	−Sin	Sin	−Sin	Sin
$2\omega_c + \omega_s$	$V_s \frac{\text{Sin } 2k\pi}{2\pi}$	Sin	−Sin	Sin	−Sin

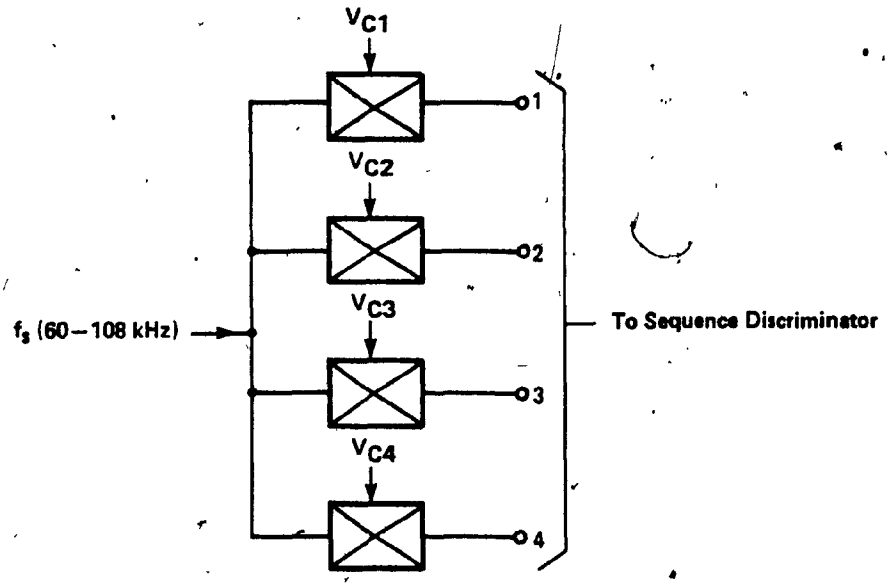

Figure 5.9 Demodulation Scheme

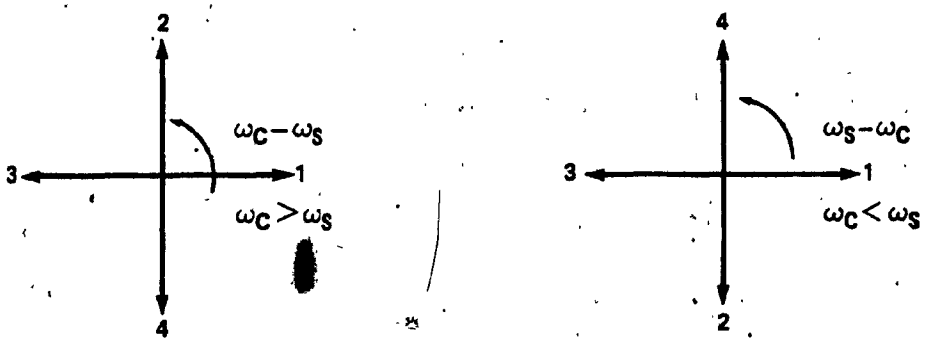

Figure 5.10 Sequences Resulting from Demodulation (Lower Side Band $f_C - f_s$)

generate single-sideband signal.

The same mathematical approach discussed in section 5.3 can be applied here for this purpose. The main difference, in the case of the switched capacitor filter design, is that the outputs of this filter are of discrete form which are functions of the switching rate. In such a case the application of sampling theorem reduces the problem of transmitting a continuously varying waveform to one of transmitting a discrete number of amplitude values.

Consider a signal f(t) which is assumed to be bandlimited*. This signal can be represented exactly by samples spaced relatively far apart such that;

$$f(t) = \sum_{k=-\infty}^{k=+\infty} f\left(\frac{k}{2w}\right) \frac{\text{Sin } (2\pi wt - k\pi)}{(2\pi wt - k\pi)}$$

this expression relates the discrete time domain {k/2w} with sample values f(k/2W) to the continuous time domain {t} of the function f(t).

The process of sampling can be thought of as the product modulation of the input signal and a set of impulses. Accordingly, the two output signals from the switched capacitor filter can be written as:

$$V_o(t) = V_o(nT_o) = A \text{ Cos } (\omega_s t + \theta_s) \qquad nT_o \leq t < (2n+1)\frac{T_o}{2}$$

$$= 0 \qquad (2n+1)\frac{T_o}{2} \leq t < (n+1)T_o$$

and

$$V'_o(t) = V'_o(nT_o) = A \text{ Cos } (\omega_s t - \frac{\pi}{2} + \theta_s) \qquad nT_o \leq t < (2n+1)\frac{T_o}{2}$$

$$= 0 \qquad (2n+1)\frac{T_o}{2} \leq t < (n+1)T_o$$

---

* A signal f(t) is said to be band limited in the interval $(-2\pi w, 2\pi w)$ if its Fourier transform $f(\omega)$ has the property $f(\omega) = 0 \qquad |\omega| > 2\pi w$

where

n is an integer, n = 0, 1, 2, ...

and T_o is the switching period.

For a negative sequence input, the four modulating signals from the sequence discriminator can be written as:

$$V_1(t) = V_1(nT_o) = A \text{ Cos } (\omega_s t + \theta_s) \quad , \quad nT_o \leq t < (2n+1)\frac{T_o}{2}$$

$$V_2(t) = V_2(nT_o) = A \text{ Cos } (\omega_s t - \frac{\pi}{2} + \theta_s) \quad , \quad nT_o \leq t < (2n+1)\frac{T_o}{2}$$

$$V_3(t) = V_3(nT_o) = A \text{ Cos } (\omega_s t - \pi + \theta_s) \quad , \quad nT_o \leq t < (2n+1)\frac{T_o}{2}$$

$$V_4(t) = V_4(nT_o) = A \text{ Cos } (\omega_s t - \frac{3\pi}{2} + \theta_s) \quad nT_o \leq t < (2n+1)\frac{T_o}{2}$$

and

$$V_1(nT_o) = V_2(nT_o) = V_3(nT_o) = V_4(nT_o) = 0 \quad (2n+1)\frac{T_o}{2} \leq t < (n+1)T_o$$

For a duty period ($k = \frac{1}{2}$), the four modulated functions take the form given by (5-9).

Following the same mathematical procedure discussed in section 5.3, the output modulated signal M_i from any modulator i can be expressed as;

$$M_i = V_i P_i$$

For simplicity take $\theta = 0$, then;

$$M_1 = A \text{ Cos } \omega_s t \left\{K \sum_{m=-\infty}^{m=+\infty} S_a(2\pi mk) \text{ Cos } m\omega_c t\right\} \quad , \quad nT_o \leq t < (2n+1)\frac{T_o}{2}$$

$$M_1 = \tfrac{1}{2} AK \sum_{m=-\infty}^{m=+\infty} S_a(2\pi mk) \left[\text{Cos}(m\omega_c + \omega_s)t + \text{Cos}(m\omega_c - \omega_s)t)\right] \quad ,$$

Similarly

$$M_2 = A \cos\left(\omega_s t - \frac{\pi}{2}\right) \left[K \sum_{m=-\infty}^{m=+\infty} S_a(2\pi mk) \cos\left\{m\omega_c\left(t - \frac{T}{4}\right)\right\}\right], \quad nT_o \le t < (2n+1)\frac{T_o}{2}$$

$$M_2 = \tfrac{1}{2} AK \sum_{m=-\infty}^{m=+\infty} S_a(2\pi mk) \left[\cos\left\{m\omega_c'\left(t - \frac{T}{4}\right) + \omega_s t - \frac{\pi}{2}\right\} + \cos\left\{m\omega_c\left(t - \frac{T}{4}\right) - \omega_s t + \frac{\pi}{2}\right\}\right]$$

$$M_3 = A \cos(\omega_s t - \pi) \left[K \sum_{m=-\infty}^{m=+\infty} S_a(2\pi mk) \cos\left\{m\omega_c\left(t - \frac{T}{2}\right)\right\}\right], \quad nT_o \le t < (2n+1)\frac{T_o}{2}$$

$$= \tfrac{1}{2} AK \sum_{m=-\infty}^{m=+\infty} S_a(2\pi mk) \left[\cos\left\{m\omega_c\left(t - \frac{T}{2}\right) + \omega_s t - \pi\right\} + \cos\left\{m\omega_c\left(t - \frac{T}{2}\right) - \omega_s t + \pi\right\}\right].$$

$$M_4 = A \cos\left(\omega_s t - \frac{3\pi}{2}\right) \left[K \sum_{m=-\infty}^{m=+\infty} S_a(2\omega mk) \cos\left\{m\omega_c\left(t - \frac{3T}{4}\right)\right\}\right], \quad nT_o \le t < (2n+1)\frac{T_o}{2}$$

$$= \tfrac{1}{2} AK \sum_{m=-\infty}^{m=+\infty} S_a(2\pi mk) \left[\cos\left\{m\omega_c\left(t - \frac{3T}{2}\right) + \omega_s t - \frac{3\pi}{2}\right\} + \cos\left\{m_\omega c\left(t - \frac{3T}{2}\right) - \omega_s t + \frac{3\pi}{2}\right\}\right]$$

and

$$M_1(nT_o) = M_2(nT_o) = M_3(nT_o) = M_4(nT_o) = 0 \quad , \qquad (2n+1)\frac{T_o}{2} \le t < (n+1)\frac{T_o}{2}$$

The summed output is given by;

$$M_o = \sum_{i=1}^{i=4} M_i$$

$$= 0 \qquad \text{for } m = 0$$

and for $m = 1$

$$M_o = 2\,AK\,S_a(2\pi k)\left[\cos(\omega_c - \omega_s)t\right]$$

From the above derivations, and for the negative input sequence, the final output M_o adds at $\omega_c - \omega_s$ while cancels at $\omega_s (m = 0)$, $\omega_c + \omega_s$ and $2\omega_c \pm \omega_s$. Similar conclusion can be reached for the positive input sequence, where the final output adds at $\omega_c + \omega_s$ and cancels at ω_s, $\omega_c - \omega_s$ and $2\omega_c \pm \omega_s$ as was explained previously in section 5.3.

5.6 PRACTICAL CONSIDERATIONS

It was clear from the foregoing analysis that the sequence discriminator networks can be used to generate single-sideband signals. This stems from the fact that both upper and lower sidebands do exist and the main operation of the sequence discriminator network is to suppress one sideband with respect to the other. In this respect, two main factors have to be taken into account in any design consideration:

1) performance of the network to the applied input sequence.
2) performance of the modulators.

Performance of the sequence discrimination type of networks, to the applied positive and negative sequence, is very critical since the sideband suppression is achieved by cancellation of modulation products and hence any inaccuracies in the design of these networks will cause loss of sideband suppression. Fortunately the networks presented in this thesis do not suffer from such a problem because of the simplicity in design which requires that only the RC products in each section be kept constant. This can easily be done by only trimming R_i's or R'_i's to the nominal RC product in each individual section. This represents an important achievement in the design of phase splitting network over the quadrature modulation design method.

One advantage of the quadrature modulation method, which employs two all pass networks, over the sequence discrimiation method can be explained by referring to Figure 2.4. It can be seen that the two output signals V_o and V'_o are frequency dependent and;

The wanted sideband is proprotional to $\frac{1}{2}\{|V_o + V_o'|\}$, and

The unwanted sideband is proportional to $\frac{1}{2}\{|V_o - V_o'|\}$

Over the specified bandwidth of the realization both V_o and V_o' are identically equal in magnitude and in phase quadrature, and hence

The wanted sideband (passband) = $20 \log |V_o(f)|$ dB,

The unwanted sideband (stopband) = $-\infty$ dB

Considering the above results, there is an obvious difference compared with the conventional all pass realization. The two outputs from the all-pass realization are identically equal in magnitude at all frequencies, i.e. $V_o(f) = V_o$. Hence the wanted and unwanted sidebands are proportional to V_o COS δ and V_o Sin δ respectively, where 2δ is the phase error between the two outputs. For $\delta = 0$, then

The wanted sideband = 0 dB

unwanted sideband = $-\infty$ dB

The performance of the modulators is very important since any errors in their gain or phase can pose severe problems. The modulators used in this thesis are of CMOS IC's type which are characterized by their excellent linearity and very low ON resistance as indicated in sec. 5.3. However the relative timing between these switches is very important, and any carrier leak due to coupling stray capacitances should cancel at f_c. As pointed out in [27] a relative error of Δt seconds, in any path, from the exact switching time has a negligible effect in the passband, while its effect is dominant in the stopband.

Consider the switching waveforms given in (5.4), for a time error of Δt seconds in the first path, it can be shown that the magnitude of the remaining components is $(2 f_s \Delta t)\, V.\ \mathrm{Sin}(k\pi)$. This may represent a problem particularly at high carrier frequency, but with the operating frequency and the available CMOS ICs no problems were encountered. The switching scheme of Figure 5.11 was suggested in [3, 25] to reduce the effect of the imbalance in the modulators. A switch which is operated at 4 times the frequency of the input signal of Figure 5.5 (i.e. $16 f_c$) is employed to reduce the carrier leak between the switches. It is arranged as shown in Figure 5.11 to chop out the signal during the ON and OFF periods between two successive switches.

Consider again the modulation process as previously described. The four phase signals which represent the inputs to the four multipliers were assumed to be identically equal in magnitude and in perfect phase quadrature. This is not practically the case and any gain or phase error in one path can be considered as a modification of the signal in that path. To study the effect of possible gain or phase error consider, for example, an error of δ has been encountered in the first path, then the four output signal to the modulators can be written as;

$$V_1 = V + \delta$$

$$V_2 = \pm V$$

$$V_3 = -V$$

$$V_4 = \mp V$$

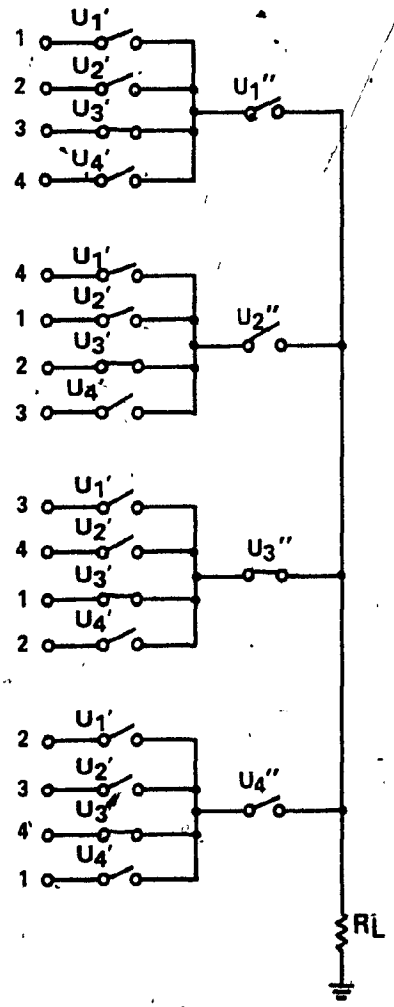

Figure 5.11 A Switching Scheme to Reduce Unbalance Effects

where the $\pm$ in V_2 and $\mp$ V_4 are used to distinguish between negative and positive sequences, respectively.

for V = 1, it can be shown that [3]:

The unwanted sideband = $\delta/4$

The wanted sideband = $1 + \delta/4$

The sideband discrimination = $20 \log \left(\frac{1 + \delta/4}{\delta/4}\right)$ dB

Similarly, for phase error ϕ in one of the paths ($V_1 = \exp(j\phi)$, say, then,

The unwanted sideband = $\frac{1}{4}$ [Cosϕ - 1 + j Sin ϕ]

The wanted sideband = $\frac{1}{4}$ [Cosϕ + 3 + j Sin ϕ]

The sideband discrimination = $10 \log \left[\frac{5 + 3 \text{Cos}\phi}{1 - \text{Cos}\phi}\right]$

During demodulation, to recover the original transmitted signal it is necessary to generate a local carrier at the receiver for the purpose of synchronous detection [47]. Ideally, the frequency of the local carrier must be identical to that of the carrier at the transmitter. Similarly, the phase of the local carrier should be identical to that of the reference carrier in the receiver signal. Any discrepancy in the frequency and phase of the local carrier gives rise to a distortion in the detector waveform. As an example consider the case of a local carrier with a frequency error of $\Delta\omega_c$. The received signal is $f(t)\text{Cos}\omega_c t$ and the local carrier is $\text{Cos}\{(\omega_c + \Delta\omega_c)t\}$, then

$f(t).\text{Cos}\omega_c t.\text{Cos}(\omega_c + \Delta\omega_c)t = \frac{1}{2} f(t) [\text{Cos}(\Delta\omega_c t) + \text{Cos}(2\omega_c + \Delta\omega_c)t]$

The second term of the above equation will be filtered out while $\text{Cos}(\Delta\omega_c.t)$ represents an extra term. Thus instead of recovering the original signal

f(t), the signal f(t) $\cos(\Delta\omega.t)$ is obtained. In general, $\Delta\omega_c \to 0$ and $f(t).\cos(\Delta\omega_c t)$ represents the original signal f(t) multiplied by a slowly varying gain constant which is rather an undesirable kind of distortion. In the scheme suggested in the next section both the modulators and demodulators waveform were driven from the same four phase carrier generator and hence no such problems were encountered.

5.7 PRACTICAL POLYPHASE MODEM

In this section a block diagram of a channel unit modulator/demodulator (MODEM) is suggested using the sequence discriminator networks introduced in the previous chapters. This block diagram is shown in Figure 5.12 where, at the transmitter side, 12 voice channel (each of 0-4 kHz) are modulated directly to 60-108 kHz as shown in Figure 5.1. At the receiver side these 12 modulated channels are demodulated to generate the original transmitted signals.

The amplifier-limiter and the audio low pass filter preceeding the sequence discriminator network at the transmitter side are used to band-limit the transmitted voice signals to the required upper band edge ($\simeq$3.4 kHz) to prevent any interference into adjacent channels. At the receiver side an audio low pass filter and an amplifier can be used to recover the original transmitted signal, reject the unnecessary channels and minimize intermodulation and noise that may be encountered from the interference of the adjacent channels.

The sequence discriminator networks are used in both the transmitter and receiver sides as shown in Figure 5.12. Both networks are

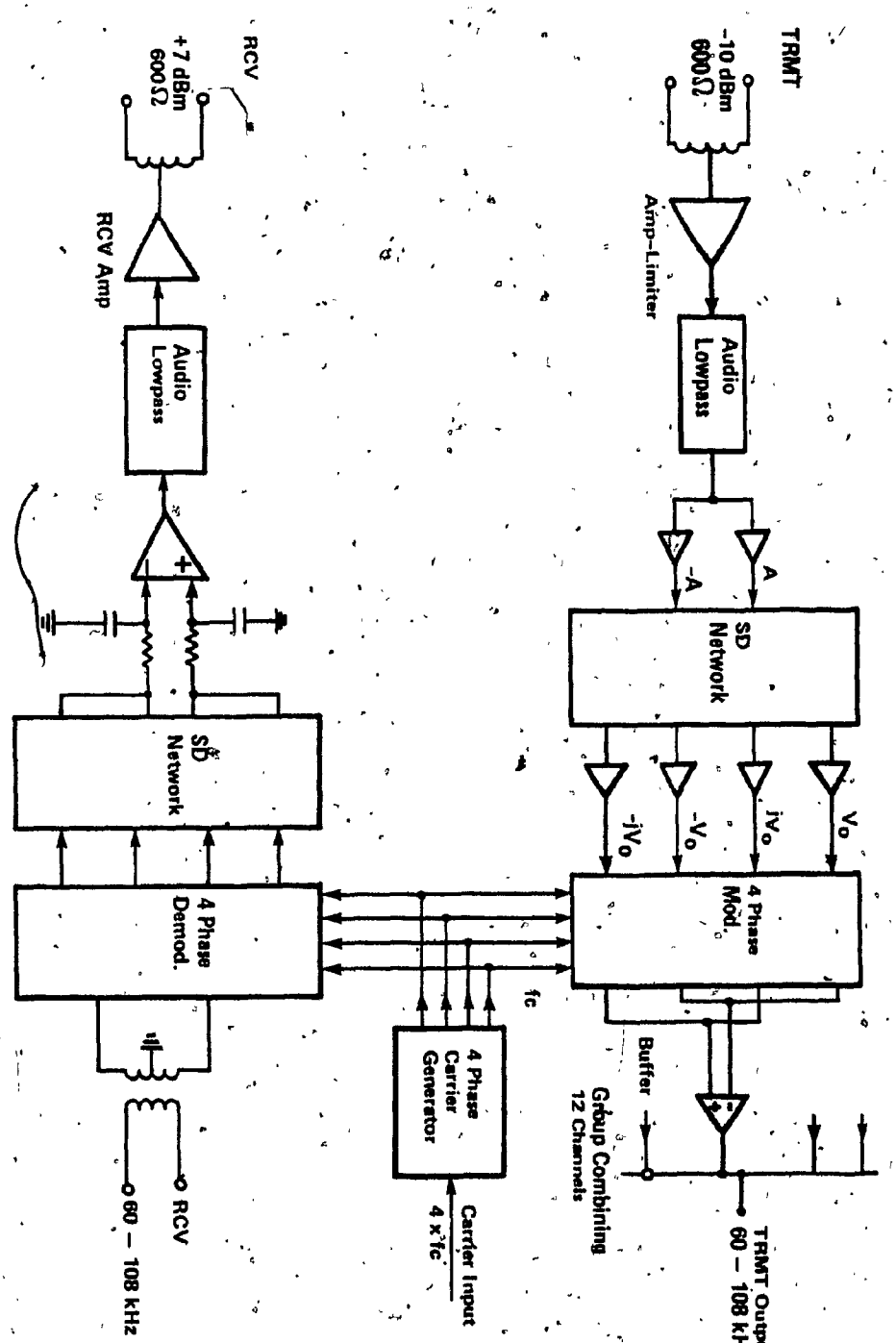

Figure 5.12 Sequence Discriminator Channel Unit Block Diagram

similar in their design but the one at the transmitter side is used to generate four signals in phase quadrature with respect to one another. The sequence discriminator network at the receiver side distinguishes between sequences in the voice frequency range and reject the adjacent channel on the other side of the carrier.

CMOS switches are best suited as switches for modulation-demodulation purposes because of their excellent characteristics as was indicated in section 5.3.

The four carrier signals, used to modulate (demodulate) the twelve channels directly to (from) 60-108 kHz on the transmitted (receiver) side, are generated from the same four phase carrier generator with its input frequency $4f_c$, where f_c is the required carrier.

Generating the modualting (demodulating) waveforms from the same source will enable us to have a local carrier at the receiver identically equal, in frequency and phase, to that of the carrier at the transmitter.

5.8 CONCLUSIONS

In this chapter we have demonstrated the practicality of the proposed sequence discriminator networks whether in the active RC forms or in the fixed-switched capacitor configurations.

The principle of frequency translation and the transmission of a large number of signals at the same time on one channel was investigated

using the technique of frequency division multiplex (FDM). A channel bank consisting of 12 voice channel (each of 0-4 kHz) was proposed for transmission to/from 60-108 kHz by modulation/demodulation.

The principle of N-path filter and its use in conjunction with single-sideband signal generation is considered for comparison with Gingel's polyphase filter, where the N filter in the former have been repalced in the latter by a single N-phase sequence asymmetric polyphase filter.

CMOS switches have been found to be the most successful candidate, as multiplier, for their excellent characteristics. The main principle of generating and detecting single-sideband signals was given, where four phase signals forming a symmetric sequence were generated from the two outputs of the sequence discriminator network. The signal were multiplied by their corresponding carriers which also form a symmetric sequence of the same polarity. By adding the four modulated signals M_1 through M_4, a single-sideband signal was generated .

CHAPTER VI

CONCLUSIONS

6.1 SUMMARY

This thesis discusses two types of phase splitting networks:

(i) Active RC networks

(ii) Switched Capacitor network

both are primarily used for the purpose of generating two signals in phase quadrature over a wide band of frequency.

A new class of active phase splitting networks has been introduced in this thesis. These networks are characterized by their abiltiy to discriminate between different types of applied polyphase input signals in the frequency domain. The realization of the active structures makes use of resistors and capacitors as the basic passive elements and the fairchild μA 741 operational amplifier as the only active device. The minimax algorithm was used to calculate the values of the resistors and capacitors. These values were chosen such that the RC product in each section is set to previously specified value (i.e. additional constrained in the minimax algorithm). The bandwidth of the realization is determined by the difference between the RC-products in the individual sections. The operational amplifiers were used in different mode of operations, either as buffers between the cascaded sections or as inverters.

Studies of both the gain and phase sensitivities to variations in the positions of the notch frequencies have shown that these networks are superior in their performance, to the all-pass realization. Further

sensitivity improvement has been achieved by a proper use of feedback. Comparison between the different types of polyphase active networks indicates that the networks with feedback and particularly the positive feedback configuration ratain the attractive features of the original design, while improving the sensitivities both in the passband and stopband. In addition to the simplicity of both structures (with and without feedback), the networks introduced are relatively less sensitive to component variations when compared to the quadrature modulation method for producing SSB which implements the 90 degree phase difference networks by employing two independent all-pass paths.

The proposed active phase splitting networks were evaluated experimentally, for the particular application of single-sideband signal generation, by measurements of the network response using four external modulating signals in phase quadrature to each other. The modulation/demodualtion schemes have been proposed in chapter 5.

In summary, the active RC structures introduced in chapters 2 and 3 have the following attractive features:

1) Simplicity of design
2) The cascaded approach is attractive for post-design adjustments as each section is isolated from the other.
3) Tuning can be done by varying the RC-product in each section separately (by simply trimming R's only).
4) Low sensitivity to component variations.
5) Either upper-sideband (USB) or lower-sideband (LSB) signal can be generated by interchanging any two modulating or carrier signals which are 180° out of phase.

As Large Scale Integration (LSI) techniques are being used to integrate systems, it is becoming increasingly important to develop new techniques to efficiently implement active RC networks. It is for this reason that the sampled data active phase spliting sequence discriminator, introduced in chapter 4, was realized by replacing all resistors, in the active RC design, by switched capacitors. It has been shown that there is an apparent equivalence between a resistor and a circuit element consisting of a capacitor and two switches if the clock rate of the switches is much higher than the higher frequency of the input signal.

The frequency response characteristics of the two realization are image of each other. In addition, a stable RC realization with all its poles in the left half of the S-plane corresponds to a stable sampled data switched capacitor realization with all its poles inside the open unit circle. The greatest assets of the switched capacitor technique are:

1) The equivalent resistor can be fully integrated using MOS technology with an efficient utilization of silicon area.
2) Reduced circuit complexity.
3) The temperature stability and linearity of the equivalent resistor are much better than for the integrated (diffused) resistor.
4) The filter characteristics such as gain, resonant frequencies and/or cut-off frequency can be modified by varying the capacitor ratios or the clock rate of the switched capacitor or both.

The sampled data active phase splitting network was used for single-sideband signal generation, and it has been found to have comparable properties to the realization using resistors.

6.2 SUGGESTIONS FOR FUTURE INVESTIGATION

This work has laid the basis for further studies in the area of active switched capacitor networks for more accurate measurements over a wider frequency band. The author feels that it should be of interest to examine the effects of the stray capacitance of the MOS switches when employing different clocks for the different cascaded sections. Such an effect is more important to consider when designing the amplifier and the network elements on a single chip. The networks behaviour should also be investigated when considering carrier frequencies higher than the one considered in this thesis (i.e. 64 kHz). The effects of the finite impedance levels of the operational amplifier (such as differential input impedance, output impedance, etc.) on the design presented in this thesis should also be investigated.

In conclusion, the author hopes that with the potential cost saving and size reduction possible with modern integrated circuit technology, many areas in communication and instrumentation will benefit from the application of the active phase splitting networks presented in this thesis.

REFERENCES

[1] J. Haine, "New Active Quadrature Phase-Shift Network", Electron. Lett. Vol. 13, No.7, pp. 216-218, March 1977.

[2] J.P. Hamaker and J. Pezij, "A Simple RC Realization of the 90° Phase-Difference network Including Source and Load Resistances", Proc. IEEE, Vol. 63, pp. 722-723, April 1975.

[3] M.J. Gingell, "The Synthesis and Applications of Polyphase Filters with Sequence Asymmetric Properties", Ph.D. Thesis, University of London, 1975.

[4] M.J. Gingell, "Polyphase Symmetrical Network", United States Patent 3,559,042, Jan. 1971.

[5] Y. Sun, "Network Functions of Quadrature N-Path Filters", IEEE Trans. Circuit Theory, Vol. CT-17, No. 4, pp. 594-600, Nov. 1970.

[6] W. Saraga, "N-Path Filter Sections with Biquadratic Transfere Functions", Electron-Lett., Vol. 5, No. 26, pp.711-714, Dec. 1969..

[7] S.D. Bedrosian, "Normalized Design of 90° Phase Difference Networks", IRE Trans. Circuit Theory, Vol. CT-7, pp. 128-136, June 1960.

[8] D.K. Weaver, Jr., "Design of RC Wide-Band 90-Degree Phase-Difference Networks", Proc. IRE, Vol. 42, No. 4, pp. 671-676, April 1954.

[9] H.J. Orchard, "Synthesis of Wideband Two-Phase Networks", Wireless Engineer, Vol. 27, pp. 72-81, March 1950.

[10] W. Saraga, "The Design of Wide-Band Phase Splitting Networks", Proc. IRE, Vol. 38, No. 7, pp. 754-770, July 1950.

[11] S. Darlington, "Realization of Constant Phase Difference", BSTJ, Vol. 29, pp. 94-104, 1950.

[12] N.F. Barber, "Bridge Networks Discriminating between Positive and Negative Sequences in Polyphase Supply". Letter in Nature, Vol. 161, pp. 685-686, May 1948.

[13] D.G.C. Luck, "Properties of Some Wide-Band Phase-Splitting Networks," Proc. IRE, Vol. 37, pp. 147-151, Feb. 1949.

[14] M.J. Gingell, "Single-Sideband Modulation Using Sequence Asymmetric Polyphase Networks", Electrical Communication, Vol. 48, No. 1 and 2, pp. 21-25, 1973.

[15] W. Saraga, "Quadrature Modulation Type Low-Pass Filters", Electron. Lett., Vol. 7, No. 18, pp. 516-517, Sept. 1971.

[16] D.R. Barber and M.J. Gingell, "Polyphase Modem for Frequency-Division Multiplex", Electrical Communication, Vol. 44, No. 2, pp. 108-114, 1969.

[17] R.K.P. Galpin, P.L. Hawkes and W. Saraga, "A Practical Tantalum 7. Thin-Film Single-Sideband Modulator Using RC-Time-Varying and Active Networks," IEEE Journal of Solid State Circuits, March 196

[18] A.A. Campora, B. Rabinovici and C.A. Renton, "Generation of Band-Pass Filters by Switching Techniques," Proc. IEEE, Vol. 51, No. 1, pp. 256-257, Jan. 1963.

[19] D.E. Norgaard, "The Phase-Shift Method of Single-Sideband Signal Generation", Proc. IRE, Vol. 44, pp. 1719-1735, Dec. 1956.

[20] I.F. Macdiarmid and D.G. Tucker, "Polyphase Modulation as a Solution of Certain Filtration Problems in Telecommunication", Proc. IEE, Vol. 97, Part III, pp. 349-358, Sept. 1950.

[21] D.K. Weaver, Jr., "A Third Method of Generation and Detection of Single-Sideband Signals", Proc. IRE, Vol. 44, pp. 1703-1705, Dec. 1956.

[22] O.G. Villard, Jr., "A High-Level Single-Sideband Transmitter", Proc. IRE, Vol. 36, pp. 1419-1425, 1948.

[23] D.G. Tucker, "A Two-Phase Telecommunication System", Electronic Engineering, Vol. 20, Part 1 and 2, May 1948.

[24] N.F. Barber, "Narrow Band-Pass Filter Using Modulation", Wireless Engineer, Vol. 24, No. 5, pp. 132-134, May 1947.

[25] G.G. Madella, "Single-Phase and Polyphase Filtering Devices Using Modulation", Wireless Engineer, Vol. 24, No. 10, pp. 310-311, Oct. 1947.

[26] B.E. Lenchan, "A new Single-Sideband Carrier Systems", Electrical Engineering, pp. 549-552, June 1947.

[27] W.B. Mikhael, "Sequence Discriminators and their Use in FDM Communication Systems", IEEE Trans. Circuits and Systems, Vol. CAS-26, pp. 117-129, Feb. 1979.

[28] R. Neumann, SYMMETRICAL COMPONENT ANALYSIS OF UNSYMMETRICAL POLYPHASE SYSTEMS, Sir Isaac Pitman & Sons Ltd., London, 1939.

[29] CCITT, General Characteristics Applicable to All Modern International Circuits and National Extension Circuits, Six Planery Assembly, Orange Book, Geneva, Vol. III.1 - Rec.G.151, pp.75, 1976.

[30] G.S. Moschytz, LINEAR INTEGRATED NETWORKS, Fundamentals, New York; Van Nostrand Reinhold Company, 1974.

[31] S.K. Mitra, ANALYSIS AND SYNTHESIS OF LIENAR ACTIVE NETOWRKS, new York: Wiley, 1969.

[32] L.P. Huelsmann, Ed., Active Filters: Lumpted, Distributed, INTEGRATED, DIGITAL AND PARAMETRIC., New York: McGraw-Hill, 1970.

[33] D.L. Fired, "Analog Sampled Data Filters", IEEE J. Solid State Circuits (Corresp.), Vol. SC-7, pp. 302-304, Aug. 1972.

[34] I.A. Young, D.A. Hodges, and P.R. Gray, "Analog NMOS Sampled-Data Recursive Filter", ISSCC Dig. Tech. Papers, pp. 156-157, Feb. 1977.

[35] E. Daoud, W.B. Mikhael and M.N.S. Swamy, "Simple Low Sensitivity Active RC Networks for Quadrature Signal Generation", Proc. ISCAS, N.Y., pp. 254-256, May 1978.

[36] P. Benedek, "MODNOD, A Preliminary User's Manual", Transmission Network Development, Bell-Northern Research, Unpublished Memorandum.

[37] _____, "LINEAR INTEGRATED CIRCUITS DATA BOOK", Fairchild Semi-Conductor, MA Linear, 1976.

[38] S.R.K. Dutta, Private Communication, Electrical Engineering Department, Concordia University, Montreal.

[39] B.J. Hostika, R.W. Brodersen and P.R. Gray, "MOS Sampled Data Recursive Filters Using Switched Capacitor Integrators", IEEE J. Solid-State Circuits, Vol. SC-12, No. 6, pp. 600-608, Dec. 1977.

[40] C.R. Hewes, "A Self-Contained 8000 Stage CCD Transversal Filter", Proc. Int. Conf. Application of Charge-Coupled Devices, pp. 809-318, 1975.

[41] J.L. McGreary and P.R. Gray, "All-MOSS Charge Redistribution Analog-to-Digital Conversion Techniques - Part I", IEEE J. Solid-State Circuits", Vol. SC-10, No. 6, pp. 371-379, Dec. 1975.

[42] R.E. Suarez, P.R. Gray and D.A. Hodges, "All-MOS Charge Redistribution Analog-to-Digital Conversion Techniques - Part II, IEEE J. Solid-State Circuits, Vol. SC-10, No. 6, pp. 379-385, Dec. 1975.

[43] G.C. Temes and I.A. Young, "An Improved Switched-Capacitor Integrator", Electron. Lett., Vol 14, No. 9, pp. 287-288, April 1978.

[44] G.C. Temes, "The Derivation of Switched Capacitor Filters from Active-RC Prototypes", Electron. Lett., Vol. 14, No. 12, pp. 361-362, June 1978.

[45] J.T. Caves, M.A. Copeland, C.F. Rahim, and S.D. Rosenbaum, "Sampled Analog Filtering Using Switched Capacitors as Resistor Equivalents", IEEE J. Solid-State Circuits, Vol. SC-12, No. 6, pp. 592-599, Dec. 1977.

[46] G. Kelson, H.H. Stellrecht and D.S. Perloff, "A Monolithic 10-b Digital-to-Analog Converter Using ION Implantation", IEEE J. Solid-State Circuits, Vol. SC-8, pp. 396-403, Dec. 1973.

[47] B.P. Lathi, COMMUNICATION SYSTEMS, John Wiley & Sons, Inc., N.Y. 1968.

[48] A.K. Mitra and V.K. Aatre, "A Note on Frequency and Q Limitations of Active Filters", IEEE Trans. Circuits and Systems, Vol. CAS-24, pp. 215-218, April 1977.

[49] A. Papoulis, THE FOURIER INTEGRAL AND ITS APPLICATIONS, New York: McGraw-Hill, 1962.

[50] _____, Digital Integrated Circuits, RCA, Solid-State Division, 1976.

APPENDIX A

DERIVATIONS OF THE ACTUAL OUTPUT VOLTAGES V_o AND V_o'

AS FUNCTIONS OF THE POSITIVE AND NEGATIVE SEQUENCES

DERIVATION OF THE ACTUAL OUTPUT VOLTAGES V_o AND V'_o AS A FUNCTION OF THE POSITIVE AND NEGATIVE SEQUENCES

For the network of Figure 2.5, the two output signals V_x and V_y, from the first section, due to both the positive and negative sequences were given in (2.3), (2.4), (2.8) and (2.9) respectively. By interchanging $V_{op}(V_{on})$ and $V'_{op}(V'_{on})$ by V_x and V_y respectively, then for the positive sequence only we get

$$V_x = \frac{1 + \zeta_1}{1 + j\zeta_1} \quad (V) \qquad (A-1)$$

and

$$V_y = \frac{1 + \zeta'_1}{1 + j\zeta'_1}, \quad (-jV) \qquad (A-2)$$

Now, V_x , V_y and $(-V_x)$ constitute the input to the second section, then;

$$V_x + j\zeta_2 V_y = V_{op}(1 + j\zeta_2) \qquad (A-3)$$

Substituting (A-1) and (A-2) into (A-3) gives V_{op} for the non-ideal case as;

$$V_{op} = \frac{1}{1 + j\zeta_2}\left[\frac{1 + \zeta_1}{1 + j\zeta_1} + \frac{\zeta_2(1 + \zeta'_1)}{1 + j\zeta'_1}\right] \quad (V) \qquad (A-4)$$

Similarly;

$$V_y - j\zeta'_2 V_x = V'_{op}(1 + j\zeta'_2)$$

then

$$V'_{op} = \frac{-j}{1 + \zeta'_2}\left[\frac{1 + \zeta'_1}{1 + j\zeta'_1} + \frac{\zeta'_2(1 + \zeta_1)}{1 + j\zeta_1}\right] \quad (V) \qquad (A-5)$$

For nominal component values and in the ideal case where $\omega_i = \omega'_i$ then equations (A-4) and (A-5) can be simplified to;

$$V_{op} = \frac{(1 + \zeta_1)(1 + \zeta_2)}{(1 + j\zeta_1)(1 + j\zeta_2)} \quad (V) \qquad (A-6)$$

and

$$V'_{op} = \frac{(1+\zeta_1)(1+\zeta_2)}{(1+j\zeta_1)(1+j\zeta_2)} \quad (\pm jV) \qquad \text{(A-7)}$$

For the negative sequence only, then;

$$V_x = \frac{1-\zeta_1}{1+j\zeta_1} \quad (V) \qquad \text{(A-8)}$$

and

$$V_x = \frac{1-\zeta'_1}{1+j\zeta'_1} \quad (jV) \qquad \text{(A-9)}$$

Following the same procedure as in the case of the positive sequence, the two output signals V_{on} and V'_{on} can be written as,

$$V_{on} = \frac{1}{(1+j\zeta_2)}\left[\frac{1-\zeta_1}{1+j\zeta_1} + \zeta_2 \frac{1-\zeta'_1}{1+\zeta'_1}\right] \quad (V) \qquad \text{(A-10)}$$

and

$$V'_{on} = \frac{j}{(1+j\zeta_2)}\left[\frac{1-\zeta'_1}{1+j\zeta'_1} - \zeta'_2 \frac{1-\zeta_1}{1+j\zeta'_1}\right] \quad (V) \qquad \text{(A-11)}$$

For nominal component values (A-10) and (A-11) or simplified to

$$V_{on} = \frac{(1-\zeta_1)(1-\zeta_2)}{(1+j\zeta_1)(1+j\zeta_2)} \quad (V) \qquad \text{(A-12)}$$

and

$$V'_{on} = \frac{(1-\zeta_1)(1-\zeta_2)}{(1+j\zeta_1)(1+j\zeta_2)} \quad (jV) \qquad \text{(A-13)}$$

The actual outputs V_o and V'_o can be obtained by adding the outputs due to both the positive and the negative sequences. From (A-4), (A-5), (A-10) and (A-11), the two outputs V_o and V'_o for the non-ideal case can be written as;

$$V_o = \frac{1}{1+j\zeta_2}\left[\frac{1}{1+j\zeta_1} + \frac{\zeta'_1\zeta_2}{1+j\zeta'_1}\right] (2V) \qquad \text{(A-14)}$$

and

$$V'_o = \frac{1}{1+j\zeta'_2} \left[\frac{1}{1+j\zeta'_1} + \frac{\zeta'_2}{1+j\zeta_1} \right] (-2jV) \qquad \text{(A-15)}$$

where, as it can be seen from (A-14) and (A-15), the output signals V_o and V'_o are functions of the actual input signals ($\pm$2V).

For nominal component values, the two output signals can be simplified to;

$$V_o = \frac{1 + \zeta_1\zeta_2}{(1+j\zeta_1)(1+j\zeta_2)} \quad (2V),$$

and

$$V'_o = \frac{\zeta_1 + \zeta_2}{(1+j\zeta_1)(1+j\zeta_2)} \quad (-j2V)$$

As were given in (2.22) and (2.23) respectively.

APPENDIX B

SENSITIVITY ANALYSIS FOR THE NON-GROUNDED NETWORK

SENSITIVITY ANALYSIS FOR THE NON-GROUNDED NETWORKS

Passband Sensitivity

Recall the passband expression as given by (2.33) and let

$$\omega_2' = \omega_2 \pm \Delta\omega_2 \qquad \text{(B-1)}$$

Substituting (B-1) into (2.33) and for first degree of approximation then;

$$V_p' = (1+j)\frac{(1+j\frac{\omega}{\omega_1})+ j\frac{\omega}{\omega_2}(1-j\frac{\omega}{\omega_1})}{(1+j\frac{\omega}{\omega_1})(1+j\frac{\omega}{\omega_2})} \mp \frac{2\frac{\omega}{\omega_2}}{(1+j\frac{\omega}{\omega_1})(1+j\frac{\omega}{\omega_2})^2}\frac{\Delta\omega_2}{\omega_2} \qquad \text{(B-2)}$$

$$= V_p \mp \Delta V_p$$

$$\frac{\Delta V_p}{V_p} = \mp (1-j)\frac{\frac{\omega}{\omega_2}}{(1+j\frac{\omega}{\omega_2})(1+\frac{\omega}{\omega_1})(1+\frac{\omega}{\omega_2})}\cdot\frac{\Delta\omega_2}{\omega_2} \qquad \text{(B-3)}$$

The passband sensitivity to ω_2 is;

$$S^{V_p}_{\omega_2} = \frac{\Delta V_p/V_p}{\Delta\omega_2/\omega_2}$$

$$S^{V_p}_{\omega_2} = \pm (1-j)\frac{\frac{\omega}{\omega_2}}{(1+j\frac{\omega}{\omega_2})(1+\frac{\omega}{\omega_1})(1+\frac{\omega}{\omega_2})} \qquad \text{(B-4)}$$

Stopband Sensitivity

The stopband expression is given by (2.34). By substituting (B-1) into (2.34) and for first degree of approximation then;

$$V_s' = V_s \mp \Delta V_s$$

where

$$\Delta V_s = \frac{2\,\frac{\omega}{\omega_2}}{(1+j\,\frac{\omega}{\omega_1})(1+j\,\frac{\omega}{\omega_2})^2} \qquad \text{(B-5)}$$

Then, the stopband sensitivity is given by;

$$S^{V_p}_{\omega_2} = \frac{\Delta V_s/V_s}{\Delta\omega_2/\omega_2}$$

$$= \pm\,(1+j)\,\frac{\frac{\omega}{\omega_2}}{(1+j\,\frac{\omega}{\omega_2})(1-\frac{\omega}{\omega_1})(1-\frac{\omega}{\omega_2})} \qquad \text{(B-6)}$$

By separating (B-4) and (B-6) into their real and imaginary parts both the gain and phase sensitivities, to the variations in the RC-product of the second section, can be obtained

APPENDIX C

THE COMPUTER PROGRAM FOR CALCULATING THE PASSBAND AND STOPBAND SENSITIVITIES TO COMPONENT VARIATIONS FOR THE VARIOUS TYPES OF NETWORKS DISCUSSED

PROGRAM SENS 73/172 OPT=1 FTN 4.6+446 78/03/0

```
      PROGRAM SENS(INPUT,OUTPUT)
      DIMENSION X1(250),T(250),XX(250),YY(250),Z(250),TT(250)
      DIMENSION T1(250),T2(250),T3(250)
      COMPLEX SEN,SEN1,SEN2,SEN3,SEN4,SEN5,P,SEN6,SEN7,SEN8,SEN9
      COMPLEX A,A1,A2,A3,A4,A5,A6,A7,A8,A9
      COMPLEX B,B1,B2,B3,B4,B5,B6,B7,B8,B9
      COMPLEX B61,B62,AA,BA,AAL,BAL
      COMPLEX A12,A13,A11,A21,A31,A32,A22,AZ,A33,AZ1,AX,AY,AY1
      COMPLEX A14,A24,A44,A15,A25,A35,A55,A66
      COMPLEX SEN10,SEN11,SEN12,SEN13,SENAL,SENA
      DEL1=.05
      DEL2=.05
      PRINT 1
      PRINT 2
      PRINT 5,DEL1
      PRINT 7,DEL2
    5  FORMAT(10X,*PERCENTAGE VARIATION IN W1 IS =*,E12.6/)
    7  FORMAT(10X,*PERCENTAGE VARIATION IN W2 IS =*,E12.6/)
    1  FORMAT(1H1)
    2  FORMAT(20X,*PASS BAND SENSTIVITIES*//)
      PRINT 6
    6  FORMAT(5X,*FREQUENCY-KHZ*,6X,*GAIN3*,11X,*GAIN4*,11X,*GAIN5*,12X,*
     $GAIN6*,11X,*GAIN7*,11X,*GAIN10*7X,*GAIN12* ////)
      PI=3.14159265364
      I=1
      F=.01
      FI=.02
      F2=4.
      N=F2/FI
      R1=.4
      R2=.5
      C1=.25
      C2=.1
      W1=1./(R1*C1)
      W2=1./(R2*C2)
    3 F=F+FI
      W=2.*PI*F
      P=(0.,E-50,1.)*W
      X=W/W2
      Y=W/W1
C     PASS BAND SENSITIVITIES W.R.T. W1
C     GROUNDED NETWORK
      A3=Y
      B3=(1.+(P/W1))*(1.+Y)
      SEN3=(A3/B3)*DEL1
      GAIN3=ABS(REAL(SEN3))
      PHI3=180.0*AIMAG(SEN3)/PI
C     POSITIVE FEEDBACK CASE
      A6=Y*(1.+(P/W2))
      B61=(1.+Y)
      B62=-2.*X*Y+2.*((P/W1)+(P/W2))+(((1./W1)+(1./W2))**2)*W1*W2
      B6=B61+B62
      SEN6=(A6/B6)*DEL1
      GAIN6=ABS(REAL(SEN6))
      PHI6=180.0*AIMAG(SEN6)/PI
C     NEGATIVE FEEDBACK CASE
      A1=((P/W2)**2-(P/W1))
```

PROGRAM SENS 73/172 OPT=1 FTN 4.6+446 78/03/0

```
      A12=AX*((1.-((P**2)/(W1*W2)))*(2.+(P/W1)+(P/W2))+((P/W1)
     $+(P/W2))**2)
      A13=AY*(((P**2)/(W1*W2))+2.*((P/W2)**2)+(P/W2)-(P/W1)-1.)
      AY=(((P**3)/((W1**2)*W2))+((P**3)/(W1*(W2**2)))+2.*((P**2)
     $/(W1*W2))+(P/W1)+(P/W2))
C
      A11=A12+A13
      A21=AX*(((P/W1)+(P/W2))*((P**2)/(W1*W2))+(P/W1)+(P/W2)+1.)
      A31=AY*(((P**2)/(W1*W2))+(P/W1)+(P/W2))
      A32=A21-A31
      A22=A11-A31*(P/W)
      AZ=(1.+X)*(1.+Y)*(2.+(P/W1)+(P/W2)-X-Y)
      SEN10=(((P/W1)*A22)/((1.+(P/W1))*AY*AZ))*DEL1
      GAIN10=ABS(REAL(SEN10))
      PHI10=180.0*AIMAG(SEN10)/PI
C     PASS BAND SENSITIVITIES W.R.T.   W2
C     ALL PASS NETWORK
      AAL=.1815*(-W*(1.+.0285*W)+P*(1.-.0285))
      BAL=(1.+.1815*P)*(1.+.153*W+.0052*(W**2))
      SENAL=(AAL/BAL)*DEL2
      GAINL=ABS(REAL(SENAL))
      PHIAL=180.0*AIMAG(SENAL)
C     GROUNDED NETWORK
      A4=X*(1.-(P/W1))
      B4=(1.+(P/W2))*(1.+X)*(1.+Y)
      SEN4=(A4/B4)*DEL2
      GAIN4=ABS(REAL(SEN4))
      PHI4=180.0*AIMAG(SEN4)/PI
C     NON GROUNDED NETWORK
      A5=X-(P/W2)
      B5=(1.+(P/W2))*(1.+X)*(1.+Y)
      SEN5=(A5/B5)*DEL2
      GAIN5=ABS(REAL(SEN5))
      PHI5=180.0*AIMAG(SEN5)/PI
C      POSITIVE FEEDBACK CASE
      A7=Y*(1.+(P/W1))*(1.+(P/W2))
      B7=(1.+X)*(1.+Y)*B62
      SEN7=(A7/B7)*DEL2
      GAIN7=ABS(REAL(SEN7))
      PHI7=180.0*AIMAG(SEN7)/PI
C     NEGATIVE FEEDBACK CASE...
      AY1=2.*AY
      A14=(2.*((P**3)/((W1**2)*W2))+(P/W1)**2+(P**2/(W1*W2))+
     $     (P/W1)+(P/W2))
      A24=(2.+(P/W1)+(P/W2)+(P/W1)**2+(P/W2)**2-2.*((P**3)/(
     $     W1*(W2**2)))-2.*((P**3)/(W2*(W1**2))))
      A44=(A14+A24)+(((P**3)/(W2*(W1**2)))+(P/W2))*AY1
      A15=(2.*((P**3)/(W2*(W1**2)))+(P/W1)**2+(P**2)/(W1*W2)
     $+(P/W1)+(P/W2))*(AY+(P/W1)**2+(P/W2)**2)
      A25=AY1*(((P**2)/(W1*W2))+(P/W1)+(P/W2))
      A35=A15+A25
      A55=A44-(A35)*(P/W)
      SEN12=((P/W2)*A55/(AY1*AZ))*DEL2
      GAIN12=ABS(REAL(SEN12))
      PHI12=180.0*AIMAG(SEN12)/PI
C     STOP BAND SENSTIVITIES W.R.T.  W1
C     GROUNDED NETWORK
```

PROGRAM SENS 73/172 OPT=1 FTN 4.6+446 78/03/0

```
      A=Y
      B=(1.+(P/W1))*(1.-Y)
      SEN=(A/B)*DEL1
      GAIN=ABS(REAL(SEN))
      PHI=180.0*AIMAG(SEN)/PI
C     POSITIVE FEEDBACK CASE.
      A8=A6
      B8=(1.-Y)*B62
      SEN8=(A8/B8)*DEL1
      GAIN8=ABS(REAL(SEN8))
      PHI8=180.0*AIMAG(SEN8)/PI
C     NEGATIVE FEEDBACK CASE...
      A33=A21+A31*(P/W)
      AZ1=(1.-X)*(1.-Y)*(2.+(P/W1)+(P/W2)+X+Y)
      SEN11=(((P/W1)*A33)/((1.+(P/W1))*AY*AZ1))*DEL1
      GAIN11=ABS(REAL(SEN11))
      PHI11=180.0*AIMAG(SEN11)/PI
C     STOP BAND SENSITIVITIES W.R.T. W2
C     ALL PASS NETWORK
      AA=.1815*(W*(1.-.0285*W)+P*(1.+.0285*W))
      BA=(1.+.1815*P)*(1.-.153*W+.0052*(W**2))
      SENA=(AA/BA)*DEL2
      GAINA=ABS(REAL(SENA))
      PHIA=180.0*AIMAG(SENA)
C     GROUNDED NETWORK
      A1=X*(1.-(P/W1))
      B1=(1.+(P/W2))*(1.-X)*(1.-Y)
      SEN1=(A1/B1)*DEL2
      GAIN1=ABS(REAL(SEN1))
      PHI1=180.0*AIMAG(SEN1)/PI
C     NON GROUNDED NETWORK
      A2=X+P/W2
      B2=(1+(P/W2))*(1.-X)*(1.-Y)
      SEN2=(A2/B2)*DEL2
      GAIN2=ABS(REAL(SEN2))
      PHI2=180.0*AIMAG(SEN2)/PI
C     POSITIVE FEEDBACK CASE
      A9=A7
      B9=(1.-X)*(1.-Y)*B62
      SEN9=(A9/B9)*DEL2
      GAIN9=ABS(REAL(SEN9))
      PHI9=180.0*AIMAG(SEN9)/PI
      A66=A44+(A35)*(P/W)
      SEN13=((P/W2)*A66/(AY1*AZ1))*DEL2
      GAIN13=ABS(REAL(SEN13))
      PHI13=180.0*AIMAG(SEN13)/PI
C     PRINT 4,F,GAIN3,GAIN4,GAIN5,GAIN6,GAIN7,GAIN10,GAIN12,GAINL
      PRINT 4,F,PHI3,PHI6,PHI10,PHI4,PHI5,PHI7,PHI12,PHIAL
    4 FORMAT(1X,9(1X,E14.7))
      X1(I)=F
      XX(I)=PHI
      YY(I)=PHI8
      Z(I)=PHI11
      T(I)=PHI1
      TT(I)=PHI2
      T1(I)=PHI9
      T2(I)=PHI13
```

PROGRAM SENS 73/172 OPT=1 FTN 4.6+446 78/03/1

```
      T3(I)=PHIA
      I=I+1
      IF(F.LT.F2)  GO TO 3
      PRINT 14
   14 FORMAT(//)
      PRINT 15
   15 FORMAT(20X,*STOP BAND SENSITIVITIES*//)
      PRINT 8
    8 FORMAT(5X,*FREQUENCY-KHZ*,6X,*GAIN*,11X,*GAIN1*,11X,*GAIN2*,8X,*
     $GAIN8*,12X,*GAIN9*,13X,*GAIN11*,13X,*GAIN13*///)
      DO 40 J=1,N
      PRINT 50,X1(J),XX(J),YY(J),Z(J),T(J),TT(J),T1(J),T2(J),T3(J)
   50  FORMAT(1X,9(1X,E14.7))
   40 CONTINUE
      STOP
      END
```

SYMBOLIC REFERENCE MAP (R=1)

ENTRY POINTS

VARIABLES

SN	TYPE	RELOCATION			
	COMPLEX	5651	AA	COMPLEX	
	COMPLEX	5705	AX	COMPLEX	
	COMPLEX	5711	AY1	COMPLEX	
	COMPLEX	5703	AZ1	COMPLEX	
	COMPLEX	5665	A11	COMPLEX	
	COMPLEX	5663	A13	COMPLEX	
	COMPLEX	5721	A15	COMPLEX	
	COMPLEX	5667	A21	COMPLEX	
	COMPLEX	5715	A24	COMPLEX	
	COMPLEX	5603	A3	COMPLEX	
	COMPLEX	5673	A32	COMPLEX	
	COMPLEX	5725	A35	COMPLEX	
	COMPLEX	5717	A44	COMPLEX	
	COMPLEX	5727	A55	COMPLEX	
	COMPLEX	5731	A66	COMPLEX	
	COMPLEX	5615	A8	COMPLEX	
	COMPLEX	5621	B	COMPLEX	
	COMPLEX	5657	BAL	COMPLEX	
	COMPLEX	5625	B2	COMPLEX	
	COMPLEX	5631	B4	COMPLEX	
	COMPLEX	5635	B6	COMPLEX	
	COMPLEX	5647	B62	COMPLEX	
	COMPLEX	5641	B8	COMPLEX	
	COMPLEX	5761	C1	REAL	
	REAL	5747	DEL1	REAL	
2	REAL	5753	F	REAL	
	REAL	5755	F2	REAL	
N	REAL	6016	GAINA	REAL	
NL	REAL	6020	GAIN1	REAL	
N10	REAL	6014	GAIN11	REAL	

APPENDIX D

DERIVATIONS OF THE OUTPUT SEQUENCE SIGNALS IN TERMS OF THE POSITIVE AND NEGATIVE INPUT SEQUENCES FOR THE SWITCHED CAPACITOR NETWORK

DERIVATIONS OF THE OUTPUT SEQUENCE SIGNALS IN TERMS OF THE POSITIVE AND NEGATIVE INPUT SEQUENCES FOR THE SWITCHED CAPACITOR NETWORK

Consider the network shown in Fig. 4.4, by applying the negative sequence (V_{in}, jV_{in}, $-jV_{in}$)* shown in Fig. 4.4 the charge conservation equation yeidls:

$$C_x[V_{xn}(n) - V_{in}(n-1)] = -C_1[\{V_{xn}(n) - V_{xp}(n-1)\} - j\{V_{in}(n) - V_{in}(n-1)\}] \quad (D-1)$$

and

$$C'_x[V'_{xn}(n) - jV_{in}(n-1)] = -C'_1[\{V'_{yn}(n) - V'_{yn}(n-1)\} - \{V_{in}(n) - V_{in}(n-1)\}] \quad (D-2)$$

Z-transformation yields

$$V_{xn}(z) = \frac{j}{1+\alpha_1} \cdot \frac{z - (1+j\alpha_1)}{z - \frac{1}{1+\alpha_1}} \cdot V_{in}(z) \quad (D-3)$$

and

$$V_{yn}(z) = \frac{-1}{1+\alpha_1} \cdot \frac{z - (1+j\alpha'_1)}{z - \frac{1}{1+\alpha'_1}} \cdot V_{in}(z) \quad (D-4)$$

let $\alpha = \alpha'$ then,

$$V_{yn} = jV_{xn} \quad (D-5)$$

From (3), (4) and (5) the two output signals from the first section are equal in magnitude and in phase quadrature to each other.

Using the same analytical approach, the outputs from the second section can be written as:

---

*When analyzing the input signal to its positive and negative sequence equivalences the magnitude of the actual input is twice that of the sequence. i.e. V_{in} (actual) = $2V_{in}$ (sequence).

$$V_{on}(z) = \frac{-1}{(1+\alpha_1)(1+\alpha_2)} \cdot \frac{\{z - (1+j\alpha_1)\}\{z - (1+j\alpha_2)\}}{\{z - \frac{1}{1+\alpha_1}\}\{z - \frac{1}{1+\alpha_2}\}} V_{in}(z) \quad \text{(D-6)}$$

and

$$V'_{on}(z) = \frac{-j}{(1+\alpha_1)(1+\alpha_2)} \cdot \frac{\{z - (1+j\alpha_1)\}\{z - (1+j\alpha_2)\}}{\{z - \frac{1}{1+\alpha_1}\}\{z - \frac{1}{1+\alpha_2}\}} V_{in}(z) \quad \text{(D-7)}$$

From (6) and (7) then

$$V'_{on} = jV_{on}$$

Now, for the positive sequence input ($V_{in} - jV_{in}$, $-V_{in}$), the charge conservation equation yeilds:

$$C_x[V_{xp}(n) - V_{in}(n-1)] = -C_1[\{V_{xp}(n) - V_{xp}(n-1)\} + j\{V_{in}(n) - V_{in}(n-1)\}] \quad \text{(D-8)}$$

and

$$C'_x[V_{yp}(n) + jV_n(n-1)] = -C'_1[\{V_{yp}(n) - V_{yp}(n-1)\} + \{V_{in}(n) - V_{in}(n-1)\}] \quad \text{(D-9)}$$

Z-transformation yeilds

$$V_{xp}(z) = -\frac{j}{1+\alpha_1} \cdot \frac{z - (1-j\alpha_1)}{z - \frac{1}{1+\alpha_1}} \cdot V_{in}(z) \quad \text{(D-10)}$$

and

$$V_{yp}(z) = -\frac{1}{1+\alpha'_1} \cdot \frac{z - (1-j\alpha'_1)}{z - \frac{1}{1+\alpha'_1}} \cdot V_{in}(z) \quad \text{(D-11)}$$

Following the same procedure as in the negative sequence input case, the two outputs from the network of Fig. 4.4 are for the ideal case are;

$$V_{op}(z) = \frac{-1}{(1+\alpha_1)(1+\alpha_2)} \cdot \frac{\{z - (1-j\alpha_1)\}\{z - (1-j\alpha_2)\}}{\{z - \frac{1}{1+\alpha_1}\}\{z - \frac{1}{1+\alpha_2}\}} \cdot V_{in}(z) \quad \text{(D-12)}$$

and

$$V'_{op}(z) = \frac{j}{(1+\alpha_1)(1+\alpha_2)} \cdot \frac{\{z - (1-j\alpha_1)\}\{z - (1-j\alpha_2)\}}{\{z - \frac{1}{1+\alpha_1}\}\{z - \frac{1}{1+\alpha_2}\}} \cdot V_{in}(z) \quad \text{(D-13)}$$

As can be seen from (10), (11) or (12) and (13), the two outputs from each individual section are identically equal in magnitude and in phase quadrature, where:

$$V_{yp} = -jV_{xp} \qquad (\alpha_1 = \alpha_1')$$

and

$$V_{op} = -jV_{op} \qquad (\alpha_i = \alpha_i')$$

These results agree with the previously obtained ones from the RC active realizations.

APPENDIX E

FREQUENCY COMPONENTS OF THE FOUR DEMODULATED WAVEFORMS

FREQUENCY COMPONENTS OF THE FOUR DEMODULATED WAVEFORMS

Consider the demodulated waveforms D_1, D_2, D_3 and D_4 as given in (5-16). Applying the frequency shifting property, the Fourier spectrum of the four demodulated signals are given by;

$$D_1(t) \leftrightarrow jk\Pi V_s[\delta(\omega + \omega_s) - \delta(\omega - \omega_s)] + jk\frac{\Pi}{2} V_s \sum_{m=1}^{m=\infty} Sa(2\Pi mk) \cdot [[\delta\{\omega - (m\omega_c - \omega_s)\} - \delta\{\omega - (m\omega_c + \omega_s)\}] + [\delta\{\omega + (m\omega_c + \omega_s)\} - \delta\{\omega + (m\omega_c - \omega_s)\}]] \quad \text{E-1}$$

$$D_2(t) \leftrightarrow jk\Pi V_s[\delta(\omega + \omega_s) - \delta(\omega - \omega_s)] + jk\frac{\Pi}{2} V_s \sum_{m=1}^{m=\infty} Sa(2\Pi mk) \cdot [\exp(-j\frac{T}{4} m\omega_c)[\delta\{\omega - (m\omega_c - \omega_s)\} - \delta\{\omega - (m\omega_c + \omega_s)\}] + \exp(+j\frac{T}{4} m\omega_c)[\delta\{\omega + (m\omega_c + \omega_s)\} - \delta\{\omega + (m\omega_c - \omega_s)\}] \quad \text{E-2}$$

$$D_3(t) \leftrightarrow jk\Pi V_s[\delta(\omega + \omega_s) - \delta(\omega - \omega_s)] + jk\frac{\Pi}{2} V_s \sum_{m=1}^{m=\infty} Sa(2\Pi mk) \cdot [\exp(-j\frac{Tm}{2}\omega_c)[\delta\{\omega - (m\omega_c - \omega_s)\} - \delta\{\omega - (m\omega_c + \omega_s)\}] + \exp(+j\frac{Tm}{2}\omega_c)[\delta\{\omega + (m\omega_c + \omega_s)\} - \delta\{\omega + (m\omega_c - \omega_s)\}]] \quad \text{E-3}$$

$$D_4(t) \leftrightarrow jk\Pi V_s[\delta(\omega + \omega_s) - \delta(\omega - \omega_s)] + jk\frac{\Pi}{2} V_s \sum_{m=-\infty}^{m=\infty} Sa(2\Pi mk) \cdot [\exp(-j\frac{3Tm}{4}\omega_c)[\delta(\omega + (m\omega_c - \omega_s)\} - \delta(\omega - (m\omega_c + \omega_c)\}] + \exp(+j\frac{3Tm}{4}\omega_c)[\delta(\omega + (m\omega_c + \omega_s)\} - \delta(\omega + (m\omega_c + \omega_s)\}]] \quad \text{E-4}$$

The exponential values were given in table 5.1 for m = 1, 2.

Summing up all the demodulated functions, the summed output D_o is given by

$$D_o = \sum_{i=1}^{i=4} D_i$$

$$D_o \leftrightarrow 4kV_s j\Pi [\delta(\omega + \omega_s) - \delta(\omega - \omega_s)]$$

for duty period of $k = \frac{1}{4}$, then;

$$D_o(t) \leftrightarrow V_s j\Pi [\delta(\omega + \omega_s) - \delta(\omega - \omega_s)]$$

Inverse fourier transform gives

$$D_o(f) = V_s \text{Sin } \omega_s t$$

which is the original transmitted signal.

END 14-02-80 FIN